Received: 2 August 2022 | Revised: 24 February 2023 | Accepted: 25 February 2023

DOI: 10.1111/sapm.12573

STUDIES IN APPLIED MATHEMATICS WILEY

ORIGINAL ARTICLE

Rogue wave patterns associated with Okamoto polynomial hierarchies

Bo Yang[1] | **Jianke Yang**[2]

[1]School of Mathematics and Statistics, Ningbo University, Ningbo, China

[2]Department of Mathematics and Statistics, University of Vermont, Burlington, Vermont, USA

Correspondence
Jianke Yang, Department of Mathematics and Statistics, University of Vermont, Burlington, VT 05405, USA.
Email: jxyang@uvm.edu

Funding information
National Science Foundation, Grant/Award Number: DMS-1910282; National Natural Science Foundation of China, Grant/Award Number: 12201326

Abstract

We show that new types of rogue wave patterns exist in integrable systems, and these rogue patterns are described by root structures of Okamoto polynomial hierarchies. These rogue patterns arise when the τ functions of rogue wave solutions are determinants of Schur polynomials with index jumps of three, and an internal free parameter in these rogue waves gets large. We demonstrate these new rogue patterns in the Manakov system and the three-wave resonant interaction system. For each system, we derive asymptotic predictions of its rogue patterns under a large internal parameter through Okamoto polynomial hierarchies. Unlike the previously reported rogue patterns associated with the Yablonskii–Vorob'ev hierarchy, a new feature in the present rogue patterns is that the mapping from the root structure of Okamoto-hierarchy polynomials to the shape of the rogue pattern is linear only to the leading order, but becomes nonlinear to the next order. As a consequence, the current rogue patterns are often deformed, sometimes strongly deformed, from Okamoto-hierarchy root structures, unless the underlying internal parameter is very large. Our analytical predictions of rogue patterns are compared to true solutions, and excellent agreement is observed, even when rogue patterns are strongly deformed from Okamoto-hierarchy root structures.

KEYWORDS
Manakov system, pattern formation, rogue waves, three-wave interaction system

1 | INTRODUCTION

Rogue waves are large and spontaneous nonlinear wave excitations that "come from nowhere and disappear with no trace." Such waves were first studied in oceanography, because they posed a threat even to large ships.[2,3] Later, these waves were also investigated in optics and other physical fields due to their peculiar nature.[4,5] From a theoretical point of view, an important fact is that many integrable nonlinear wave equations admit explicit rational solutions that correspond to rogue waves. This fact was first reported by Peregrine,[6] who presented a simple rogue wave solution for the nonlinear Schrödinger (NLS) equation. Peregrine's solution was later generalized, and more intricate rogue wave solutions in the NLS equation were derived.[7–11] Since the NLS equation governs nonlinear wave packet evolution in a wide range of physical systems,[12,13] these theoretical rogue wave solutions of the NLS equation then motivated a lot of rogue-wave experiments, ranging from water waves to optical waves to acoustic waves.[14–20] These combined theoretical and experimental studies significantly deepened our understanding of physical rogue wave events. Due to this success, rogue wave solutions have also been derived in many other physically important integrable equations, such as the derivative NLS equations for circularly polarized nonlinear Alfvén waves in plasmas and short-pulse propagation in a frequency-doubling crystal,[21–26] the Manakov equations for light transmission in randomly birefringent fibers and interaction between two incoherent light beams in crystals,[27–34] and the three-wave resonant interaction equations in diverse physical situations.[13,35–39] Such theoretical rogue wave solutions have further stimulated experiments on optical rogue waves in randomly birefringent fibers.[40,41] In addition to these rogue waves that arise from a uniform background, rogue waves that arise from a nonuniform background have also been predicted or observed in several wave systems.[42–46]

Pattern formation of rogue waves is an important question, because this information allows for the prediction of later rogue wave events from earlier wave forms. Rogue wave patterns were first studied for the NLS equation in Refs. [7–11, 47–53], where the maximum-amplitude rogue waves and their near-field profiles were determined. In addition, clear geometric shapes of rogue waves on the spatial-temporal plane, such as triangles, pentagons, and heptagons, were numerically reported under certain parameters, and analytically explained for the case of triangles.[52] Regarding the latter question of geometric shapes, significant progress was made recently in Ref. [54], where an intimate connection between geometric shapes of NLS rogue waves and root structures of the Yablonskii–Vorob'ev polynomial hierarchy was revealed when one of the internal parameters in the rogue solutions is large. Since roots of the Yablonskii–Vorob'ev polynomial hierarchy on the complex plane come in shapes such as triangles, pentagons, and heptagons, previous numerical reports on this subject can then be analytically explained. Further significant progress in this direction was made in Ref. [55], where NLS rogue patterns associated with the Yablonskii–Vorob'ev hierarchy were shown to be universal in integrable systems, as long as rogue wave solutions of the integrable systems can be expressed by τ functions whose matrix elements contain Schur polynomials with index jumps of two, as in the generalized derivative NLS equations, the Boussinesq equation, the Manakov system, and many others.[55–58]

A natural next question is, are there other shapes of rogue wave patterns in integrable systems? If so, what special polynomials would be associated with such rogue patterns?

In this article, we show that there are indeed other shapes of rogue patterns in integrable systems. These new rogue patterns would arise if rogue solutions can be expressed by τ functions whose matrix elements contain Schur polynomials with index jumps of three, which occurs in integrable systems such as the Manakov equations (see later text), the three-wave resonant interaction equations,[59] and many others. Special polynomials associated with these new rogue patterns are the Okamoto polynomial hierarchies. We demonstrate these new rogue patterns in the Manakov system and the three-wave resonant interaction system. For each system, we derive asymptotic predictions of its rogue shapes through Okamoto polynomial hierarchies when one of the internal free parameters in the rogue waves gets large. Since roots of Okamoto-hierarchy polynomials exhibit shapes such as double triangles, rhombuses, and squares, we then get new rogue patterns in such shapes. However, unlike the previously reported rogue patterns associated with the Yablonskii–Vorob'ev hierarchy, a new feature in the present case is that the mapping from the root structure of Okamoto hierarchies to the shape of the rogue pattern is linear only to the leading order, but becomes nonlinear to the next order of size $O(1)$. This nonlinear nature of the mapping then generates rogue shapes that are often deformed, sometimes strongly deformed, from Okamoto-hierarchy root structures, unless the underlying internal parameter is very large so that the next-order nonlinear correction of the mapping becomes insignificant. Our analytical predictions of rogue patterns are compared to true solutions, and excellent agreement is observed, even when rogue shapes are strongly deformed from Okamoto-hierarchy root structures.

This paper is structured as follows. In Section 2, we describe some preliminary facts and results. Here, we introduce Okamoto polynomial hierarchies and study their root structures. We also provide explicit rogue wave expressions through Schur polynomials in the Manakov and three-wave-interaction systems. In Section 3, we present our main results on rogue patterns in these two systems under a large internal parameter. In Section 4, we compare these analytical rogue-pattern predictions to true solutions in the two systems. In Section 5, we prove the analytical results stated in Section 3. Section 6 summarizes the paper. In Appendix A, we provide alternative definitions of Okamoto polynomial hierarchies. In Appendices B and C, we prove root-structure results of Okamoto-hierarchy polynomials, and derive the bilinear rogue wave expression in the Manakov system, both of which have been stated in Section 2.

2 | PRELIMINARIES

2.1 | Okamoto polynomials and their hierarchies

Okamoto polynomials first arose in Okamoto's study of rational solutions to the Painlevé IV equation.[60] He showed that a class of such rational solutions can be expressed as the logarithmic derivative of certain special polynomials, which are now called Okamoto polynomials. Later, determinant expressions of these polynomials were discovered by Kajiwara and Ohta.[61] Let $p_j(z)$ be Schur polynomials defined by

$$\sum_{j=0}^{\infty} p_j(z)\epsilon^j = \exp\left(z\epsilon + \epsilon^2\right), \tag{1}$$

with $p_j(z) \equiv 0$ for $j < 0$. Then, the monic Okamoto polynomials $Q_N(z)$ and $R_N(z)$ with $N \geq 1$ are defined as[61,62]

$$Q_N(z) = c_N \begin{vmatrix} p_2(z) & p_1(z) & \cdots & p_{3-N}(z) \\ p_5(z) & p_4(z) & \cdots & p_{6-N}(z) \\ \vdots & \vdots & \vdots & \vdots \\ p_{3N-1}(z) & p_{3N-2}(z) & \cdots & p_{2N}(z) \end{vmatrix}, \tag{2}$$

and

$$R_N(z) = d_N \begin{vmatrix} p_1(z) & p_0(z) & \cdots & p_{2-N}(z) \\ p_4(z) & p_3(z) & \cdots & p_{5-N}(z) \\ \vdots & \vdots & \vdots & \vdots \\ p_{3N-2}(z) & p_{3N-3}(z) & \cdots & p_{2N-1}(z) \end{vmatrix}, \tag{3}$$

where

$$c_N = 3^{-\frac{1}{2}N(N-1)} \frac{2!5! \cdots (3N-1)!}{0!1! \cdots (N-1)!}, \tag{4}$$

and

$$d_N = 3^{-\frac{1}{2}N(N-1)} \frac{1!4! \cdots (3N-2)!}{0!1! \cdots (N-1)!}. \tag{5}$$

Note that these two determinants are both Wronskians, because $p'_{j+1}(z) = p_j(z)$ from the definition of $p_j(z)$ in Equation (1), where the prime denotes differentiation. The first three $Q_N(z)$ and $R_N(z)$ polynomials are

$$Q_1(z) = z^2 + 2,$$

$$Q_2(z) = z^6 + 10z^4 + 20z^2 + 40,$$

$$Q_3(z) = z^{12} + 28z^{10} + 260z^8 + 1120z^6 + 2800z^4 + 11200z^2 + 11200,$$

$$R_1(z) = z,$$

$$R_2(z) = z^4 + 4z^2 - 4,$$

$$R_3(z) = z(z^8 + 16z^6 + 56z^4 - 560).$$

Compared to the Okamoto polynomials introduced in Refs. [60–62], the polynomials above are related to them through a simple scaling in z and (Q_N, R_N).

Like the Yablonskii–Vorob'ev polynomials,[63] these Okamoto polynomials can also be generalized to hierarchies. This generalization has not been done before (to our knowledge). Thus, we do it now. Let $p_j^{[m]}(z)$ be Schur polynomials defined by

$$\sum_{j=0}^{\infty} p_j^{[m]}(z)\epsilon^j = \exp\left(z\epsilon + \epsilon^m\right), \tag{6}$$

where m is a positive integer larger than one, and $p_j^{[m]}(z) \equiv 0$ if $j < 0$. Then, we define the monic Okamoto polynomial hierarchies $R_N^{[m]}(z)$ and $Q_N^{[m]}(z)$ by the Wronskians

$$Q_N^{[m]}(z) = c_N \begin{vmatrix} p_2^{[m]}(z) & p_1^{[m]}(z) & \cdots & p_{3-N}^{[m]}(z) \\ p_5^{[m]}(z) & p_4^{[m]}(z) & \cdots & p_{6-N}^{[m]}(z) \\ \vdots & \vdots & \vdots & \vdots \\ p_{3N-1}^{[m]}(z) & p_{3N-2}^{[m]}(z) & \cdots & p_{2N}^{[m]}(z) \end{vmatrix}, \tag{7}$$

and

$$R_N^{[m]}(z) = d_N \begin{vmatrix} p_1^{[m]}(z) & p_0^{[m]}(z) & \cdots & p_{2-N}^{[m]}(z) \\ p_4^{[m]}(z) & p_3^{[m]}(z) & \cdots & p_{5-N}^{[m]}(z) \\ \vdots & \vdots & \vdots & \vdots \\ p_{3N-2}^{[m]}(z) & p_{3N-3}^{[m]}(z) & \cdots & p_{2N-1}^{[m]}(z) \end{vmatrix}. \tag{8}$$

If $m \bmod 3 = 0$, then $Q_N^{[m]}(z) = z^{N(N+1)}$ and $R_N^{[m]}(z) = z^{N^2}$. Proofs for them would be a simple modification of our proofs in Appendix B for Theorems 1 and 2 to be stated below and are thus omitted for brevity. But such m values turn out to be irrelevant to our rogue pattern problem. Thus, in this article, we require $m \bmod 3 \neq 0$, that is, $m = 2, 4, 5, 7, 8, 10, \ldots$. When $m = 2$, $Q_N^{[2]}(z)$ and $R_N^{[2]}(z)$ are the Okamoto polynomials $Q_N(z)$ and $R_N(z)$. When $m > 2$, $Q_N^{[m]}(z)$ and $R_N^{[m]}(z)$ give higher members of Okamoto hierarchies.

The above Okamoto hierarchy polynomials can also be defined through Schur functions associated with Young diagrams. Such alternative definitions will be provided in Appendix A.

We should point out that these Okamoto hierarchy polynomials are different from the generalized Okamoto polynomials $Q_{m,n}(z)$ introduced and studied earlier in Refs. [62, 64, 65]. Those generalized Okamoto polynomials are built from the original $p_j(z)$ polynomials of Equation (1), but adding additional matrix elements into the original determinants (2)–(3). Our Okamoto hierarchy polynomials, on the other hand, are built from the new $p_j^{[m]}(z)$ polynomials of Equation (6), while preserving the forms of the original determinants (2)–(3). Loosely speaking, the generalized Okamoto polynomials are horizontal generalizations, whereas Okamoto hierarchy polynomials are vertical generalizations.

2.2 | Root structures of Okamoto polynomial hierarchies

Root structures of Okamoto-hierarchy polynomials will play a key role in our analytical study of rogue wave patterns. For Okamoto polynomials $Q_N(z)$ and $R_N(z)$, their root structures have been investigated in Refs. [62, 66, 67]. It has been shown that for every positive integer N, $Q_N(z)$ and $R_N(z)$ have simple roots.[66,67] In addition, graphs of root locations for many $Q_N(z)$ and $R_N(z)$ polynomials have been plotted, and double-triangle as well as rhombus-shape root structures have been observed.[62] But for higher members of Okamoto hierarchies, their root structures have not been studied yet since those polynomials have not been introduced before.

In this subsection, we examine root structures of Okamoto hierarchies $Q_N^{[m]}(z)$ and $R_N^{[m]}(z)$. Defining integer N_0 as the remainder of N divided by m, that is,

$$N_0 \equiv N \bmod m, \tag{9}$$

and denoting $[a]$ as the largest integer less than or equal to a real number a, then our results are summarized by the following two theorems.

Theorem 1. *The Okamoto hierarchy polynomial $Q_N^{[m]}(z)$ is monic with degree $N(N+1)$, and is of the form*

$$Q_N^{[m]}(z) = z^{N_Q} q_N^{[m]}(\zeta), \quad \zeta \equiv z^m, \tag{10}$$

where $q_N^{[m]}(\zeta)$ is a monic polynomial of ζ with all-real coefficients and a nonzero constant term. The nonnegative integer N_Q is the multiplicity of the zero root in $Q_N^{[m]}(z)$ and is given by the formula

$$N_Q = N_{1Q}(N_{1Q} - N_{2Q} + 1) + N_{2Q}^2, \tag{11}$$

where N_{1Q} and N_{2Q} are nonnegative integers. If $m > 1$ and $m \bmod 3 = 1$, these (N_{1Q}, N_{2Q}) values are

$$(N_{1Q}, N_{2Q}) = \begin{cases} (N_0, 0), & \text{when } 0 \le N_0 \le \left[\frac{m}{3}\right], \\ \left(\left[\frac{m}{3}\right], N_0 - \left[\frac{m}{3}\right]\right), & \text{when } \left[\frac{m}{3}\right] + 1 \le N_0 \le 2\left[\frac{m}{3}\right], \\ (m-1-N_0,\, m-1-N_0), & \text{when } 2\left[\frac{m}{3}\right] + 1 \le N_0 \le m-1; \end{cases} \tag{12}$$

and if $m \bmod 3 = 2$, these (N_{1Q}, N_{2Q}) values are

$$(N_{1Q}, N_{2Q}) = \begin{cases} (N_0, 0), & \text{when } 0 \le N_0 \le \left[\frac{m}{3}\right], \\ \left(N_0 - \left[\frac{m}{3}\right] - 1, \left[\frac{m}{3}\right]\right), & \text{when } \left[\frac{m}{3}\right] + 1 \le N_0 \le 2\left[\frac{m}{3}\right], \\ (m-1-N_0,\, m-1-N_0), & \text{when } 2\left[\frac{m}{3}\right] + 1 \le N_0 \le m-1. \end{cases} \tag{13}$$

If $N_Q = 0$, then zero is not a root of $Q_N^{[m]}(z)$.

Theorem 2. *The Okamoto hierarchy polynomial $R_N^{[m]}(z)$ is monic with degree N^2, and is of the form*

$$R_N^{[m]}(z) = z^{N_R} r_N^{[m]}(\zeta), \quad \zeta \equiv z^m, \tag{14}$$

where $r_N^{[m]}(\zeta)$ is a monic polynomial of ζ with all-real coefficients and a nonzero constant term. The nonnegative integer N_R is the multiplicity of the zero root in $R_N^{[m]}(z)$ and is given by the formula

$$N_R = N_{1R}(N_{1R} - N_{2R} + 1) + N_{2R}^2, \tag{15}$$

where N_{1R} and N_{2R} are nonnegative integers. If $m > 1$ and $m \bmod 3 = 1$, these (N_{1R}, N_{2R}) values are

$$(N_{1R}, N_{2R}) = \begin{cases} (0, N_0), & \text{when } 0 \le N_0 \le \left[\frac{m}{3}\right], \\ \left(\left[\frac{m}{3}\right] - 1, N_0 - 1 - \left[\frac{m}{3}\right]\right), & \text{when } \left[\frac{m}{3}\right] + 1 \le N_0 \le 2\left[\frac{m}{3}\right], \\ (m - 1 - N_0,\ m - N_0), & \text{when } 2\left[\frac{m}{3}\right] + 1 \le N_0 \le m - 1; \end{cases} \tag{16}$$

and if $m \bmod 3 = 2$, these (N_{1R}, N_{2R}) values are

$$(N_{1R}, N_{2R}) = \begin{cases} (0, N_0), & \text{when } 0 \le N_0 \le \left[\frac{m}{3}\right], \\ \left(N_0 - 1 - \left[\frac{m}{3}\right], \left[\frac{m}{3}\right] + 1\right), & \text{when } \left[\frac{m}{3}\right] + 1 \le N_0 \le 2\left[\frac{m}{3}\right], \\ (m - 1 - N_0,\ m - N_0), & \text{when } 2\left[\frac{m}{3}\right] + 1 \le N_0 \le m - 1. \end{cases} \tag{17}$$

If $N_R = 0$, then zero is not a root of $R_N^{[m]}(z)$.

Proofs of these two theorems will be provided in Appendix B.

The most significant piece of information in these two theorems is the formulae for N_Q and N_R, which give the multiplicities of the zero root in $Q_N^{[m]}(z)$ and $R_N^{[m]}(z)$ polynomials. These root-multiplicity formulae are particularly important for the analysis of rogue waves in the inner region under a large parameter (see later text). Compared to the multiplicity formula of the zero root in the Yablonskii–Vorob'ev polynomial hierarchy,[54,55] the present multiplicity formulae for Okamoto hierarchies are more involved, but their connection to the multiplicity formula of the Yablonskii–Vorob'ev hierarchy is still visible (see especially Ref. [55]). For Okamoto polynomials $Q_N(z)$ and $R_N(z)$ (where $m = 2$), these multiplicity formulae show that $N_Q = 0$ for all N values, and $N_R = 0$ if N is even and $N_R = 1$ if N is odd. This means that for any N, zero is not a root of $Q_N(z)$. In addition, for $R_N(z)$, zero is not a root when N is even and is a simple root when N is odd.

Another piece of information from formulae (10) and (14) of these theorems is that root structures of both $Q_N^{[m]}(z)$ and $R_N^{[m]}(z)$ polynomials are invariant under $2\pi/m$-angle rotation in the complex z plane. This rotational symmetry of the root structures will have implications on shapes of rogue patterns away from the origin under a large parameter, as we will see later.

The only major piece of information missing from the above two theorems is multiplicities of *nonzero* roots in these $Q_N^{[m]}(z)$ and $R_N^{[m]}(z)$ polynomials. For Okamoto polynomials $Q_N(z)$ and $R_N(z)$ (where $m = 2$), it has been shown that all their roots are simple.[66,67] For higher members of these hierarchies, their zero root clearly can be nonsimple in view of the above N_Q and N_R formulae. However, it is unclear whether their nonzero roots can also be nonsimple. We numerically studied this question for many particular polynomials in the two hierarchies, and found their nonzero roots to be always simple. Based on this numerical evidence, we propose the following conjecture.

Conjecture 1. *Nonzero roots of Okamoto-hierarchy polynomials $Q_N^{[m]}(z)$ and $R_N^{[m]}(z)$ are all simple for arbitrary integers $N \ge 1$ and $m > 1$.*

FIGURE 1 Root structures of the $Q_N^{[m]}(z)$ polynomial hierarchy for $2 \le N \le 4$ and $m = 2, 4, 5, 7$. In all panels, $-8 \le \mathrm{Re}(z), \mathrm{Im}(z) \le 8$.

If this conjecture holds, then from Theorems 1–2, numbers of nonzero roots in $Q_N^{[m]}(z)$ and $R_N^{[m]}(z)$ would be

$$M_Q = N(N+1) - N_Q, \quad M_R = N^2 - N_R, \tag{18}$$

respectively, where N_Q and N_R are given in Equations (11) and (15).

To get a visual impression of root structures in Okamoto polynomial hierarchies, we plot in Figure 1 roots of the $Q_N^{[m]}(z)$ hierarchy in the complex z plane with $2 \le N \le 4$ and $m = 2, 4, 5, 7$. The first column of this figure (with $m = 2$), for roots of Okamoto polynomials $Q_N(z)$, exhibits "double triangles" as reported in Ref. [62]. We caution the reader that sides of these double triangles are not exactly straight; thus, our use of the term "double triangles" is only in an approximate sense. The second column of this figure, for roots of $Q_N^{[4]}(z)$ polynomials, exhibit a "square" shape with curved sides, intricate interiors, and some very close roots. The third column, for roots of $Q_N^{[5]}(z)$, exhibits a pentagon shape; while the fourth column, for roots of $Q_N^{[7]}(z)$, exhibits a heptagon shape. Compared to root shapes of the Yablonskii–Vorob'ev polynomial hierarchy, the present double-triangle and square shapes are new. The pentagon and heptagon shapes are not new, as they have appeared in the Yablonskii–Vorob'ev hierarchy before.[54,55,63] However, compared to pentagons and heptagons of Yablonskii–Vorob'ev-hierarchy roots, the current pentagons and heptagons of Okamoto-hierarchy roots have different interiors.

In Figure 2, we plot root structures of the $R_N^{[m]}(z)$ hierarchy in the complex plane with $2 \le N \le 4$ and $m = 2, 4, 5, 7$. Shapes of these roots are somewhat similar to their counterparts for $Q_N^{[m]}(z)$

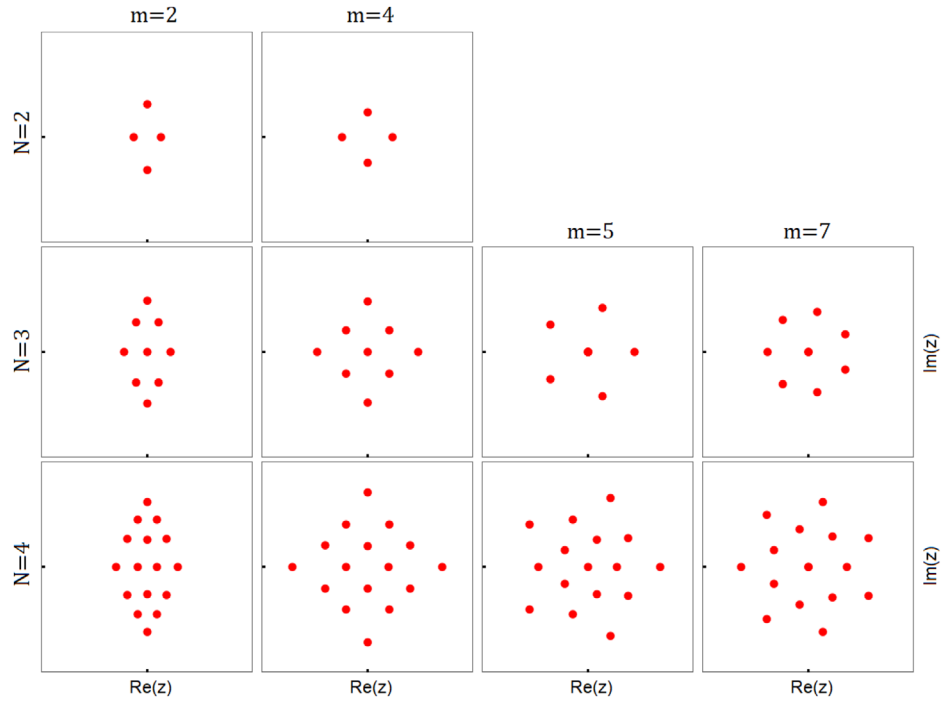

FIGURE 2 Root structures of the $R_N^{[m]}(z)$ polynomial hierarchy for $2 \le N \le 4$ and $m = 2, 4, 5, 7$. In all panels, $-7 \le \mathrm{Re}(z), \mathrm{Im}(z) \le 7$.

in the previous figure, but plenty of differences also exist between them. One difference is that while the first column of Figure 1 exhibits two separate triangles, the first column of the current figure exhibits two triangles that are joined together at the base to form a rhombus. Another difference is that interior roots in the second column of the current figure are more orderly than their counterparts in Figure 1. A third difference is that even though shapes of roots in the fourth columns of the two figures are quite similar to each other, zero roots in corresponding panels actually have different multiplicities. For example, the zero root has multiplicity 5 in the upper panel of the fourth column of Figure 1, but has multiplicity 2 in the corresponding panel of Figure 2.

The aim of this paper is to show that geometric shapes of certain types of rogue waves in integrable systems are closely related with root structures of Okamoto polynomial hierarchies. For this purpose, we present such rogue waves in two integrable systems below.

2.3 | Rogue waves in the Manakov system

The Manakov system is[68]

$$\begin{aligned} (\mathrm{i}\partial_t + \partial_x^2)u_1 + (\epsilon_1|u_1|^2 + \epsilon_2|u_2|^2)u_1 = 0, \\ (\mathrm{i}\partial_t + \partial_x^2)u_2 + (\epsilon_1|u_1|^2 + \epsilon_2|u_2|^2)u_2 = 0, \end{aligned} \tag{19}$$

where the nonlinear coefficients $\epsilon_1 = \pm 1$ and $\epsilon_2 = \pm 1$. These equations govern many physical processes such as the interaction of two incoherent light beams in crystals,[28,29,69] transmission

of light in randomly birefringent optical fibers,[27,70,71] and evolution of two-component Bose–Einstein condensates.[72,73] Integrability of this system can be found in Ref. [68] for $\epsilon_1 = \epsilon_2$ and in Ref. [74] for arbitrary (ϵ_1, ϵ_2) values.

Rogue waves in the Manakov system are rational solutions that satisfy the following boundary conditions:

$$\begin{aligned} u_1(x,t) &\to \rho_1 e^{\mathrm{i}(k_1 x+\omega_1 t)}, \quad x,t \to \pm\infty, \\ u_2(x,t) &\to \rho_2 e^{\mathrm{i}(k_2 x+\omega_2 t)}, \quad x,t \to \pm\infty, \end{aligned} \tag{20}$$

where (k_1, k_2) and (ω_1, ω_2) are wave numbers and frequencies of the two components in the plane-wave background, and (ρ_1, ρ_2) are their amplitudes that will be set real positive using phase invariance of the system. Parameters of the background plane wave satisfy the following relations:

$$\begin{aligned} \omega_1 &= \epsilon_1\rho_1^2 + \epsilon_2\rho_2^2 - k_1^2, \\ \omega_2 &= \epsilon_1\rho_1^2 + \epsilon_2\rho_2^2 - k_2^2. \end{aligned} \tag{21}$$

Due to Galilean invariance of the Manakov system, we can set $k_1 = -k_2$ without loss of generality. In this case, $\omega_1 = \omega_2$.

Rogue waves in the Manakov system have been derived in Refs. [30–34, 55] by various methods. Some of those waves, whose τ functions are determinants of Schur polynomials with index jumps of two, are asymptotically related to the Yablonski–Vorob'ev polynomial hierarchy when one of the internal free parameters in such waves is large.[55] The rogue waves that are asymptotically related to Okamoto hierarchies under a large internal parameter turn out to be those whose τ functions are determinants of Schur polynomials with index jumps of three. This asymptotic connection between such rogue waves and Okamoto hierarchies naturally arises, since Okamoto-hierarchy polynomials are also determinants of Schur polynomials with index jumps of three (see Equations (7)–(8)), similar to those rogue waves. In this case, when an internal parameter in such rogue waves is large, the rogue-wave determinants with Schur-polynomial elements simplify to Okamoto-hierarchy polynomials under proper scalings (details on this will be seen in Section 5 later).

In the framework of Darboux transformation, Manakov rogue waves in the form of determinants of Schur polynomials with index jumps of three would arise when the underlying 3×3 scattering matrix admits a triple eigenvalue. Derivation of such rogue waves by Darboux transformation can be found in Refs. [32–34]. However, those rogue from Darboux transformation are not general nor explicit for asymptotic analysis. Thus, we will first present explicit and general expressions of those rogue waves, which we will derive by the bilinear method.

Before presenting our rogue-wave expressions, we need to introduce elementary Schur polynomials. These polynomials $S_j(\boldsymbol{x})$ with $\mathbf{x} = (x_1, x_2, ...)$ are defined by the generating function

$$\sum_{j=0}^{\infty} S_j(\boldsymbol{x})\epsilon^j = \exp\left(\sum_{j=1}^{\infty} x_j \epsilon^j\right), \tag{22}$$

or more explicitly,

$$S_0(\mathbf{x}) = 1, \quad S_1(\boldsymbol{x}) = x_1, \quad S_2(\boldsymbol{x}) = \frac{1}{2}x_1^2 + x_2, \ \ldots, \quad S_j(\boldsymbol{x}) = \sum_{l_1+2l_2+\cdots+ml_m=j} \left(\prod_{j=1}^{m} \frac{x_j^{l_j}}{l_j!}\right). \tag{23}$$

In addition, we define $S_j(\mathbf{x}) = 0$ when $j < 0$.

Our Manakov rogue waves whose τ functions are determinants of Schur polynomials with index jumps of three are given by the following theorem.

Theorem 3. *When the nonlinear coefficients in the Manakov system (19) are $\epsilon_1 = \epsilon_2 = 1$, and background amplitudes and wave numbers in the boundary conditions (20) satisfy the following constraints:*

$$\rho_1 = \rho_2 = \sqrt{2}|k_1 - k_2|, \quad k_1 \neq k_2, \tag{24}$$

the algebraic equation

$$\mathcal{F}_1'(p) = 0, \tag{25}$$

where

$$\mathcal{F}_1(p) = \frac{\rho_1^2}{p - \mathrm{i}k_1} + \frac{\rho_1^2}{p - \mathrm{i}k_2} + 2p, \tag{26}$$

would admit a double root

$$p_0 = \frac{\sqrt{3}}{2}(k_1 - k_2) + \frac{\mathrm{i}}{2}(k_1 + k_2). \tag{27}$$

In this case, the Manakov system (19) under boundary conditions (20) would admit nonsingular (N_1, N_2)th-order rogue wave solutions

$$u_{1,N_1,N_2}(x,t) = \rho_1 \frac{g_{1,N_1,N_2}}{f_{N_1,N_2}} e^{\mathrm{i}(k_1 x + \omega_1 t)}, \tag{28}$$

$$u_{2,N_1,N_2}(x,t) = \rho_1 \frac{g_{2,N_1,N_2}}{f_{N_1,N_2}} e^{\mathrm{i}(k_2 x + \omega_2 t)}, \tag{29}$$

where N_1 and N_2 are arbitrary nonnegative integers,

$$f_{N_1,N_2} = \sigma_{0,0}, \quad g_{1,N_1,N_2} = \sigma_{1,0}, \quad g_{2,N_1,N_2} = \sigma_{0,1}, \tag{30}$$

$\sigma_{n,k}$ is given by the following 2×2 block determinant

$$\sigma_{n,k} = \det \begin{pmatrix} \sigma_{n,k}^{[1,1]} & \sigma_{n,k}^{[1,2]} \\ \sigma_{n,k}^{[2,1]} & \sigma_{n,k}^{[2,2]} \end{pmatrix}, \tag{31}$$

$$\sigma_{n,k}^{[I,J]} = \left(\phi_{3i-I,\,3j-J}^{(n,k,I,J)} \right)_{1 \le i \le N_I,\, 1 \le j \le N_J}, \tag{32}$$

the matrix elements in $\sigma_{n,k}^{[I,J]}$ are defined by

$$\phi_{i,j}^{(n,k,I,J)} = \sum_{\nu=0}^{\min(i,j)} \left[\frac{|p_1|^2}{(p_0 + p_0^*)^2} \right]^{\nu} S_{i-\nu}(\mathrm{x}_I^+(n,k) + \nu \mathrm{s})\, S_{j-\nu}(\mathrm{x}_J^-(n,k) + \nu \mathrm{s}^*), \tag{33}$$

vectors $\mathrm{x}_I^+(n,k)=(x_{1,I}^+,x_{2,I}^+,\ldots)$ *and* $\mathrm{x}_J^-(n,k)=(x_{1,J}^-,x_{2,J}^-,\ldots)$ *are defined by*

$$x_{r,I}^+(n,k)=p_r x+\left(\sum_{l=0}^{r}p_l p_{r-l}\right)(\mathrm{i}t)+n\theta_r+k\lambda_r+a_{r,I},\ \text{if } r \bmod 3\neq 0, \tag{34}$$

$$x_{r,J}^-(n,k)=p_r^* x-\left(\sum_{l=0}^{r}p_l^* p_{r-l}^*\right)(\mathrm{i}t)-n\theta_r^*-k\lambda_r^*+a_{r,J}^*,\ \text{if } r \bmod 3\neq 0, \tag{35}$$

$$x_{r,I}^+(n,k)=x_{r,J}^-(n,k)=0,\ \text{if } r \bmod 3=0, \tag{36}$$

the asterisk "" represents complex conjugation, and* θ_r, λ_r, *and* s_r *are coefficients from the expansions*

$$\ln\left[\frac{p(\kappa)-\mathrm{i}k_1}{p_0-\mathrm{i}k_1}\right]=\sum_{r=1}^{\infty}\theta_r\kappa^r,\ln\left[\frac{p(\kappa)-\mathrm{i}k_2}{p_0-\mathrm{i}k_2}\right]=\sum_{r=1}^{\infty}\lambda_r\kappa^r, \tag{37}$$

$$\ln\left[\frac{1}{\kappa}\left(\frac{p_0+p_0^*}{p_1}\right)\left(\frac{p(\kappa)-p_0}{p(\kappa)+p_0^*}\right)\right]=\sum_{r=1}^{\infty}s_r\kappa^r, \tag{38}$$

the function $p(\kappa)$ *is defined by the equation*

$$\mathcal{F}_1[p(\kappa)]=\frac{\mathcal{F}_1(p_0)}{3}\left[e^{\kappa}+2e^{-\kappa/2}\cos\left(\frac{\sqrt{3}}{2}\kappa\right)\right], \tag{39}$$

$p_r=p^{(r)}(0)/r!$, *with the superscript "(r)" denoting the rth derivative of* $p(\kappa)$, *and*

$$(a_{1,1},a_{2,1},a_{4,1},a_{5,1},\ldots,a_{3N_1-1,1}),\quad (a_{1,2},a_{2,2},a_{4,2},a_{5,2},\ldots,a_{3N_2-2,2}) \tag{40}$$

are free complex constants.

The proof of this theorem will be provided in Appendix C. Graphs for some simple solutions in this theorem will be illustrated in Section 2.6 later. Note that for other (ϵ_1,ϵ_2) values, these rogue waves as determinants with index jumps of three will not exist.

Remark 1. Regarding the polynomial degree of $\sigma_{n,k}$ in the above theorem, we can show, by rewriting $\sigma_{n,k}$ into a larger determinant similar to what was done in Ref. [11], that

$$\deg(\sigma_{n,k})=2\left[N_1(N_1-N_2+1)+N_2^2\right] \tag{41}$$

in both x and t.

Remark 2. The algebraic equation (25) is a quartic equation. Under parameter conditions (24), this quartic equation admits two double roots, one being $p_0^{(1)}=p_0$, and the other being $p_0^{(2)}=-p_0^*$. If we replace p_0 by $p_0^{(2)}$ in Equations (33)–(39), the resulting functions (28)–(29) are still Manakov rogue waves. However, these other Manakov rogue waves are equivalent to those given in Theorem 3 when parameters $(a_{r,1},a_{r,2})$ in them are properly related. See Remark 2 in Ref. [59] for details.

Remark 3. Regarding coefficients s_r defined in the expansion (38), we can show that $s_r=0$ for $r \bmod 3\neq 0$. In addition, if we normalize $k_2=-k_1$ through a Galilean transformation to the

Manakov system, then s_r would be specific numbers without parameter dependence. Proofs of these facts will be given in Appendix D. In the latter case, the first few values of these s_r numbers are found to be

$$s_1 = s_2 = 0,\ s_3 = -\frac{1}{40},\ s_4 = s_5 = 0,\ s_6 = \frac{1669}{1814400},\ s_7 = s_8 = 0,\ s_9 = -\frac{6047}{133056000},$$
$$s_{10} = s_{11} = 0,\ \ldots. \tag{42}$$

Remark 4. There are three functions of $p(\kappa)$ that satisfy Equation (39), and these three functions are related as $p(\kappa e^{\mathrm{i}2j\pi/3})$, where $j = 0, 1, 2$. We can choose any one of these three functions in the above theorem and keep complex parameters $a_{r,I}$ free without loss of generality. See Remark 3 in Ref. [59] for details. The choice of these three $p(\kappa)$ functions is made by the choice of the p_1 value in $p(\kappa)$'s Taylor expansion. This p_1 is any one of the three cubic roots of a certain constant. After p_1 is picked, $p(\kappa)$ will be uniquely determined.

2.4 | Rogue waves in the three-wave resonant interaction system

The (1+1)-dimensional three-wave resonant interaction system is

$$\begin{aligned}(\partial_t + c_1\partial_x)u_1 &= \epsilon_1 u_2^* u_3^*,\\ (\partial_t + c_2\partial_x)u_2 &= \epsilon_2 u_1^* u_3^*,\\ (\partial_t + c_3\partial_x)u_3 &= \epsilon_3 u_1^* u_2^*,\end{aligned} \tag{43}$$

where (c_1, c_2, c_3) are group velocities of the three waves, and $(\epsilon_1, \epsilon_2, \epsilon_3)$ are real-valued nonlinear coefficients. To remove ambiguity, we order the three group velocities as $c_1 > c_2 > c_3$, and make $c_3 = 0$ by choosing a coordinate system that moves with velocity c_3. The nonlinear coefficients ϵ_n can be normalized to ± 1 by variable scalings. In addition, we can fix $\epsilon_1 = 1$ without loss of generality.

Rogue waves in this three-wave interaction system are rational solutions that approach plane-wave backgrounds as $x, t \to \pm\infty$, that is,

$$\begin{aligned}&u_1(x,t) \to \rho_1 e^{\mathrm{i}(k_1 x+\omega_1 t)}, && x,t \to \pm\infty,\\ &u_2(x,t) \to \rho_2 e^{\mathrm{i}(k_2 x+\omega_2 t)}, && x,t \to \pm\infty,\\ &u_3(x,t) \to \mathrm{i}\rho_3 e^{-\mathrm{i}[(k_1+k_2)x+(\omega_1+\omega_2)t]}, && x,t \to \pm\infty,\end{aligned} \tag{44}$$

where (k_1, k_2) and (ω_1, ω_2) are wave numbers and frequencies of the first two waves, and (ρ_1, ρ_2, ρ_3) are the complex amplitudes of the three waves. Parameters of these plane waves satisfy the following relations:

$$\begin{aligned}\rho_1(\omega_1 + c_1 k_1) &= -\epsilon_1 \rho_2^* \rho_3^*,\\ \rho_2(\omega_2 + c_2 k_2) &= -\epsilon_2 \rho_1^* \rho_3^*,\\ \rho_3(\omega_1 + \omega_2) &= \epsilon_3 \rho_1^* \rho_2^*.\end{aligned} \tag{45}$$

In this article, we assume that ρ_1, ρ_2, and ρ_3 are all nonzero. In view of the phase invariance, we can normalize ρ_1 and ρ_2 to be real. Then the above relations show that ρ_3 is real as well.

In addition, the gauge invariance allows us to impose a restriction on the four parameters $(k_1, k_2, \omega_1, \omega_2)$, such as fixing one of them as zero, or equating $k_1 = k_2$, or equating $\omega_1 = \omega_2$, without any loss of generality. Under such a restriction, wave number and frequency parameters $(k_1, k_2, \omega_1, \omega_2)$ would be fully determined from the three real background-amplitude parameters (ρ_1, ρ_2, ρ_3) through Equations (45).

General rogue-wave solutions in the three-wave interaction system (43) have been derived by the bilinear method in Ref. [59]. To present these rogue waves, we introduce notations

$$\gamma_1 \equiv \epsilon_1 \frac{\rho_2 \rho_3}{\rho_1}, \ \gamma_2 \equiv \epsilon_2 \frac{\rho_1 \rho_3}{\rho_2}, \ \gamma_3 \equiv \epsilon_3 \frac{\rho_1 \rho_2}{\rho_3}, \tag{46}$$

and

$$\mathcal{F}_2(p) = \left(\frac{\gamma_1 c_2}{\gamma_3 (c_2 - c_1)} \right) \frac{1}{p} - \left(\frac{\gamma_2 c_1}{\gamma_3 (c_2 - c_1)} \right) \frac{1}{p - \mathrm{i}} - p. \tag{47}$$

Then, rogue waves in the three-wave system whose τ functions are determinants of Schur polynomials with index jumps of three are given by the following theorem.

Theorem 4 [59]. *In the soliton-exchange case where* $(\epsilon_1, \epsilon_2, \epsilon_3) = (1, -1, 1)$*, and under parameter conditions*

$$\rho_2 = \pm \sqrt{\frac{c_1}{c_2}} \rho_1, \quad \rho_3 = \pm \sqrt{\frac{c_1 - c_2}{c_2}} \rho_1, \tag{48}$$

the algebraic equation

$$\mathcal{F}_2'(p) = 0 \tag{49}$$

admits a double root $p_0 = (\sqrt{3} + \mathrm{i})/2$*. In this case, the three-wave interaction system (43) under boundary conditions (44) admits nonsingular* (N_1, N_2)*th-order rogue-wave solutions*

$$u_{1,N_1,N_2}(x,t) = \rho_1 \frac{g_{1,N_1,N_2}}{f_{N_1,N_2}} e^{\mathrm{i}(k_1 x + \omega_1 t)}, \tag{50}$$

$$u_{2,N_1,N_2}(x,t) = \rho_2 \frac{g_{2,N_1,N_2}}{f_{N_1,N_2}} e^{\mathrm{i}(k_2 x + \omega_2 t)}, \tag{51}$$

$$u_{3,N_1,N_2}(x,t) = \mathrm{i}\rho_3 \frac{g_{3,N_1,N_2}}{f_{N_1,N_2}} e^{-\mathrm{i}[(k_1 + k_2)x + (\omega_1 + \omega_2)t]}, \tag{52}$$

where N_1 *and* N_2 *are arbitrary nonnegative integers,*

$$f_{N_1,N_2} = \sigma_{0,0}, \quad g_{1,N_1,N_2} = \sigma_{1,0}, \quad g_{2,N_1,N_2} = \sigma_{0,-1}, \quad g_{3,N_1,N_2} = \sigma_{-1,1}, \tag{53}$$

$\sigma_{n,k}$ *is given by the following* 2×2 *block determinant*

$$\sigma_{n,k} = \det \begin{pmatrix} \sigma_{n,k}^{[1,1]} & \sigma_{n,k}^{[1,2]} \\ \sigma_{n,k}^{[2,1]} & \sigma_{n,k}^{[2,2]} \end{pmatrix}, \tag{54}$$

$$\sigma_{n,k}^{[I,J]} = \left(\phi_{3i-I,\,3j-J}^{(n,k,I,J)} \right)_{1 \le i \le N_I,\, 1 \le j \le N_J}, \tag{55}$$

the matrix elements in $\sigma_{n,k}^{[I,J]}$ *are defined by*

$$\phi_{i,j}^{(n,k,I,J)} = \sum_{\nu=0}^{\min(i,j)} \left[\frac{|p_1|^2}{(p_0+p_0^*)^2}\right]^{\nu} S_{i-\nu}(\mathrm{x}_I^+(n,k)+\nu\mathrm{s})\, S_{j-\nu}(\mathrm{x}_J^-(n,k)+\nu\mathrm{s}^*), \tag{56}$$

vectors $\mathrm{x}_I^+(n,k) = (x_{1,I}^+, x_{2,I}^+, ...)$ *and* $\mathrm{x}_J^-(n,k) = (x_{1,J}^-, x_{2,J}^-, ...)$ *are defined by*

$$x_{r,I}^+(n,k) = (\alpha_r - \beta_r)\, x + (c_1\beta_r - c_2\alpha_r)\, t + n\theta_r + k\lambda_r + a_{r,I},\ \textit{if}\ r\ \textit{mod}\ 3 \neq 0, \tag{57}$$

$$x_{r,J}^-(n,k) = (\alpha_r^* - \beta_r^*)\, x + (c_1\beta_r^* - c_2\alpha_r^*)\, t - n\theta_r^* - k\lambda_r^* + a_{r,J}^*,\ \textit{if}\ r\ \textit{mod}\ 3 \neq 0, \tag{58}$$

$$x_{r,I}^+(n,k) = x_{r,J}^-(n,k) = 0,\ \textit{if}\ r\ \textit{mod}\ 3 = 0, \tag{59}$$

α_r, β_r, θ_r, λ_r *and the vector* $\mathrm{s} = (s_1, s_2, ...)$ *are defined through the expansions*

$$\frac{\gamma_1}{c_1-c_2}\left(\frac{1}{p(\kappa)} - \frac{1}{p_0}\right) = \sum_{r=1}^{\infty} \alpha_r \kappa^r, \tag{60}$$

$$\frac{\gamma_2}{c_1-c_2}\left(\frac{1}{p(\kappa)-\mathrm{i}} - \frac{1}{p_0-\mathrm{i}}\right) = \sum_{r=1}^{\infty} \beta_r \kappa^r, \tag{61}$$

$$\ln\frac{p(\kappa)}{p_0} = \sum_{r=1}^{\infty} \lambda_r \kappa^r, \quad \ln\frac{p(\kappa)-\mathrm{i}}{p_0-\mathrm{i}} = \sum_{r=1}^{\infty} \theta_r \kappa^r, \tag{62}$$

$$\ln\left[\frac{1}{\kappa}\left(\frac{p_0+p_0^*}{p_1}\right)\left(\frac{p(\kappa)-p_0}{p(\kappa)+p_0^*}\right)\right] = \sum_{r=1}^{\infty} s_r \kappa^r, \tag{63}$$

the function $p(\kappa)$ *that appears in Equations (60)–(63) is defined by the equation*

$$\mathcal{F}_2[p(\kappa)] = \frac{\mathcal{F}_2(p_0)}{3}\left[e^{\kappa} + 2e^{-\kappa/2}\cos\left(\frac{\sqrt{3}}{2}\kappa\right)\right], \tag{64}$$

$\mathcal{F}_2(p)$ *is given by Equation (47), or equivalently,*

$$\mathcal{F}_2(p) = -\left(\frac{1}{p} + \frac{1}{p-\mathrm{i}} + p\right) \tag{65}$$

in view of the parameter constraints (48), $p_1 \equiv (dp/d\kappa)|_{\kappa=0}$, *and*

$$(a_{1,1}, a_{2,1}, a_{4,1}, a_{5,1}, ..., a_{3N_1-1,1}), \quad (a_{1,2}, a_{2,2}, a_{4,2}, a_{5,2}, ..., a_{3N_2-2,2}) \tag{66}$$

are free complex constants.

We note that the above rogue expressions are a bit simpler than those presented in Ref. [59], because $x_{r,I}^+(n,k)$ and $x_{r,J}^-(n,k)$ for r-indices of $r \bmod 3 = 0$ have been set as zero here. The reason for this simplification is analogous to that explained in Appendix A of Ref. [54] in a different setting. We also note that there was a typo in the β_r expansion equation (35) of Ref. [59], where $c_2 - c_1$ there should have been $c_1 - c_2$. That typo has been fixed in our current β_r expansion equation (61).

As in the Manakov case, the quartic equation (49) under parameter conditions (48) also admits another double root $-p_0^* = (-\sqrt{3}+\mathrm{i})/2$, but that other double root does not lead to new rogue solutions.[59] In addition, from the expansion (63) for s_r, we find numerically that

$$s_1 = s_2 = 0,\ s_3 = -\frac{1}{40} - \frac{\sqrt{3}}{324}\mathrm{i},\ s_4 = s_5 = 0,\ s_6 = \frac{14321}{16329600} + \frac{\sqrt{3}}{4320}\mathrm{i},\ s_7 = s_8 = 0,\ \ldots. \tag{67}$$

So, $s_r = 0$ when $r \bmod 3 \neq 0$ here as well. This fact will also be proved in Appendix D. The previous Remark 4 holds here too.

2.5 | Special rogue solutions to be studied

Rogue waves in Theorems 3 and 4 for the Manakov and three-wave-interaction systems with general (N_1, N_2) values contain a wide variety of solutions that exhibit different wave patterns. In this article, we will only study rogue waves in these two theorems where $N_1 = 0$ or $N_2 = 0$. In these cases, the 2×2 block determinants in Equations (31) and (54) reduce to a single-block determinant, which makes our analysis a little simpler. For convenience, we introduce the terminology:

- *Q-type Nth-order rogue waves*: rogue waves in Theorems 3 and 4 where $N_1 = N\,(>0)$ and $N_2 = 0$;
- *R-type Nth-order rogue waves*: rogue waves in Theorems 3 and 4 where $N_1 = 0$ and $N_2 = N\,(>0)$.

The reason for the word choices of "Q-type" and "R-type" here is that the underlying rogue waves will be related to $Q_N^{[m]}(z)$ and $R_N^{[m]}(z)$ polynomials, respectively, as we will show later.

For Q-type Nth-order rogue waves, $\sigma_{n,k}$ in Equations (31) and (54) becomes

$$\sigma_{n,k}^{(Q)} = \left(\phi_{3i-1,\,3j-1}^{(n,k)}\right)_{1\le i,j\le N}, \tag{68}$$

and for R-type Nth-order rogue waves, $\sigma_{n,k}$ in Equations (31) and (54) is

$$\sigma_{n,k}^{(R)} = \left(\phi_{3i-2,\,3j-2}^{(n,k)}\right)_{1\le i,j\le N}, \tag{69}$$

where $\phi_{i,j}^{(n,k)}$ is given by Equation (33) for the Manakov system and (56) for the three-wave system, but with indices I and J removed. Internal parameters are $(a_1, a_2, a_4, a_5, \ldots, a_{3N-1})$ for Q-type waves, and $(a_1, a_2, a_4, a_5, \ldots, a_{3N-2})$ for R-type waves. We normalize $a_1 = 0$ by a shift of the (x,t) axes. Then, internal complex parameters in these rogue waves are $(a_2, a_4, a_5, \ldots, a_{3N-1})$ for Q-type, and $(a_2, a_4, a_5, \ldots, a_{3N-2})$ for R-type. Notice that this parameter vector does not contain $(a_3, a_6, \ldots)$. As we will see later, this explains why Okamoto hierarchy polynomials $Q_N^{[m]}(z)$ and $R_N^{[m]}(z)$ with $m = 3, 6, \ldots$ are irrelevant to our rogue pattern studies.

2.6 | Lowest-order Q-type and R-type rogue waves

The lowest-order Q-type and R-type rogue waves are those where $N = 1$. For the Manakov system, the lowest-order R-type rogue wave can be obtained from Theorem 3 and further simplified as

$$u_1(x,t) = \hat{u}_1(x,t)\, e^{\mathrm{i}(k_1 x+\omega_1 t)}, \quad u_2(x,t) = \hat{u}_2(x,t)\, e^{\mathrm{i}(k_2 x+\omega_2 t)}, \tag{70}$$

where

$$\hat{u}_1(x,t) = \rho_1 \frac{\left(x+2\mathrm{i}p_0 t+\hat{\theta}_1\right)\left(x-2\mathrm{i}p_0^* t-\hat{\theta}_1^*\right)+\hat{\xi}_0}{|x+2\mathrm{i}p_0 t|^2+\hat{\xi}_0}, \tag{71}$$

$$\hat{u}_2(x,t) = \rho_1 \frac{\left(x+2\mathrm{i}p_0 t+\hat{\lambda}_1\right)\left(x-2\mathrm{i}p_0^* t-\hat{\lambda}_1^*\right)+\hat{\xi}_0}{|x+2\mathrm{i}p_0 t|^2+\hat{\xi}_0}, \tag{72}$$

and

$$\hat{\theta}_1 = \frac{1}{p_0-\mathrm{i}k_1}, \hat{\lambda}_1 = \frac{1}{p_0-\mathrm{i}k_2}, \hat{\xi}_0 = \frac{1}{(p_0+p_0^*)^2}. \tag{73}$$

This rogue wave is a ratio of degree-2 polynomials in x and t, which is the simplest among all rogue waves in the Manakov system. Thus, we will call it the fundamental Manakov rogue wave. If we choose background wave numbers as $k_2 = -k_1$, which is always possible through a Galilean transformation, then p_0 would be real, see Equation (27). In this case, it is easy to see that this fundamental rogue wave admits the symmetry of $\hat{u}_2(x,t) = \hat{u}_1(-x,t)$, that is, $\hat{u}_2(x,t)$ would be a mirror image of $\hat{u}_1(x,t)$ around the t-axis in the (x,t) plane. To illustrate, let we take $k_1 = -k_2 = 1/\sqrt{12}$, which we will also use later in Section 4.1. Then, the explicit expression of this fundamental Manakov rogue wave is

$$\hat{u}_1(x,t) = \sqrt{\frac{2}{3}}\frac{x^2+t^2-\mathrm{i}(3t-\sqrt{3}x)-2}{x^2+t^2+1}, \quad \hat{u}_2(x,t) = \sqrt{\frac{2}{3}}\frac{x^2+t^2-\mathrm{i}(3t+\sqrt{3}x)-2}{x^2+t^2+1}. \tag{74}$$

This solution is plotted in the left column of Figure 3. It is seen that both the $|u_1|$ and $|u_2|$ components of this solution have a single elongated hump of equal amplitude, and orientations of these two humps are opposite of each other with respect to the vertical axis.

The lowest-order Q-type Manakov rogue wave can also be obtained from Theorem 3. This solution is a ratio of polynomials of degree 4 in x and t, and it contains an irreducible free complex parameter a_2. When we choose $k_1 = -k_2 = 1/\sqrt{12}$, this solution with $a_2 = 0$ is

$$u_1(x,t) = \rho_1 \frac{g_1(x,t)}{f(x,t)}\, e^{\mathrm{i}(k_1 x+\omega_1 t)}, \quad u_2(x,t) = \rho_1 \frac{g_2(x,t)}{f(x,t)}\, e^{\mathrm{i}(k_2 x+\omega_2 t)}, \tag{75}$$

where $\rho_1 = \sqrt{2/3}$, and

$$\begin{aligned}
f(x,t) &= 4+t^4+8x^2+4x^3+x^4+2t^2(10+6x+x^2),\\
g_1(x,t) &= -2-6\mathrm{i}\sqrt{3}-6\mathrm{i}t^3+t^4-4\mathrm{i}\sqrt{3}x+(-1+3\mathrm{i}\sqrt{3})x^2+(4+2\mathrm{i}\sqrt{3})x^3+x^4\\
&\quad +6t\left[-\mathrm{i}+3\sqrt{3}+(-3\mathrm{i}+\sqrt{3})x-\mathrm{i}x^2\right]+t^2\left[5+9\mathrm{i}\sqrt{3}+2(6+\mathrm{i}\sqrt{3})x+2x^2\right],\\
g_2(x,t) &= -2+6\mathrm{i}\sqrt{3}-6\mathrm{i}t^3+t^4+4\mathrm{i}\sqrt{3}x+(-1-3\mathrm{i}\sqrt{3})x^2+(4-2\mathrm{i}\sqrt{3})x^3+x^4\\
&\quad -6t\left[\mathrm{i}+3\sqrt{3}+(3\mathrm{i}+\sqrt{3})x+\mathrm{i}x^2\right]+t^2\left[5-9\mathrm{i}\sqrt{3}+2(6-\mathrm{i}\sqrt{3})x+2x^2\right].
\end{aligned}$$

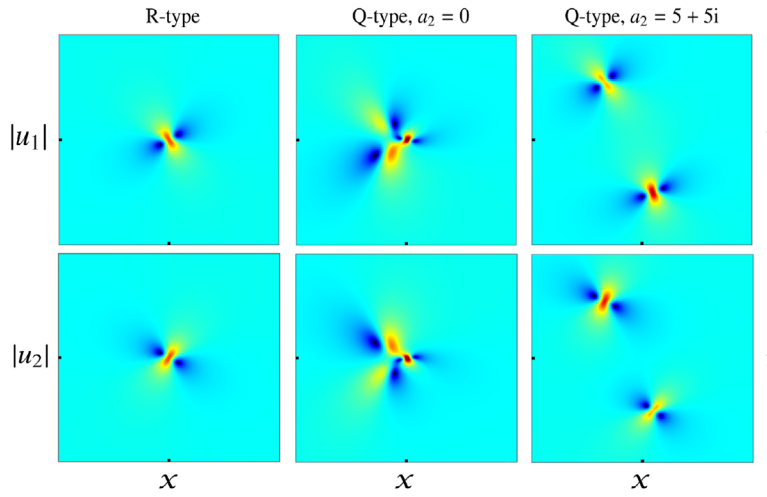

FIGURE 3 Lowest-order Q-type and R-type Manakov rogue waves ($N = 1$) for $k_1 = -k_2 = 1/\sqrt{12}$. Left column: R-type in Equation (74). Middle column: Q-type with $a_2 = 0$ in Equation (75). Right column: Q-type with $a_2 = 5 + 5\mathrm{i}$. In all panels, $-15 \le x, t \le 15$.

This solution is plotted in the middle column of Figure 3. It is seen that the profile of this solution is more complicated.

If $a_2 \neq 0$, the expression for this lowest-order Q-type solution would be more lengthy and will not be produced in this article. When we take $a_2 = 5 + 5\mathrm{i}$, this solution is plotted in the right column of Figure 3. We can see that this solution splits approximately into two fundamental Manakov rogue waves. Notice that this splitting occurs when the internal parameter $|a_2|$ is large. In the next section, we will present an analytical theory that can asymptotically predict this splitting of the solution into fundamental rogue waves under a large internal parameter. With that theory, the solution graph in the right column of Figure 3 would be analytically understood (simply speaking, this splitting is due to the Okamoto polynomial $Q_1^{[2]}(z) = z^2 + 2$ having two simple roots).

For the three-wave system, the lowest-order R-type rogue wave can be obtained from Theorem 4, which can be further simplified as

$$u_1(x,t) = \hat{u}_1(x,t)\, e^{\mathrm{i}(k_1 x + \omega_1 t)}, \quad u_2(x,t) = \hat{u}_2(x,t)\, e^{\mathrm{i}(k_2 x + \omega_2 t)}, \quad u_3(x,t) = \hat{u}_3(x,t)\, e^{-\mathrm{i}[(k_1+k_2)x + (\omega_1+\omega_2)t]}, \tag{76}$$

where

$$\hat{u}_1(x,t) = \rho_1 \frac{\hat{g}_1}{\hat{f}}, \quad \hat{u}_2(x,t) = \rho_2 \frac{\hat{g}_2}{\hat{f}}, \quad \hat{u}_3(x,t) = \mathrm{i}\rho_3 \frac{\hat{g}_3}{\hat{f}},$$

$$\hat{f} = \left|(\hat{\alpha}_1 - \hat{\beta}_1)x + (c_1\hat{\beta}_1 - c_2\hat{\alpha}_1)t\right|^2 + \hat{\xi}_0,$$

$$\hat{g}_1 = \left[(\hat{\alpha}_1 - \hat{\beta}_1)x + (c_1\hat{\beta}_1 - c_2\hat{\alpha}_1)t + \hat{\theta}_1\right]\left[(\hat{\alpha}_1^* - \hat{\beta}_1^*)x + (c_1\hat{\beta}_1^* - c_2\hat{\alpha}_1^*)t - \hat{\theta}_1^*\right] + \hat{\xi}_0,$$

$$\hat{g}_2 = \left[(\hat{\alpha}_1 - \hat{\beta}_1)x + (c_1\hat{\beta}_1 - c_2\hat{\alpha}_1)t - \hat{\lambda}_1\right]\left[(\hat{\alpha}_1^* - \hat{\beta}_1^*)x + (c_1\hat{\beta}_1^* - c_2\hat{\alpha}_1^*)t + \hat{\lambda}_1^*\right] + \hat{\xi}_0,$$

$$\hat{g}_3 = \left[(\hat{\alpha}_1 - \hat{\beta}_1)x + (c_1\hat{\beta}_1 - c_2\hat{\alpha}_1)t - \hat{\theta}_1 + \hat{\lambda}_1\right]\left[(\hat{\alpha}_1^* - \hat{\beta}_1^*)x + (c_1\hat{\beta}_1^* - c_2\hat{\alpha}_1^*)t + \hat{\theta}_1^* - \hat{\lambda}_1^*\right] + \hat{\xi}_0,$$

$$\hat{\alpha}_1 = -\frac{\gamma_1}{p_0^2(c_1 - c_2)}, \hat{\beta}_1 = -\frac{\gamma_2}{(p_0 - \mathrm{i})^2(c_1 - c_2)}, \hat{\theta}_1 = \frac{1}{p_0 - \mathrm{i}}, \hat{\lambda}_1 = \frac{1}{p_0}, \hat{\xi}_0 = \frac{1}{(p_0 + p_0^*)^2}. \tag{77}$$

This rogue wave is a ratio of polynomials of degree 2 in x and t, which is the lowest possible degree of all rogue waves in the three-wave system. Thus, it will be called the fundamental rogue wave of the three-wave system. The graph of this solution, with parameter values of $c_1 = 1, c_2 = 0.5$, and $\rho_1 = 1$, has been displayed in Ref. [59] (see the top row of Figure 5 there). Thus, it will not be plotted here to avoid repetition.

The lowest-order Q-type rogue wave in the three-wave system can also be obtained from Theorem 4. As in the Manakov case, this solution is a ratio of polynomials of degree 4 in x and t, and it contains an irreducible free complex parameter a_2. For parameter values of $c_1 = 1, c_2 = 0.5$, and $\rho_1 = 1$, this solution with $a_2 = 10 + 10\mathrm{i}$ has been plotted in Ref. [59] (upper row of Figure 6 there). It was seen that this solution splits into two fundamental rogue waves, similar to the Manakov case (see the right column of Figure 3). The analytical reason for this splitting will become clear in the next section (since the Okamoto polynomial $Q_1^{[2]}(z) = z^2 + 2$ contains two simple roots). If a_2 is not large (in magnitude), this splitting will not occur, and the resulting solution would exhibit a more complicated profile due to strong interference between the two fundamental rogue waves in close proximity, akin to the middle column of Figure 3 of the Manakov case.

3 | ROGUE WAVE PATTERNS UNDER A LARGE PARAMETER IN THE MANAKOV AND THREE-WAVE SYSTEMS

Now, we consider solution patterns of Q-type and R-type rogue waves in the Manakov and three-wave-interaction systems when a single complex internal parameter a_m in them is large (in magnitude), where $2 \le m \le 3N - 1$ for Q-type, and $2 \le m \le 3N - 2$ for R-type. In both cases, $m \bmod 3 \ne 0$.

3.1 | Rogue-pattern results in the Manakov system

Our results on patterns of Q-type and R-type rogue waves in the Manakov system under a large internal parameter are summarized in the following two theorems.

Theorem 5. *For the Q-type Nth-order rogue wave $[u_{1,N,0}(x,t), u_{2,N,0}(x,t)]$ in the Manakov system, suppose $|a_m| \gg 1$ and all other internal parameters are $O(1)$. In addition, suppose all nonzero roots of $Q_N^{[m]}(z)$ are simple. Then, the following asymptotics for this rogue wave holds.*

1. *In the outer region on the (x,t) plane, where $\sqrt{x^2 + t^2} = O(|a_m|^{1/m})$, this rogue wave asymptotically separates into M_Q isolated fundamental rogue waves, where M_Q is given in Equation (18). These fundamental rogue waves are $[\hat{u}_1(x - \hat{x}_0, t - \hat{t}_0)\, e^{\mathrm{i}(k_1 x + \omega_1 t)},\ \hat{u}_2(x - \hat{x}_0, t - \hat{t}_0)\, e^{\mathrm{i}(k_2 x + \omega_2 t)}]$, where $[\hat{u}_1(x,t), \hat{u}_2(x,t)]$ are given in Equations (71)–(72), and their positions $(\hat{x}_0, \hat{t}_0)$ are given by*

$$\hat{x}_0 = \frac{1}{\Re(p_0)}\Re\left[\frac{p_0^*}{p_1}\left(z_0 a_m^{1/m} - \Delta_Q\right)\right], \tag{78}$$

$$\hat{t}_0 = \frac{1}{2\Re(p_0)}\Im\left[\frac{1}{p_1}\left(z_0 a_m^{1/m} - \Delta_Q\right)\right], \tag{79}$$

where $\Re$ and $\Im$ represent the real and imaginary parts of a complex number, z_0 is each of the M_Q nonzero simple roots of $Q_N^{[m]}(z)$, and Δ_Q is a z_0-dependent $O(1)$ quantity whose formula will be given by Equation (126) in later text. The error of this fundamental rogue wave approximation is $O(|a_m|^{-1/m})$. Expressed mathematically, when $|a_m| \gg 1$ and $(x-\hat{x}_0)^2 + (t-\hat{t}_0)^2 = O(1)$, we have the following solution asymptotics:

$$\begin{aligned} u_{1,N,0}(x,t) &= \hat{u}_1(x-\hat{x}_0, t-\hat{t}_0)\, e^{\mathrm{i}(k_1 x+\omega_1 t)} + O(|a_m|^{-1/m}), \\ u_{2,N,0}(x,t) &= \hat{u}_2(x-\hat{x}_0, t-\hat{t}_0)\, e^{\mathrm{i}(k_2 x+\omega_2 t)} + O(|a_m|^{-1/m}). \end{aligned} \tag{80}$$

2. *If zero is a root of the Okamoto-hierarchy polynomial $Q_N^{[m]}(z)$, then in the neighborhood of the origin (the inner region), where $x^2+t^2 = O(1)$, $[u_{1,N,0}(x,t), u_{2,N,0}(x,t)]$ is approximately a lower (N_{1Q}, N_{2Q})th-order rogue wave $[u_{1,N_{1Q},N_{2Q}}(x,t), u_{2,N_{1Q},N_{2Q}}(x,t)]$ as given in Theorem 3, where (N_{1Q}, N_{2Q}) are provided in Theorem 1. Internal parameters $(\hat{a}_{1,1}, \hat{a}_{2,1}, \hat{a}_{4,1}, \hat{a}_{5,1}, \dots, \hat{a}_{3N_{1Q}-1,1})$ and $(\hat{a}_{1,2}, \hat{a}_{2,2}, \hat{a}_{4,2}, \hat{a}_{5,2}, \dots, \hat{a}_{3N_{2Q}-2,2})$ in this lower order rogue wave are related to those in the original rogue wave as*

$$\hat{a}_{j,1} = \hat{a}_{j,2} = a_j, \quad j = 1, 2, 4, 5, \dots. \tag{81}$$

The error of this lower order rogue wave approximation is $O(|a_m|^{-1})$. Expressed mathematically, when $|a_m| \gg 1$ and $x^2+t^2 = O(1)$,

$$\begin{aligned} u_{1,N,0}(x,t;a_2,a_4,a_5,\dots) &= u_{1,N_{1Q},N_{2Q}}(x,t;\hat{a}_{j,1},\hat{a}_{j,2}, j=1,2,4,5,\dots) + O(|a_m|^{-1}), \\ u_{2,N,0}(x,t;a_2,a_4,a_5,\dots) &= u_{2,N_{1Q},N_{2Q}}(x,t;\hat{a}_{j,1},\hat{a}_{j,2}, j=1,2,4,5,\dots) + O(|a_m|^{-1}). \end{aligned} \tag{82}$$

If zero is not a root of $Q_N^{[m]}(z)$, then in the inner region, the solution $[u_{1,N,0}(x,t), u_{2,N,0}(x,t)]$ approaches the uniform background $[\rho_1 e^{\mathrm{i}(k_1 x+\omega_1 t)}, \rho_1 e^{\mathrm{i}(k_2 x+\omega_2 t)}]$ when $|a_m| \gg 1$.

Theorem 6. *For the R-type Nth-order rogue wave $[u_{1,0,N}(x,t), u_{2,0,N}(x,t)]$ in the Manakov system, suppose $|a_m| \gg 1$ and all other internal parameters are $O(1)$. In addition, suppose all nonzero roots of $R_N^{[m]}(z)$ are simple. Then, the following asymptotics for this rogue wave holds.*

1. *In the outer region, where $\sqrt{x^2+t^2} = O(|a_m|^{1/m})$, this rogue wave asymptotically separates into M_R-isolated fundamental rogue waves, where M_R is given in Equation (18). These fundamental rogue waves are $[\hat{u}_1(x-\hat{x}_0, t-\hat{t}_0)\, e^{\mathrm{i}(k_1 x+\omega_1 t)}, \hat{u}_2(x-\hat{x}_0, t-\hat{t}_0)\, e^{\mathrm{i}(k_2 x+\omega_2 t)}]$, where $[\hat{u}_1(x,t), \hat{u}_2(x,t)]$ are given in Equations (71)–(72), and their positions $(\hat{x}_0, \hat{t}_0)$ are given by*

$$\hat{x}_0 = \frac{1}{\Re(p_0)}\Re\left[\frac{p_0^*}{p_1}\left(z_0 a_m^{1/m} - \Delta_R\right)\right], \tag{83}$$

$$\hat{t}_0 = \frac{1}{2\Re(p_0)}\Im\left[\frac{1}{p_1}\left(z_0 a_m^{1/m} - \Delta_R\right)\right], \tag{84}$$

where z_0 is each of the M_R nonzero simple roots of $R_N^{[m]}(z)$, and Δ_R is a z_0-dependent $O(1)$ quantity given by Equation (147) in later text. The error of this fundamental rogue wave approximation is $O(|a_m|^{-1/m})$. Expressed mathematically, when $|a_m| \gg 1$ and $(x-\hat{x}_0)^2 + (t-\hat{t}_0)^2 = O(1)$, we

have the following solution asymptotics:

$$\begin{aligned} u_{1,0,N}(x,t) &= \hat{u}_1(x-\hat{x}_0, t-\hat{t}_0)\, e^{\mathrm{i}(k_1 x+\omega_1 t)} + O(|a_m|^{-1/m}), \\ u_{2,0,N}(x,t) &= \hat{u}_2(x-\hat{x}_0, t-\hat{t}_0)\, e^{\mathrm{i}(k_2 x+\omega_2 t)} + O(|a_m|^{-1/m}). \end{aligned} \tag{85}$$

2. *If zero is a root of the Okamoto-hierarchy polynomial $R_N^{[m]}(z)$, then in the inner region, where $x^2+t^2=O(1)$, $[u_{1,0,N}(x,t), u_{2,0,N}(x,t)]$ is approximately a lower (N_{1R}, N_{2R})th-order rogue wave $[u_{1,N_{1R},N_{2R}}(x,t),\ u_{2,N_{1R},N_{2R}}(x,t)]$ as given in Theorem 3, where (N_{1R}, N_{2R}) are provided in Theorem 2. Internal parameters $(\hat{a}_{1,1}, \hat{a}_{2,1}, \hat{a}_{4,1}, \hat{a}_{5,1}, \dots, \hat{a}_{3N_{1R}-1,1})$ and $(\hat{a}_{1,2}, \hat{a}_{2,2}, \hat{a}_{4,2}, \hat{a}_{5,2}, \dots, \hat{a}_{3N_{2R}-2,2})$ in this lower order rogue wave are related to those in the original rogue wave as*

$$\hat{a}_{j,1} = \hat{a}_{j,2} = a_j, \quad j = 1, 2, 4, 5, \dots. \tag{86}$$

The error of this lower order rogue wave approximation is $O(|a_m|^{-1})$. Expressed mathematically, when $|a_m| \gg 1$ and $x^2+t^2=O(1)$,

$$\begin{aligned} u_{1,0,N}(x,t;a_2,a_4,a_5,\dots) &= u_{1,N_{1R},N_{2R}}(x,t;\hat{a}_{j,1},\hat{a}_{j,2}, j=1,2,4,5,\dots) + O(|a_m|^{-1}), \\ u_{2,0,N}(x,t;a_2,a_4,a_5,\dots) &= u_{2,N_{1R},N_{2R}}(x,t;\hat{a}_{j,1},\hat{a}_{j,2}, j=1,2,4,5,\dots) + O(|a_m|^{-1}). \end{aligned} \tag{87}$$

If zero is not a root of $R_N^{[m]}(z)$, then in the inner region, the solution $[u_{1,0,N}(x,t), u_{2,0,N}(x,t)]$ approaches the uniform background $[\rho_1 e^{\mathrm{i}(k_1 x+\omega_1 t)}, \rho_1 e^{\mathrm{i}(k_2 x+\omega_2 t)}]$ when $|a_m| \gg 1$.

Theorems 5 and 6 show that when the internal parameter $|a_m|$ is large, then in the outer region, patterns of Q- and R-type Manakov rogue waves comprise isolated fundamental rogue waves, which are the same with each other, except for their locations that are determined by root structures of $Q_N^{[m]}(z)$ and $R_N^{[m]}(z)$ polynomials through formulae (78)–(79) and (83)–(84). To the leading order of these positions, that is, to $O(|a_m|^{1/m})$, rogue patterns formed by these fundamental rogue waves are linear transformations of the underlying root structures. However, the next-order corrections of size $O(1)$ to these leading-order terms, induced by Δ_Q and Δ_R in Equations (78)–(79) and (83)–(84), depend on the root z_0 in a nonlinear way (see Equations (126) and (147) in later text). These next-order nonlinear corrections will introduce deformations to rogue patterns and make them look different from linear transformations of root structures, as we will see graphically in the next section. This behavior contrasts rogue patterns reported in Refs. [54, 55] for some other types of rogue waves, where those patterns are just linear transformations of root structures of the Yablonskii–Vorob'ev polynomial hierarchy, even after next-order position corrections are included. We do note, though, that these nonlinear deformations of rogue patterns in the present case are subdominant compared to the leading-order term, and will become less significant as $|a_m|$ gets larger. In other words, as $|a_m|$ increases, rogue patterns for Q- and R-type Manakov rogue waves will look more and more like the linear transformation of root structures of $Q_N^{[m]}(z)$ and $R_N^{[m]}(z)$.

Theorems 5 and 6 also show that when the internal parameter $|a_m|$ is large, then in the inner region, the original rogue wave reduces to a lower order rogue wave, or to the uniform background, depending on whether zero is a root of $Q_N^{[m]}(z)$ or $R_N^{[m]}(z)$. If zero is a root, then its multiplicity will determine the order of this reduced rogue wave.

In these theorems, which element a_m in the internal parameter vector $(a_2, a_4, a_5, ...)$ is taken to be large has profound consequences on the prediction of rogue patterns. Once the index m of the large parameter a_m is fixed, that choice determines not only the size of the outer region and the convergence rates of predictions, but also the polynomial $Q_N^{[m]}(z)$ or $R_N^{[m]}(z)$ whose roots predict the locations of peaks of isolated fundamental rogue waves in the outer region. Since the outer region is of size $O(|a_m|^{1/m})$, we see that internal parameters a_m with lower index numbers m have a stronger effect on the solutions if the magnitudes of a_m are fixed.

It may be interesting to notice from these theorems that in the outer region, both the Q-type and R-type rogue waves, under a large internal parameter, split into a number of the lowest-order R-type rogue waves (the fundamental rogue waves) *only*, never to the lowest-order Q-type rogue waves. There are two ways to understand this. An intuitive way is that, as we have explained in Section 2.6, the lowest-order R-type rogue wave (with $N_1 = 0$ and $N_2 = 1$) is the fundamental rogue wave with degree-2 polynomials. The lowest-order Q-type rogue wave (with $N_1 = 1$ and $N_2 = 0$), however, is a ratio of degree-4 polynomials. This latter solution should be viewed as a composition of two fundamental rogue waves, and it would split up into two separate fundamental rogue waves when its internal parameter a_2 is large (see Figure 3). A mathematical way to understand this is that, as long as the nonzero roots in $Q_N^{[m]}(z)$ and $R_N^{[m]}(z)$ are simple, then under a large internal parameter, both the Q-type and R-type rogue waves in the outer region would reduce to ratios of degree-2 polynomials (see Section 5), which can only be the fundamental rogue waves, not the lowest-order Q-type rogue waves of degree-4 polynomials.

3.2 | Rogue-pattern results in the three-wave-interaction system

Our results on Q-type and R-type rogue patterns in the three-wave-interaction system under a large internal parameter are summarized in the following two theorems.

Theorem 7. *For the Q-type Nth-order rogue wave* $[u_{1,N,0}(x,t), u_{2,N,0}(x,t), u_{3,N,0}(x,t)]$ *in the three-wave resonant interaction system, suppose* $|a_m| \gg 1$ *and all other internal parameters are* $O(1)$*. In addition, suppose all nonzero roots of* $Q_N^{[m]}(z)$ *are simple. Then, the following asymptotics for this rogue wave holds.*

1. *In the outer region, where* $\sqrt{x^2+t^2} = O(|a_m|^{1/m})$*, this rogue wave asymptotically separates into* M_Q *isolated fundamental rogue waves, where* M_Q *is given in Equation (18). These fundamental rogue waves are* $[\hat{u}_1(x-\hat{x}_0, t-\hat{t}_0)\, e^{\mathrm{i}(k_1 x+\omega_1 t)}$, $\hat{u}_2(x-\hat{x}_0, t-\hat{t}_0)\, e^{\mathrm{i}(k_2 x+\omega_2 t)}$, $\hat{u}_3(x-\hat{x}_0, t-\hat{t}_0)\, e^{-\mathrm{i}[(k_1+k_2)x+(\omega_1+\omega_2)t]}]$*, where* $[\hat{u}_1(x,t), \hat{u}_2(x,t), \hat{u}_3(x,t)]$ *are given in Equation (77), and their positions* $(\hat{x}_0, \hat{t}_0)$ *are given by*

$$\hat{x}_0 = \frac{\Im\left[\frac{z_0 a_m^{1/m} - \hat{\Delta}_Q}{c_1\beta_1 - c_2\alpha_1}\right]}{\Im\left[\frac{\alpha_1-\beta_1}{c_1\beta_1-c_2\alpha_1}\right]}, \quad \hat{t}_0 = \frac{\Im\left[\frac{z_0 a_m^{1/m} - \hat{\Delta}_Q}{\alpha_1-\beta_1}\right]}{\Im\left[\frac{c_1\beta_1-c_2\alpha_1}{\alpha_1-\beta_1}\right]}, \tag{88}$$

where z_0 *is each of the* M_Q *nonzero simple roots of* $Q_N^{[m]}(z)$*,* (α_1, β_1) *are given in the expansions (60)–(61), and* $\hat{\Delta}_Q$ *is a* z_0*-dependent* $O(1)$ *quantity given by Equation (162) in later text. The error of this fundamental rogue wave approximation is* $O(|a_m|^{-1/m})$*. Expressed mathematically, when*

$|a_m| \gg 1$ and $(x-\hat{x}_0)^2 + (t-\hat{t}_0)^2 = O(1)$, we have the following solution asymptotics:

$$\begin{aligned} u_{1,N,0}(x,t) &= \hat{u}_1(x-\hat{x}_0, t-\hat{t}_0)\, e^{\mathrm{i}(k_1 x+\omega_1 t)} + O(|a_m|^{-1/m}), \\ u_{2,N,0}(x,t) &= \hat{u}_2(x-\hat{x}_0, t-\hat{t}_0)\, e^{\mathrm{i}(k_2 x+\omega_2 t)} + O(|a_m|^{-1/m}), \\ u_{3,N,0}(x,t) &= \hat{u}_3(x-\hat{x}_0, t-\hat{t}_0)\, e^{-\mathrm{i}[(k_1+k_2)x+(\omega_1+\omega_2)t]} + O(|a_m|^{-1/m}). \end{aligned} \tag{89}$$

2. *If zero is a root of the Okamoto-hierarchy polynomial $Q_N^{[m]}(z)$, then in the inner region, where $x^2+t^2 = O(1)$, $[u_{1,N,0}(x,t), u_{2,N,0}(x,t), u_{3,N,0}(x,t)]$ is approximately a lower (N_{1Q}, N_{2Q})th-order rogue wave $[u_{1,N_{1Q},N_{2Q}}(x,t), u_{2,N_{1Q},N_{2Q}}(x,t), u_{3,N_{1Q},N_{2Q}}(x,t)]$ as given in Theorem 4, where (N_{1Q}, N_{2Q}) are provided in Theorem 1. Internal parameters $(\hat{a}_{1,1}, \hat{a}_{2,1}, \hat{a}_{4,1}, \hat{a}_{5,1}, \dots, \hat{a}_{3N_{1Q}-1,1})$ and $(\hat{a}_{1,2}, \hat{a}_{2,2}, \hat{a}_{4,2}, \hat{a}_{5,2}, \dots, \hat{a}_{3N_{2Q}-2,2})$ in this lower order rogue wave are related to those in the original rogue wave as*

$$\hat{a}_{j,1} = \hat{a}_{j,2} = a_j, \quad j = 1, 2, 4, 5, \dots. \tag{90}$$

The error of this lower order rogue wave approximation is $O(|a_m|^{-1})$. Expressed mathematically, when $|a_m| \gg 1$ and $x^2+t^2 = O(1)$,

$$\begin{aligned} u_{1,N,0}(x,t;a_2,a_4,a_5,\dots) &= u_{1,N_{1Q},N_{2Q}}(x,t;\hat{a}_{j,1},\hat{a}_{j,2}, j=1,2,4,5,\dots) + O(|a_m|^{-1}), \\ u_{2,N,0}(x,t;a_2,a_4,a_5,\dots) &= u_{2,N_{1Q},N_{2Q}}(x,t;\hat{a}_{j,1},\hat{a}_{j,2}, j=1,2,4,5,\dots) + O(|a_m|^{-1}), \\ u_{3,N,0}(x,t;a_2,a_4,a_5,\dots) &= u_{3,N_{1Q},N_{2Q}}(x,t;\hat{a}_{j,1},\hat{a}_{j,2}, j=1,2,4,5,\dots) + O(|a_m|^{-1}). \end{aligned} \tag{91}$$

If zero is not a root of $Q_N^{[m]}(z)$, then in the inner region, the solution $[u_{1,N,0}(x,t), u_{2,N,0}(x,t), u_{3,N,0}(x,t)]$ approaches the uniform background $[\rho_1 e^{\mathrm{i}(k_1 x+\omega_1 t)}, \rho_2 e^{\mathrm{i}(k_2 x+\omega_2 t)}, \mathrm{i}\rho_3 e^{-\mathrm{i}[(k_1+k_2)x+(\omega_1+\omega_2)t]}]$ when $|a_m| \gg 1$.

Theorem 8. *For the R-type Nth-order rogue wave $[u_{1,0,N}(x,t), u_{2,0,N}(x,t), u_{3,0,N}(x,t)]$ in the three-wave resonant interaction system, suppose $|a_m| \gg 1$ and all other internal parameters are $O(1)$. In addition, suppose all nonzero roots of $R_N^{[m]}(z)$ are simple. Then, the following asymptotics for this rogue wave holds.*

1. *In the outer region, where $\sqrt{x^2+t^2} = O(|a_m|^{1/m})$, this rogue wave asymptotically separates into M_R isolated fundamental rogue waves, where M_R is given in Equation (18). These fundamental rogue waves are $[\hat{u}_1(x-\hat{x}_0, t-\hat{t}_0)\, e^{\mathrm{i}(k_1 x+\omega_1 t)}, \hat{u}_2(x-\hat{x}_0, t-\hat{t}_0)\, e^{\mathrm{i}(k_2 x+\omega_2 t)}, \hat{u}_3(x-\hat{x}_0, t-\hat{t}_0)\, e^{-\mathrm{i}[(k_1+k_2)x+(\omega_1+\omega_2)t]}]$, where $[\hat{u}_1(x,t), \hat{u}_2(x,t), \hat{u}_3(x,t)]$ are given in Equation (77), and their positions $(\hat{x}_0, \hat{t}_0)$ are given by*

$$\hat{x}_0 = \frac{\Im\left[\frac{z_0 a_m^{1/m} - \hat{\Delta}_R}{c_1\beta_1 - c_2\alpha_1}\right]}{\Im\left[\frac{\alpha_1-\beta_1}{c_1\beta_1-c_2\alpha_1}\right]}, \quad \hat{t}_0 = \frac{\Im\left[\frac{z_0 a_m^{1/m} - \hat{\Delta}_R}{\alpha_1-\beta_1}\right]}{\Im\left[\frac{c_1\beta_1-c_2\alpha_1}{\alpha_1-\beta_1}\right]}, \tag{92}$$

where z_0 is each of the M_R nonzero simple roots of $R_N^{[m]}(z)$, (α_1, β_1) are given in the expansions (60)–(61), and $\hat{\Delta}_R$ is a z_0-dependent $O(1)$ quantity given by Equation (165) in the later text. The error of this fundamental rogue wave approximation is $O(|a_m|^{-1/m})$. Expressed mathematically,

when $|a_m| \gg 1$ *and* $(x-\hat{x}_0)^2+(t-\hat{t}_0)^2 = O(1)$, *we have the following solution asymptotics:*

$$\begin{aligned} u_{1,0,N}(x,t) &= \hat{u}_1(x-\hat{x}_0, t-\hat{t}_0)\, e^{\mathrm{i}(k_1 x+\omega_1 t)} + O(|a_m|^{-1/m}),\\ u_{2,0,N}(x,t) &= \hat{u}_2(x-\hat{x}_0, t-\hat{t}_0)\, e^{\mathrm{i}(k_2 x+\omega_2 t)} + O(|a_m|^{-1/m}),\\ u_{3,0,N}(x,t) &= \hat{u}_3(x-\hat{x}_0, t-\hat{t}_0)\, e^{-\mathrm{i}[(k_1+k_2)x+(\omega_1+\omega_2)t]} + O(|a_m|^{-1/m}). \end{aligned} \tag{93}$$

2. *If zero is a root of the Okamoto-hierarchy polynomial* $R_N^{[m]}(z)$, *then in the inner region, where* $x^2+t^2 = O(1)$, $[u_{1,0,N}(x,t), u_{2,0,N}(x,t), u_{3,0,N}(x,t)]$ *is approximately a lower* (N_{1R}, N_{2R})*th-order rogue wave* $[u_{1,N_{1R},N_{2R}}(x,t), u_{2,N_{1R},N_{2R}}(x,t), u_{3,N_{1R},N_{2R}}(x,t)]$ *as given in Theorem 4, where* (N_{1R}, N_{2R}) *are provided in Theorem 2. Internal parameters* $(\hat{a}_{1,1}, \hat{a}_{2,1}, \hat{a}_{4,1}, \hat{a}_{5,1}, \dots, \hat{a}_{3N_{1R}-1,1})$ *and* $(\hat{a}_{1,2}, \hat{a}_{2,2}, \hat{a}_{4,2}, \hat{a}_{5,2}, \dots, \hat{a}_{3N_{2R}-2,2})$ *in this lower order rogue wave are related to those in the original rogue wave as*

$$\hat{a}_{j,1} = \hat{a}_{j,2} = a_j, \quad j = 1,2,4,5,\dots. \tag{94}$$

The error of this lower order rogue wave approximation is $O(|a_m|^{-1})$. *Expressed mathematically, when* $|a_m| \gg 1$ *and* $x^2+t^2 = O(1)$,

$$\begin{aligned} u_{1,0,N}(x,t;a_2,a_4,a_5,\dots) &= u_{1,N_{1R},N_{2R}}(x,t;\hat{a}_{j,1},\hat{a}_{j,2}, j=1,2,4,5,\dots) + O(|a_m|^{-1}),\\ u_{2,0,N}(x,t;a_2,a_4,a_5,\dots) &= u_{2,N_{1R},N_{2R}}(x,t;\hat{a}_{j,1},\hat{a}_{j,2}, j=1,2,4,5,\dots) + O(|a_m|^{-1}),\\ u_{3,0,N}(x,t;a_2,a_4,a_5,\dots) &= u_{3,N_{1R},N_{2R}}(x,t;\hat{a}_{j,1},\hat{a}_{j,2}, j=1,2,4,5,\dots) + O(|a_m|^{-1}). \end{aligned} \tag{95}$$

If zero is not a root of $R_N^{[m]}(z)$, *then in the inner region, the solution* $[u_{1,0,N}(x,t), u_{2,0,N}(x,t), u_{3,0,N}(x,t)]$ *approaches the uniform background* $[\rho_1 e^{\mathrm{i}(k_1 x+\omega_1 t)}, \rho_2 e^{\mathrm{i}(k_2 x+\omega_2 t)}, \mathrm{i}\rho_3 e^{-\mathrm{i}[(k_1+k_2)x+(\omega_1+\omega_2)t]}]$ *when* $|a_m| \gg 1$.

Similar to the Manakov case, patterns of Q- and R-type rogue waves in the three-wave-interaction system are linear transformations of root structures of $Q_N^{[m]}(z)$ and $R_N^{[m]}(z)$ to the leading order, but are nonlinear transformations of those root structures when the next-order position corrections are included. Most other comments we have made after Theorem 6 in the previous subsection are valid here as well.

Proofs of these four theorems will be presented in Section 5.

4 | COMPARISON BETWEEN ANALYTICAL PREDICTIONS AND TRUE ROGUE SOLUTIONS

In this section, we compare our analytical predictions of rogue patterns in Theorems 5–8 to true rogue solutions in the Manakov and three-wave-interaction systems.

4.1 | Comparison in the Manakov system

For the Manakov system, we choose background wave numbers $k_1 = -k_2 = 1/\sqrt{12}$. Then background amplitudes are obtained from conditions (24) as $\rho_1 = \rho_2 = \sqrt{2/3}$, and background wave frequencies can be obtained from Equations (21).

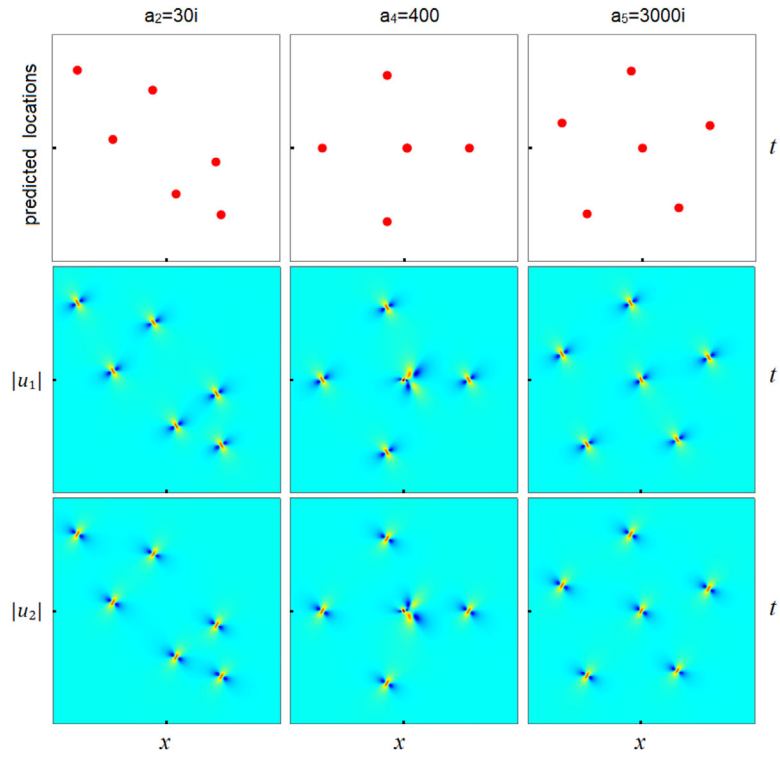

FIGURE 4 Predicted Q-type second-order Manakov rogue waves from Theorem 5. Each column is for a rogue wave with a single large parameter a_m, whose value is indicated on top, and all other internal parameters are set as zero. Top row: predicted $(\hat{x}_0, \hat{t}_0)$ locations by formulae (78)–(79) applied to all roots of $Q_2^{[m]}(z)$. Middle row: predicted $|u_1(x,t)|$. Bottom row: predicted $|u_2(x,t)|$. These $(|u_1|, |u_2|)$ predictions are assembled as $|u_k^{(p)}(x,t)| = |u_{k,N_{1Q},N_{2Q}}(x,t)| + \sum_{j=1}^{M_Q}(|\hat{u}_k(x-\hat{x}_0^{(j)}, t-\hat{t}_0^{(j)})| - \rho_k)$, where $k = 1, 2$, $u_{k,N_{1Q},N_{2Q}}(x,t)$ are the predicted inner solutions on the right sides of Equations (82), and $[\hat{x}_0^{(j)}, \hat{t}_0^{(j)}]$ are the predicted locations (78)–(79) of outer fundamental rogue waves in the top row (with $z_0 \neq 0$). In all panels, $-40 \leq x, t \leq 40$.

4.1.1 | Q-type

First, we consider Q-type Manakov rogue waves. Specifically, we take $N = 2$; thus, these are second-order waves with three internal parameters (a_2, a_4, a_5). We set one of these parameters large and the other parameters zero. Then, when that large parameter is chosen as one of

$$a_2 = 30\mathrm{i}, \quad a_4 = 400, \quad a_5 = 3000\mathrm{i}, \tag{96}$$

the three predicted rogue waves from Theorem 5 are displayed in the three columns of Figure 4, respectively. The top row of this figure shows the predicted $(\hat{x}_0, \hat{t}_0)$ locations by formulae (78)–(79) applied to all roots of $Q_2^{[m]}(z)$. In these formulae, $p_0 = 1/2$ from Equation (27), $(p_1, p_2) = (12^{-1/3}, 144^{-1/3})$ from Equation (39), and Δ_Q is calculated from Equation (126). Note that these $(\hat{x}_0, \hat{t}_0)$ predictions contain not only the dominant $O(|a_m|^{1/m})$ contribution, but also the subdominant $O(1)$ contribution.

According to Theorem 5, at each of the $(\hat{x}_0, \hat{t}_0)$ locations obtained from formulae (78)–(79) for nonzero roots of $Q_2^{[m]}(z)$, a fundamental Manakov rogue wave $[\hat{u}_1(x-\hat{x}_0,$

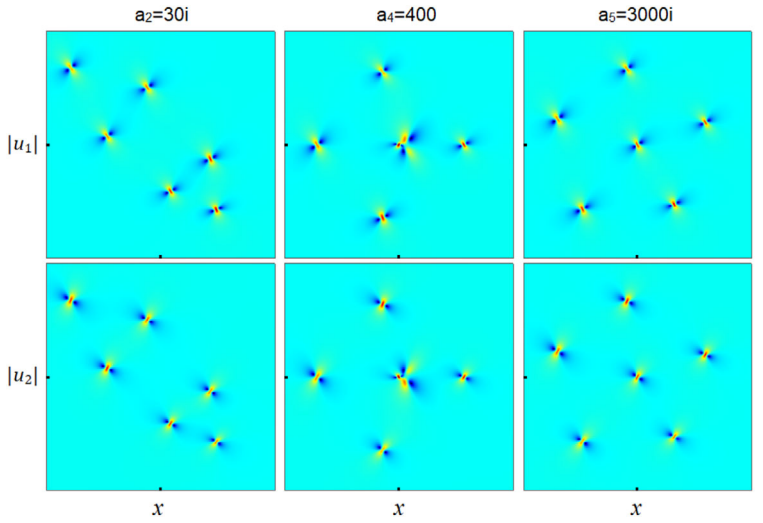

FIGURE 5 True Q-type second-order Manakov rogue waves for the same parameters and (x, t) intervals as in Figure 4.

$t - \hat{t}_0)\, e^{\mathrm{i}(k_1 x+\omega_1 t)}$, $\hat{u}_2(x - \hat{x}_0, t - \hat{t}_0)\, e^{\mathrm{i}(k_2 x+\omega_2 t)}]$ is predicted, where $[\hat{u}_1(x, t), \hat{u}_2(x, t)]$ are as given in Equations (71)–(72). The amplitude fields of these predicted fundamental rogue waves are plotted in the middle and bottom rows of Figure 4, respectively.

Theorem 5 also predicts that if zero is a root of $Q_2^{[m]}(z)$, as is the case for $m = 4$ and 5, then in the inner region, that is, the region near the $(\hat{x}_0, \hat{t}_0)$ location from formulae (78)–(79) with $z_0 = 0$, a lower (N_{1Q}, N_{2Q})th-order rogue wave would appear. These (N_{1Q}, N_{2Q}) values are calculated from Theorem 1 as

$$(N_{1Q}, N_{2Q}) = (0, 0),\ (1, 1),\ (0, 1), \tag{97}$$

for the three solutions in Figure 4, respectively. The first set (0,0) indicates that zero is not a root of $Q_2^{[2]}(z)$; hence, no lower order rogue wave in the inner region. The third set (0,1) indicates that the lower order rogue wave in the inner region is a fundamental rogue wave, wheeas the second set (1,1) indicates that the rogue wave in the inner region is a nonfundamental rogue wave. Internal parameters in these predicted lower (N_{1Q}, N_{2Q})th-order rogue waves are all zero, due to our choices of internal parameters in the original rogue waves and the s_j values shown in Equation (42). Plotting these (N_{1Q}, N_{2Q})th-order rogue waves, we get the center-region predictions in the middle and bottom rows of Figure 4.

Looking at these predicted rogue solutions in Figure 4, we see that the large-a_2 solution exhibits a skewed double-triangle, reminiscent of the double-triangle root structure of $Q_2^{[2]}(z)$ in Figure 1. The large-a_4 solution exhibits a square, reminiscent of the square-shaped root structure of $Q_2^{[4]}(z)$ in Figure 1. The large-a_5 solution exhibits a pentagon, reminiscent of the pentagon-shaped root structure of $Q_2^{[5]}(z)$ in Figure 1. This pentagon-shaped rogue pattern has been seen in the NLS and other equations before,[9–11,55] but the double-triangle and square patterns are new.

Now, we compare these predictions to true solutions. The corresponding true solutions are plotted directly from Theorem 3 and displayed in Figure 5. Comparing these true solution graphs with the predicted ones in Figure 4, they clearly match each other very well.

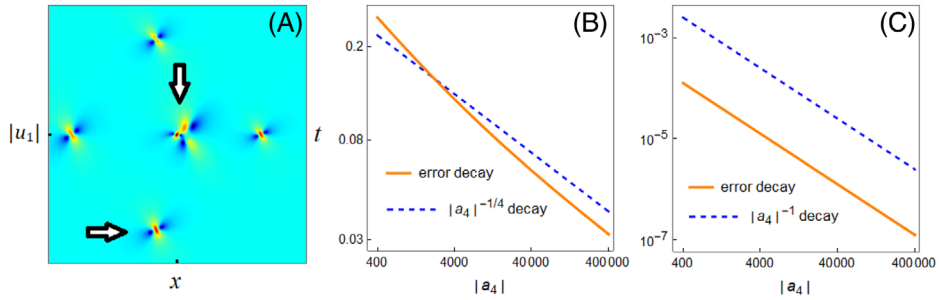

FIGURE 6 Decay of errors in our predictions of Theorem 5 for the outer and inner regions of the Q-type second-order Manakov rogue wave with various large real values of a_4, whereas the other internal parameters are set as zero. (A) $|u_1(x,t)|$ of the true rogue wave with $a_4 = 400$. (B) Decay of error versus a_4 for the outer fundamental rogue wave marked by the lower arrow in Panel (A), together with the $|a_4|^{-1/4}$ decay for comparison. (C) Decay of error versus a_4 at $x = t = 0$ of the inner region marked by the upper arrow in Panel (A), together with the $|a_4|^{-1}$ decay for comparison.

To quantitatively compare our prediction with the true solution and verify Theorem 5's error decay rates with the large parameter a_m, we choose a_4 to be the large parameter, corresponding to the second-column solution in Figures 4 and 5. For simplicity, we choose all a_4 to be real. As before, the other two internal parameters (a_2, a_5) in the rogue wave will be set as zero. We will vary this a_4 value, from 400 to 400000, and for each value, we measure the errors of our prediction in the outer and inner regions and then plot these errors versus a_4. In the outer region, this error is defined as the distance in the (x,t) plane between the predicted and true positions of the fundamental rogue wave marked by the lower arrow in Panel (A) of Figure 6. In the inner region, marked by the upper arrow in Panel (A), the error is defined as the magnitude of the difference between the predicted and true solution values at the origin $x = t = 0$. These error curves are plotted in Panels (B) and (C), for the outer and inner regions, respectively. For comparison, decay rates of $|a_4|^{-1/4}$ and $|a_4|^{-1}$ are also plotted in the corresponding panels. These error curves clearly show that the error decay rate is $|a_4|^{-1/4}$ in the outer region and $|a_4|^{-1}$ in the inner region, which fully agree with our theoretical predictions in Theorem 5.

4.1.2 | R-type

Next, we compare R-type rogue waves in the Manakov system. Here, we set $N = 3$. Thus, these are third-order waves with internal parameters (a_2, a_4, a_5, a_7). We choose one of these parameters large and the other parameters zero. Then, when that large parameter is chosen as one of

$$a_2 = 30\mathrm{i}, \quad a_4 = 300, \quad a_5 = 1000\mathrm{i}, \quad a_7 = 3000, \tag{98}$$

the four predicted rogue waves from Theorem 6 are displayed in the four columns of Figure 7, respectively. The top row of this figure shows the predicted $(\hat{x}_0, \hat{t}_0)$ locations by formulae (83)–(84) applied to all roots of $R_3^{[m]}(z)$. At each of the $(\hat{x}_0, \hat{t}_0)$ locations resulting from nonzero roots of $R_3^{[m]}(z)$, Theorem 6 predicts a fundamental Manakov rogue wave, whose amplitude fields are plotted in the middle and bottom rows of Figure 7, respectively. Our prediction for the center regions in these rows is based on Equation (87) of Theorem 6. In this prediction, the (N_{1R}, N_{2R})

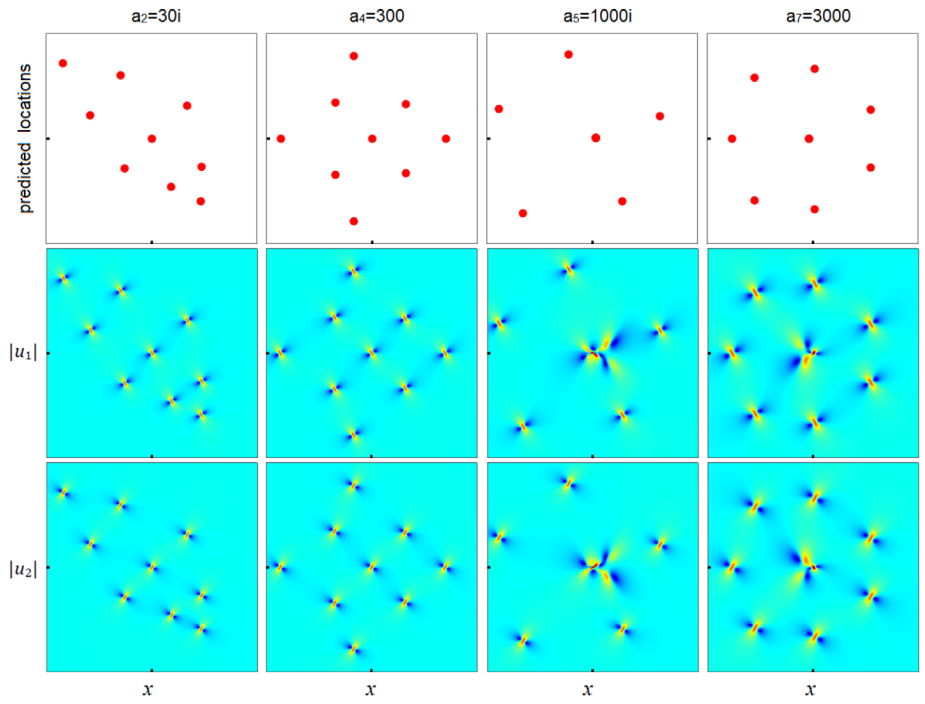

FIGURE 7 Predicted R-type third-order Manakov rogue waves from Theorem 6. Each column is for a rogue wave with a single large parameter a_m, whose value is indicated on top, and all other internal parameters are set as zero. Top row: predicted $(\hat{x}_0, \hat{t}_0)$ locations by formulae (83)–(84) applied to all roots of $R_3^{[m]}(z)$. Middle row: predicted $|u_1(x,t)|$. Bottom row: predicted $|u_2(x,t)|$. The (x,t) intervals in the four columns are $-46 \le x,t \le 46$, $-41 \le x,t \le 41$, $-35 \le x,t \le 35$, and $-28 \le x,t \le 28$, respectively.

values for these four rogue solutions are obtained from Theorem 2 as

$$(N_{1R}, N_{2R}) = (0,1),\ (0,1),\ (1,2),\ (1,0), \tag{99}$$

respectively. These values show that the center region of the first two rogue solutions hosts a fundamental rogue wave, whereas that region in the last two rogue solutions hosts a nonfundamental rogue wave. Internal parameters in these predicted lower (N_{1R}, N_{2R})th-order rogue waves of the center region are all zero, due to our choices of internal parameters in the original rogue waves as well as the s_j values shown in Equation (42). Plotting these (N_{1R}, N_{2R})th-order rogue waves from Theorem 3, we get the center-region predictions in the middle and bottom rows of Figure 7.

These predicted rogue solutions in Figure 7 exhibit various patterns, such as a skewed and deformed rhombus (first column), a deformed square (second column), a deformed pentagon (third column), and a heptagon (last column). Of these patterns, rhombus-shaped and square-shaped ones are new.

Now, we compare these predictions to true solutions. The corresponding true solutions are plotted directly from Theorem 3 and displayed in Figure 8. These true solutions clearly match the predicted ones in Figure 7 very well.

In addition to this visual agreement, we have also performed error analysis for predictions of these R-type waves, similar to what we have done for Q-type waves in Figure 6. This error analysis

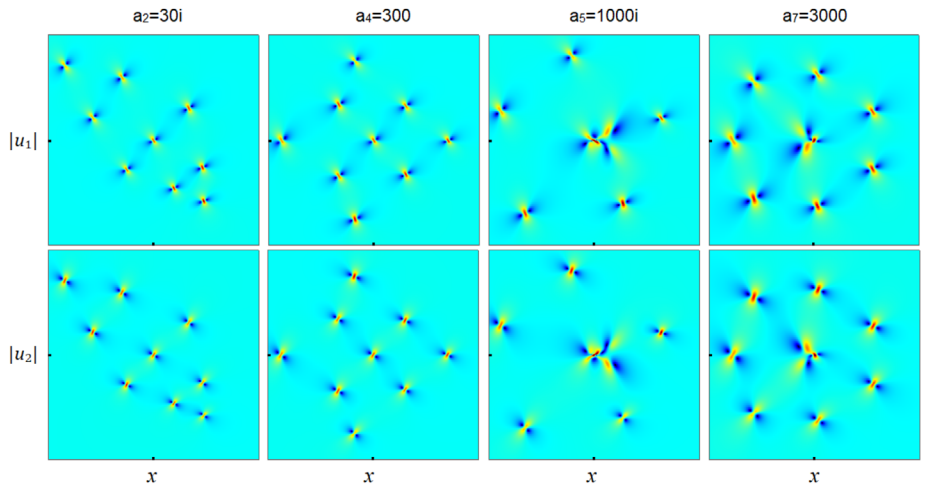

FIGURE 8 True R-type third-order Manakov rogue waves for the same parameters and (x, t) intervals as in Figure 7.

confirmed the error decay rates we predicted in Theorem 6 for the outer and inner regions. Details are omitted for brevity.

4.1.3 | Higher order Manakov rogue patterns

Rogue patterns we have seen in Figures 4–5 for $N = 2$ and Figures 7–8 for $N = 3$ are relatively simple. Using Theorems 5–6 and root structures of $Q_N^{[m]}(z)$ and $R_N^{[m]}(z)$ polynomials in Figures 1–2, we can predict more complex Manakov rogue patterns by increasing the order N.

As an example, we consider fourth-order R-type Manakov rogue waves. We take a single large parameter a_m as one of

$$a_2 = 40\mathrm{i}, \quad a_4 = 400, \quad a_5 = 3000\mathrm{i}, \quad a_7 = 60000, \tag{100}$$

and the other internal parameters are set as zero. Then, our predictions of $(\hat{x}_0, \hat{t}_0)$ from formulae (83)–(84) of Theorem 6 from roots of the $R_4^{[m]}(z)$ polynomials are plotted in the upper row of Figure 9. According to Theorem 6, each $(\hat{x}_0, \hat{t}_0)$ location away from the pattern center hosts a fundamental rogue wave. The $(\hat{x}_0, \hat{t}_0)$ location near the pattern center, generated by the zero root $z_0 = 0$ of $R_4^{[m]}(z)$ and appearing in the large-a_5 and a_7 panels only, signals a rogue wave of lower order (N_{1R}, N_{2R}), whose values are (0,1) and (2,2) for the large-a_5 and a_7 cases, respectively. This means that at the pattern center of large-a_5 and a_7 panels, a fundamental rogue wave and a nonfundamental (2,2)th-order rogue wave are predicted, respectively.

To verify these predictions, true solutions are plotted in the lower row of Figure 9. The agreement between predicted and true solutions is obvious.

Predictions and confirmations for higher-order Q-type Manakov rogue waves can also be obtained. In this case, a little caution is warranted. As one can see from Figure 1, a distinctive feature of some $Q_N^{[m]}(z)$ root structures is that some nonzero roots are extremely close to each other, see the $m = 4$ column with $N = 3$ and 4. When that happens, in order for our asymptotic theory to hold, the $|a_m|$ value would have to be chosen very large, so that the $(\hat{x}_0, \hat{t}_0)$ locations

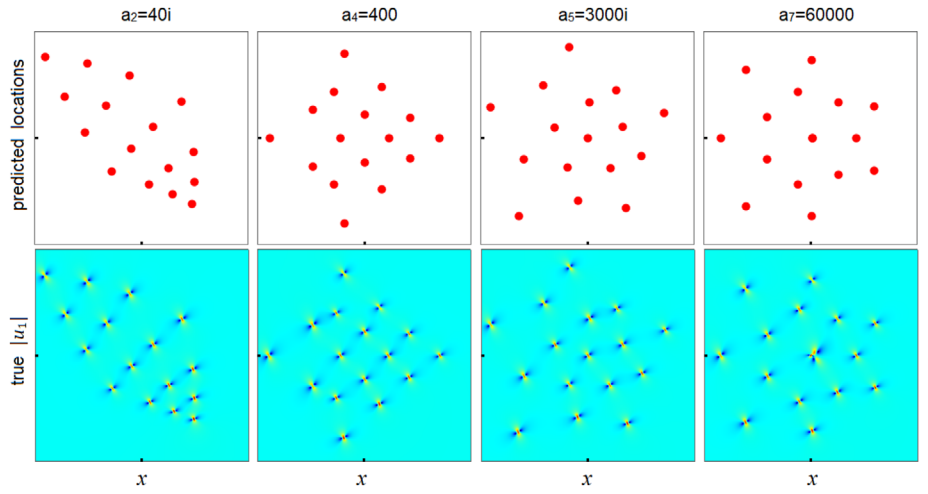

FIGURE 9 Comparison between predicted rogue patterns and true solutions for R-type fourth-order Manakov rogue waves with a single large parameter a_m, as shown on the top of each column, and other internal parameters are set as zero. Upper row: predicted $(\hat{x}_0, \hat{t}_0)$ locations by formulae (83)–(84) applied to all roots of $R_4^{[m]}(z)$. Lower row: true $|u_1(x,t)|$ solutions. In all panels, $-64 \le x, t \le 64$.

from formulae (83)–(84) for those extremely close roots can be well separated in the (x,t) plane in order for them to host an isolated fundamental rogue wave each.

4.1.4 | Effect of parameter size on rogue shapes

From the above comparisons, we have established that Manakov rogue patterns can be accurately predicted by root structures of Okamoto-hierarchy polynomials through mappings (78)–(79) and (83)–(84). The reader may have noticed that rogue shapes in the above figures are often twisted and less orderly, even though their corresponding root structures of Okamoto-hierarchy polynomials are very orderly. For example, in the R-type third-order rogue wave of Figures 7–8 with large a_4, the upper-left and lower-left sides of rogue patterns are strongly bent in, resulting in an irregular square, but the corresponding root structure of $R_3^{[4]}(z)$ in Figure 2 is like a regular square.

The reason for this irregularity in Manakov rogue patterns is apparently due to the next-order correction term in mappings (78)–(79) and (83)–(84) from the root structure of Okamoto-hierarchy polynomials to rogue peak positions in the (x,t) plane. While the leading term of $O(|a_m|^{1/m})$ in those formulae is a linear mapping, the next-order correction term of $O(1)$ is a nonlinear mapping in view of formulae (126) and (147). This nonlinear part of the mappings causes deformations in rogue shapes and makes them irregular even if the underlying root structures are.

It is important to recognize that this next-order correction term is subdominant, and its relative effect will get weaker when $|a_m|$ gets larger. Thus, if we increase $|a_m|$, this irregularity in rogue shape would diminish, and the rogue pattern would approach a linearly transformed root structure of Okamoto-hierarchy polynomials, which would be orderly if the underlying root structure is. To confirm this prediction, we take that R-type third-order rogue wave of Figures 7–8 with large a_4, and vary its a_4 value, with other internal parameters still set as zero. For three a_4 values of 30, 300, and 3000, predicted rogue locations $(\hat{x}_0, \hat{t}_0)$ from formulae (83)–(84) of Theorem 6 are

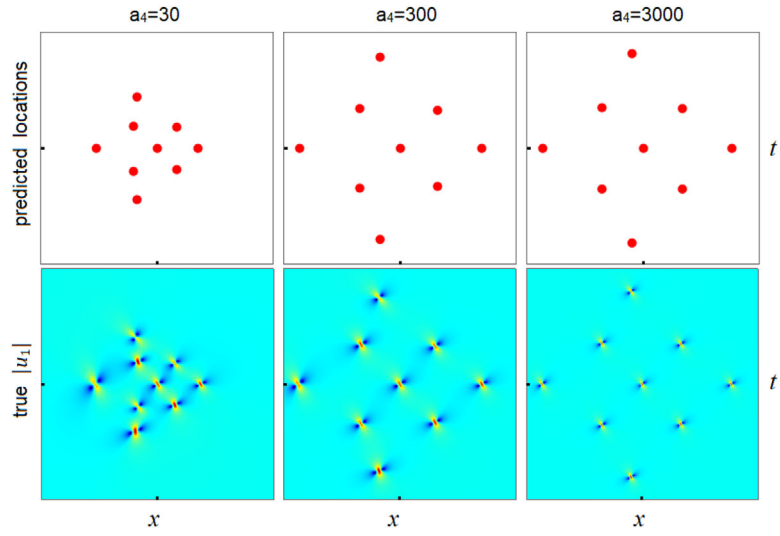

FIGURE 10 Effect of parameter size a_4 on R-type third-order Manakov rogue shapes (all other internal parameters are set as zero). Upper row: predicted $(\hat{x}_0, \hat{t}_0)$ locations by formulae (83)–(84) applied to all roots of $R_3^{[4]}(z)$. Lower row: true $|u_1(x,t)|$. The (x,t) intervals in the three columns are $-41 \le x,t \le 41$, $-41 \le x,t \le 41$, and $-70 \le x,t \le 70$, respectively.

plotted in the upper row of Figure 10, and true solutions (only the $|u_1|$ part) are plotted in the lower row. We see that when $a_4 = 30$, both the predicted and true solutions are highly irregular, almost random-like. But as a_4 increases to 300, this irregularity is significantly reduced and is visible only at the upper-left and lower-left sides of the figure. When a_4 further increases to 3000, this irregularity is almost completely gone, and the rogue shape closely resembles the root structure of $R_3^{[4]}(z)$ as shown in Figure 2.

4.2 | Comparison in the three-wave system

Now, we consider the three-wave system. We choose velocity values as $(c_1, c_2, c_3) = (1, 9/20, 0)$, and the first wave's background amplitude $\rho_1 = 1$. Then, the other two waves' background amplitudes can be derived from Equation (48) as $\rho_2 = 2\sqrt{5}/3$ and $\rho_3 = \sqrt{11}/3$ (we have taken the plus signs). Wave numbers and frequencies of the three background waves can be determined from Equation (45).

4.2.1 | Q-type

We first compare Q-type rogue waves of the three-wave system and set $N = 2$. Regarding their three internal parameters (a_2, a_4, a_5), we choose one of them large and the other two zero. Then, when that large parameter is taken as one of

$$a_2 = 40\mathrm{i}, \quad a_4 = 300, \quad a_5 = 3000\mathrm{i}, \tag{101}$$

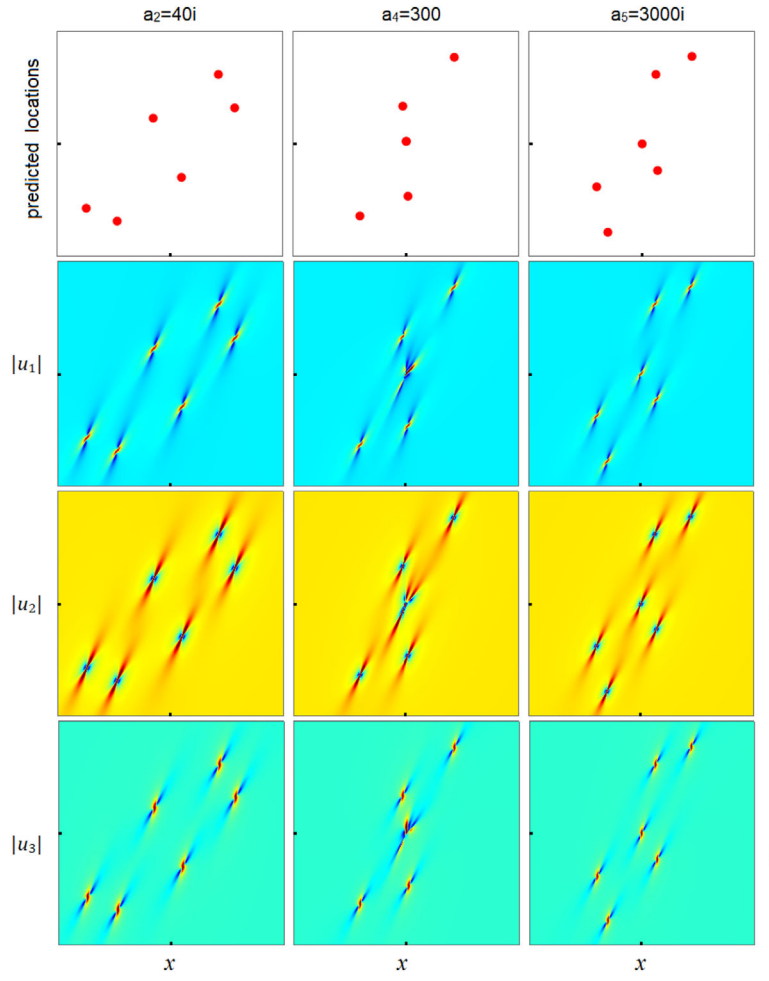

FIGURE 11 Predicted Q-type second-order rogue waves from Theorem 7 in the three-wave system. Each column shows a predicted rogue wave with a single large parameter a_m, whose value is indicated on top, and all other internal parameters are set as zero. First row: predicted $(\hat{x}_0, \hat{t}_0)$ locations from formulae (88) applied to all roots of $Q_2^{[m]}(z)$. Second row: predicted $|u_1(x,t)|$. Third row: predicted $|u_2(x,t)|$. Last row: predicted $|u_3(x,t)|$. The (x,t) intervals in the three columns are $-19 \le x,t \le 19$, $-23 \le x,t \le 23$, and $-25 \le x,t \le 25$, respectively.

the three predicted rogue waves from Theorem 7 are displayed in the three columns of Figure 11, respectively. The first row of this figure shows the predicted $(\hat{x}_0, \hat{t}_0)$ locations from formulae (88) applied to all roots of $Q_2^{[m]}(z)$. In these formulae, $(\alpha_1, \beta_1) \approx (-1.2632 + 1.8990\mathrm{i}, 0.4558 + 0.9195\mathrm{i})$ from the expansions (60)–(61), and $\hat{\Delta}_Q$ is calculated from Equation (162). At each of the $(\hat{x}_0, \hat{t}_0)$ locations resulting from nonzero roots of $Q_2^{[m]}(z)$, a fundamental rogue wave of the three-wave system is predicted. Our prediction for the center regions is based on Equation (91) of Theorem 7. In this prediction, the (N_{1Q}, N_{2Q}) values for these three rogue waves are the same as those given in Equation (97) earlier. Internal parameters in these predicted lower (N_{1Q}, N_{2Q})th-order rogue waves in the center region are all zero, due to our choices of internal parameters in the original rogue waves and the s_j values shown in Equation (67). These predictions for $(|u_1|, |u_2|, |u_3|)$ in the outer and inner regions are assembled together similar to that explained in the caption of Figure 4 and plotted in the second to fourth rows of Figure 11, respectively.

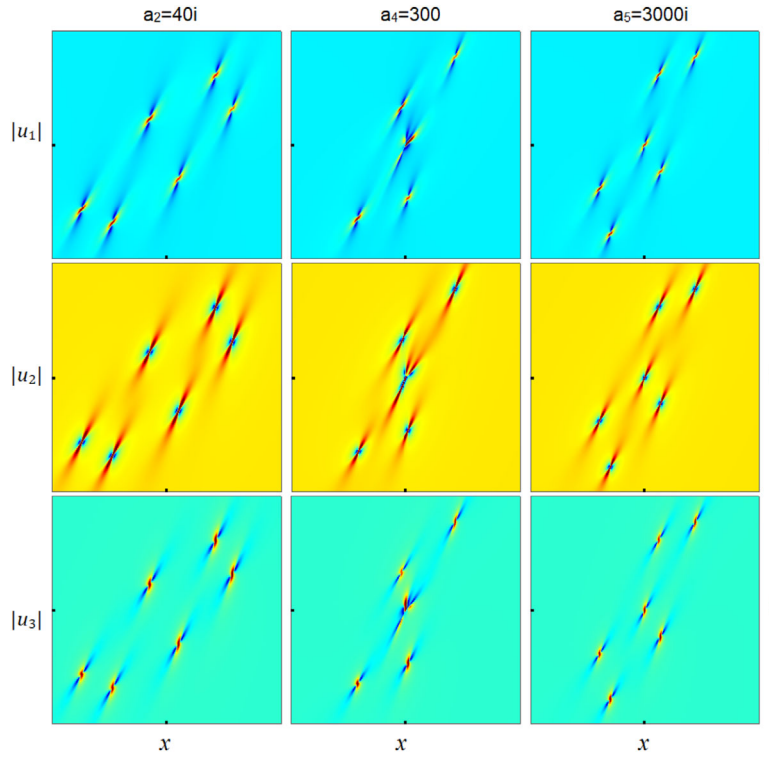

FIGURE 12 True Q-type second-order rogue waves of the three-wave system for the same parameters and (x, t) intervals as in Figure 11.

It is easy to see that these predicted rogue patterns in Figure 11, although being produced from the root structures of $Q_2^{[m]}(z)$ polynomials in Figure 1, look totally different from those root structures. The reason is the nonlinear mapping of the next-order correction term in formulae (88), which induces strong deformations to the linearly mapped result from the leading-order term in (88). These deformations, under our current velocity choices of (c_1, c_2, c_3), are much stronger than in the previous Manakov case, at comparable a_m values. As we have explained in Section 4.1.4 earlier, if we significantly increase the $|a_m|$ values, these deformations will become weaker, and rogue patterns will approach linearly transformed root structures of Okamoto-hierarchy polynomials and will thus be more recognizable.

To compare these predictions to true solutions, we plot in Figure 12 the corresponding true solutions from Theorem 4. It is easy to see that the agreement is excellent, confirming the validity of Theorem 7. This agreement also indicates that predictions from our Theorem 7 are highly accurate, even when rogue patterns are strongly deformed from Okamoto-hierarchy root structures.

4.2.2 | R-type

Next, we consider R-type rogue waves, and set $N = 3$. Regarding their internal parameters (a_2, a_4, a_5, a_7), we choose one of them large, and the others zero. Then, when that large parameter

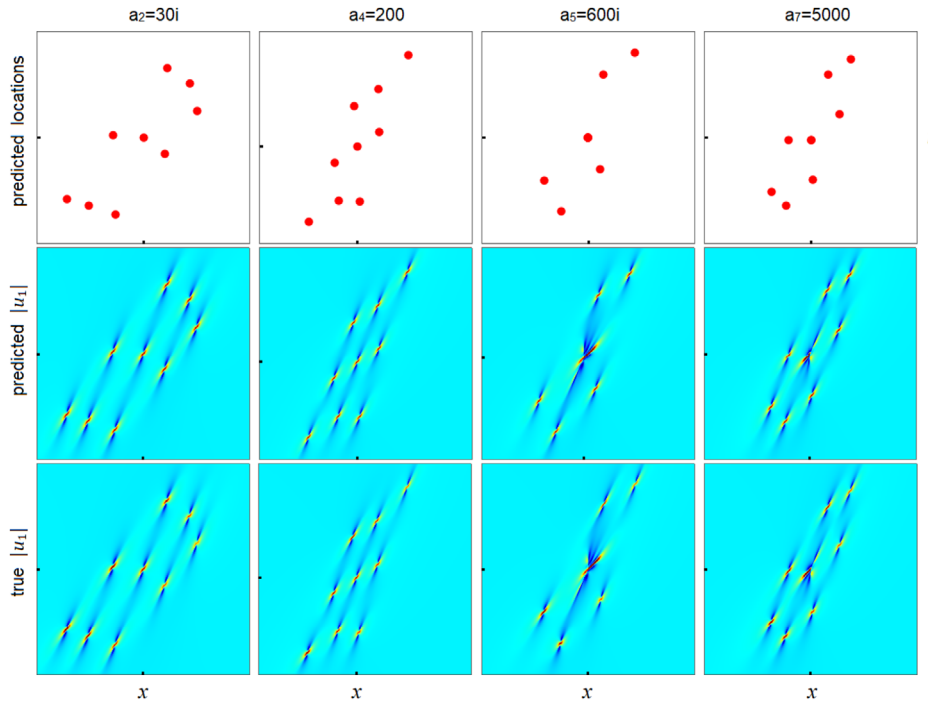

FIGURE 13 Comparison between predicted and true R-type third-order rogue waves of the three-wave system. Each column is for a rogue wave with a single large parameter a_m, whose value is indicated on top, and all other internal parameters are set as zero. Top row: predicted $(\hat{x}_0, \hat{t}_0)$ locations by formulae (92) applied to all roots of $R_3^{[m]}(z)$. Middle row: predicted $|u_1(x,t)|$. Third row: true $|u_1(x,t)|$. The (x,t) intervals in the four columns are $-21 \le x,t \le 21$, $-23 \le x,t \le 27$, $-24 \le x,t \le 24$, and $-23 \le x,t \le 23$, respectively.

a_m is taken as one of

$$a_2 = 30\mathrm{i}, \quad a_4 = 200, \quad a_5 = 600\mathrm{i}, \quad a_7 = 5000, \tag{102}$$

predicted rogue waves from Theorem 8 are displayed in the first two rows of Figure 13. The first row of this figure shows the predicted $(\hat{x}_0, \hat{t}_0)$ locations by formulae (92) applied to all roots of $R_3^{[m]}(z)$. The second row shows the predicted amplitude fields $|u_1|$ (the other two fields $|u_2|$ and $|u_3|$ are not shown for brevity). These amplitude fields in the outer region are predicted by the fundamental rogue waves in Theorem 8, and these fields in the inner region are predicted by the lower (N_{1R}, N_{2R})th-order rogue waves with all-zero internal parameters, and their (N_{1R}, N_{2R}) values are as given in Equation (99).

As in the earlier Q-case, predicted rogue patterns in Figure 13 also look very different from the underlying root structures of $R_3^{[m]}(z)$ polynomials in Figure 2.

In the bottom row of this same figure, the corresponding true solutions $|u_1|$ from Theorem 4 are plotted. Again, perfect agreement is seen between our prediction and the true solution, confirming the predictive power of our Theorem 8.

5 | PROOFS OF THEOREMS 5 TO 8

In this section, we prove Theorems 5–8 on rogue patterns in the Manakov and three-wave systems. Our proof is based on an asymptotic analysis of the two systems' rogue wave solutions, or equivalently, the determinant $\sigma_{n,k}$ in Equations (68)–(69), in the large $|a_m|$ limit.

Proof of Theorem 5 for the outer region. First, we use determinant identities and the Laplace expansion to rewrite $\sigma_{n,k}^{(Q)}$ in Equation (68) as[11]

$$\sigma_{n,k}^{(Q)} = \sum_{0\le\nu_1<\nu_2<\cdots<\nu_N\le 3N-1} \det_{1\le i,j\le N}\left[(h_0)^{\nu_j} S_{3i-1-\nu_j}(\boldsymbol{x}^+(n,k)+\nu_j \boldsymbol{s})\right] \times \det_{1\le i,j\le N}\left[(h_0^*)^{\nu_j} S_{3i-1-\nu_j}(\boldsymbol{x}^-(n,k)+\nu_j \boldsymbol{s}^*)\right], \tag{103}$$

where $h_0 = p_1/(p_0+p_0^*)$. We need to derive the asymptotics of this $\sigma_{n,k}^{(Q)}$ when $|a_m|$ is large and the other parameters $O(1)$. In this parameter regime, when (x,t) is in the outer region of $\sqrt{x^2+t^2} = O(|a_m|^{1/m})$, we have

$$S_j(\boldsymbol{x}^+(n,k)+\nu\boldsymbol{s}) = S_j(x_1^+, x_2^+, \nu s_3, x_4^+, x_5^+, \nu s_6, \dots, x_m^+ + \nu s_m, \dots) \sim S_j(\mathbf{v}), \tag{104}$$

where

$$\mathbf{v} = (p_1 x + 2p_0 p_1 \mathrm{i}t, 0, \dots, 0, a_m, 0, \dots). \tag{105}$$

Here, the fact of $s_1 = s_2 = s_4 = s_5 = 0$ from Equation (42) has been used.

Next, we see from the definition (22) of Schur polynomials that

$$\sum_{j=0}^{\infty} S_j(\mathbf{v})\epsilon^j = e^{\epsilon(p_1 x + 2p_0 p_1 \mathrm{i}t)+\epsilon^m a_m}. \tag{106}$$

Introducing the scaled variable $\hat{\epsilon} = \epsilon\, a_m^{1/m}$, we can write the right side of the above equation as $e^{\hat{\epsilon} z + \hat{\epsilon}^m}$, where

$$z = a_m^{-1/m}(p_1 x + 2p_0 p_1 \mathrm{i}t). \tag{107}$$

This $e^{\hat{\epsilon} z+\hat{\epsilon}^m}$ term is the same as the right side of Equation (6), except for a notational change of ϵ to $\hat{\epsilon}$. Using that Equation (6) with ϵ changed to $\hat{\epsilon}$ and combining the result with the above equation (106), we get

$$\sum_{j=0}^{\infty} S_j(\mathbf{v})\epsilon^j = \sum_{j=0}^{\infty} p_j^{[m]}(z)\hat{\epsilon}^j. \tag{108}$$

Then, recalling $\hat{\epsilon} = \epsilon\, a_m^{1/m}$, we arrive at the important relation

$$S_j(\mathbf{v}) = a_m^{j/m} p_j^{[m]}(z). \tag{109}$$

To proceed further, we notice that the highest order term of a_m in Equation (103) for $\sigma_{n,k}^{(Q)}$ comes from index choices of $\nu_j = j-1$. For these index choices, using the formulae (104) and (109), as

well as the definition of $Q_N^{[m]}(z)$ in Equation (7), we find that

$$\det_{1\le i,j\le N}\left[S_{3i-1-\nu_j}(\boldsymbol{x}^+(n,k)+\nu_j\boldsymbol{s})\right]=\det_{1\le i,j\le N}\left[S_{3i-j}\left(\boldsymbol{x}^+(n,k)+(j-1)\boldsymbol{s}\right)\right]\sim c_N^{-1}a_m^{N(N+1)/m}Q_N^{[m]}(z). \tag{110}$$

Similarly,

$$\det_{1\le i,j\le N}\left[S_{3i-1-\nu_j}(\boldsymbol{x}^-(n,k)+\nu_j\boldsymbol{s}^*)\right]\sim c_N^{-1}(a_m^*)^{N(N+1)/m}Q_N^{[m]}(z^*). \tag{111}$$

Thus,

$$\sigma_{n,k}^{(Q)}\sim|\alpha|^2\,|a_m|^{2N(N+1)/m}\left|Q_N^{[m]}(z)\right|^2, \tag{112}$$

where $\alpha=(h_0)^{N(N-1)/2}c_N^{-1}$. Since this leading-order asymptotics of $\sigma_{n,k}^{(Q)}$ is independent of n and k, it implies that, for $|a_m|\gg 1$, we would have $\sigma_{1,0}/\sigma_{0,0}\sim 1$ and $\sigma_{0,1}/\sigma_{0,0}\sim 1$, that is, the solution $[u_{1,N,0}(x,t),u_{2,N,0}(x,t)]$ would be on the uniform background $[\rho_1 e^{\mathrm{i}(k_1x+\omega_1t)},\rho_1 e^{\mathrm{i}(k_2x+\omega_2t)}]$, except when z is near a root z_0 of the polynomial $Q_N^{[m]}(z)$, where this leading-order asymptotics in (112) vanishes. In terms of x and t, this means that the solution $[u_{1,N,0}(x,t),u_{2,N,0}(x,t)]$ would be on the uniform background, except when (x,t) is in an $O(1)$ neighborhood of the location $(\tilde{x}_0,\tilde{t}_0)$, where

$$z_0=a_m^{-1/m}(p_1\tilde{x}_0+2\mathrm{i}p_0p_1\tilde{t}_0). \tag{113}$$

Such $(\tilde{x}_0,\tilde{t}_0)$ locations are the leading-order terms of $(\hat{x}_0,\hat{t}_0)$ in Equations (78)–(79) of Theorem 5. Due to the requirement of $\sqrt{x^2+t^2}=O(|a_m|^{1/m})$, z_0 should not be zero.

Next, we show that when (x,t) is in an $O(1)$ neighborhood of each of the $(\tilde{x}_0,\tilde{t}_0)$ locations given by Equation (113), the Q-type Manakov rogue wave $[u_{1,N,0}(x,t),u_{2,N,0}(x,t)]$ approaches a fundamental Manakov rogue wave that is located within $O(1)$ distance from $(\tilde{x}_0,\tilde{t}_0)$. In order to derive this more refined asymptotics, we need to calculate terms in Equation (103) whose order is lower than $|a_m|^{2N(N+1)/m}$, since that highest order term (112) vanishes at $(\tilde{x}_0,\tilde{t}_0)$.

First, we denote

$$\hat{x}_2^+(x,t)=p_2x+(2p_0p_2+p_1^2)(\mathrm{i}t), \tag{114}$$

which are the dominant terms of $x_2^+(x,t)$ in Equation (34) with the index "I" removed, when (x,t) is in the outer region. Then, for (x,t) in the neighborhood of $(\tilde{x}_0,\tilde{t}_0)$, we have a more refined asymptotics for $S_j(\boldsymbol{x}^+(n,k)+\nu\boldsymbol{s})$ as

$$\begin{aligned}S_j(\boldsymbol{x}^+(n,k)+\nu\boldsymbol{s})&=S_j(x_1^+,x_2^+,\nu s_3,x_4^+,x_5^+,\nu s_6,\ldots,x_m^++\nu s_m,\ldots)\\&=\left[S_j(\hat{\mathbf{v}})+\hat{x}_2^+(\tilde{x}_0,\tilde{t}_0)S_{j-2}(\hat{\mathbf{v}})\right]\left[1+O(|a_m|^{-2/m})\right],\ |a_m|\gg 1,\end{aligned} \tag{115}$$

where

$$\hat{\mathbf{v}}=\left(x_1^+,0,\ldots,0,a_m,0,\ldots\right)=(p_1x+2p_0p_1\mathrm{i}t+n\theta_1+k\lambda_1,0,\ldots,0,a_m,0,\ldots). \tag{116}$$

Here, the normalization of $a_1=0$ in x_1^+ has been used, and the second equation in (115) is obtained by using the definition (22) of Schur polynomials and splitting the $\boldsymbol{x}^+(n,k)+\nu\boldsymbol{s}$ vector into $\hat{\mathbf{v}}$ and

the rest. Polynomials $S_j(\hat{\mathbf{v}})$ are related to $p_j^{[m]}(z)$ in Equation (6) as

$$S_j(\hat{\mathbf{v}}) = a_m^{j/m} p_j^{[m]}(\hat{z}), \tag{117}$$

where $\hat{z} = a_m^{-1/m}(p_1 x + 2p_0 p_1 \mathrm{i} t + n\theta_1 + k\lambda_1)$.

Now, we derive leading order terms of a_m in Equation (103) when (x, t) is in the $O(1)$ neighborhood of $(\tilde{x}_0, \tilde{t}_0)$. These leading order terms come from two index choices, the first being $\boldsymbol{\nu} = (0, 1, \dots, N-1)$, and the second being $\boldsymbol{\nu} = (0, 1, \dots, N-2, N)$.

(i) With the first index choice, in view of Equations (115)–(117), dominant contributions to the first determinant involving $\boldsymbol{x}^+(n, k)$ in Equation (103) contain two parts. One part, coming from the $S_j(\hat{\mathbf{v}})$ term in Equation (115) for each element of that determinant, is

$$\alpha\, a_m^{N(N+1)/m} Q_N^{[m]}(\hat{z})\big[1 + O(|a_m|^{-2/m})\big], \tag{118}$$

where α is given below Equation (112). Expanding $Q_N^{[m]}(\hat{z})$ around $\hat{z} = z_0$, where z_0 is given in Equation (113), and recalling $Q_N^{[m]}(z_0) = 0$, we have

$$Q_N^{[m]}(\hat{z}) = a_m^{-1/m}[p_1(x - \tilde{x}_0) + 2p_0 p_1 \mathrm{i}(t - \tilde{t}_0) + n\theta_1 + k\lambda_1]\Big[Q_N^{[m]}\Big]'(z_0)\big[1 + O(|a_m|^{-1/m})\big]. \tag{119}$$

Inserting this equation into (118), this part of the contribution becomes

$$\alpha\, a_m^{[N(N+1)-1]/m}[p_1(x - \tilde{x}_0) + 2\mathrm{i}p_0 p_1(t - \tilde{t}_0) + n\theta_1 + k\lambda_1]\Big[Q_N^{[m]}\Big]'(z_0)\big[1 + O(|a_m|^{-1/m})\big]. \tag{120}$$

The other part of the contribution to the first determinant in Equation (103) comes from the $S_{j-2}(\hat{\mathbf{v}})$ term of (115) for each single column of that determinant and the $S_j(\hat{\mathbf{v}})$ term for the rest of the columns. This part of the contribution gives

$$\hat{x}_2^+(\tilde{x}_0, \tilde{t}_0) \sum_{j=1}^{N} \det_{1\le i\le N}\Big[S_{3i-1}(\hat{\mathbf{v}}), \dots, h_0^{j-1} S_{3i-j-2}(\hat{\mathbf{v}}), \dots, h_0^{N-1} S_{3i-N}(\hat{\mathbf{v}})\Big]\big[1 + O(|a_m|^{-1/m})\big]. \tag{121}$$

Here, the matrix of the determinant is $(h_0^{j-1} S_{3i-j}(\hat{\mathbf{v}}))_{1\le i,j\le N}$, except for its jth column, which is $h_0^{j-1} S_{3i-j-2}(\hat{\mathbf{v}})$ instead, that is, the index of the Schur polynomial in the jth column is reduced by two. Replacing $S_j(\hat{\mathbf{v}})$ by its leading-order term $S_j(\mathbf{v})$, utilizing the relation (109), and further replacing z by its leading-order term z_0, the above contribution reduces to

$$\alpha\, a_m^{[N(N+1)-2]/m} \hat{x}_2^+(\tilde{x}_0, \tilde{t}_0) \sum_{j=1}^{N} \det_{1\le i\le N}\Big[p_{3i-1}^{[m]}(z_0), \dots, p_{3i-j-2}^{[m]}(z_0), \dots, p_{3i-N}^{[m]}(z_0)\Big]\big[1 + O(|a_m|^{-1/m})\big]. \tag{122}$$

Since $\hat{x}_2^+(\tilde{x}_0, \tilde{t}_0) = O(|a_m|^{1/m})$, this contribution is of the same order as the previous contribution in Equation (120). Combining these two contributions, the first determinant involving

$\boldsymbol{x}^{+}(n,k)$ in Equation (103) is found to be

$$\alpha\, a_m^{[N(N+1)-1]/m}\left[p_1(x-\tilde{x}_0)+2p_0p_1\mathrm{i}(t-\tilde{t}_0)+n\theta_1+k\lambda_1+\Delta_Q\right]\left[Q_N^{[m]}\right]'(z_0)\left[1+O(|a_m|^{-1/m})\right], \tag{123}$$

where

$$\Delta_Q=\frac{\hat{x}_2^{+}(\tilde{x}_0,\tilde{t}_0)}{a_m^{1/m}}\frac{\sum_{j=1}^{N}\det_{1\le i\le N}\left[p_{3i-1}^{[m]}(z_0),\ldots,p_{3i-j-2}^{[m]}(z_0),\ldots,p_{3i-N}^{[m]}(z_0)\right]}{\left[Q_N^{[m]}\right]'(z_0)}. \tag{124}$$

Denoting $\varphi_m\equiv\arg(a_m^{1/m})$ and then using the $(\tilde{x}_0,\tilde{t}_0)$ expressions as obtained from Equation (113), we find that

$$\frac{\hat{x}_2^{+}(\tilde{x}_0,\tilde{t}_0)}{a_m^{1/m}}=\frac{p_2}{p_1}z_0+\frac{\mathrm{i}p_1^2}{2\Re(p_0)}\frac{\Im\left(z_0e^{\mathrm{i}\varphi_m}/p_1\right)}{e^{\mathrm{i}\varphi_m}}. \tag{125}$$

Thus,

$$\Delta_Q=\left(\frac{p_2}{p_1}z_0+\frac{\mathrm{i}p_1^2}{2\Re(p_0)}\frac{\Im\left(z_0e^{\mathrm{i}\varphi_m}/p_1\right)}{e^{\mathrm{i}\varphi_m}}\right)\frac{\sum_{j=1}^{N}\det_{1\le i\le N}\left[p_{3i-1}^{[m]}(z_0),\ldots,p_{3i-j-2}^{[m]}(z_0),\ldots,p_{3i-N}^{[m]}(z_0)\right]}{\left[Q_N^{[m]}\right]'(z_0)}. \tag{126}$$

Here, the determinant inside the summation of the above formula is the determinant of $Q_N^{[m]}(z_0)$, that is, $\det_{1\le i,j\le N}[p_{3i-j}^{[m]}(z_0)]$, except that the subindices of its jth column are reduced by two. This Δ_Q is an $O(1)$ quantity that is dependent on $m,N,z_0,\varphi_m,p_0,p_1$, and p_2. Absorbing this Δ_Q term into $(\tilde{x}_0,\tilde{t}_0)$ in Equation (123), we find that the contribution to the first determinant in Equation (103) under the first index choice of $\boldsymbol{\nu}=(0,1,\ldots,N-1)$ is

$$\alpha\, a_m^{[N(N+1)-1]/m}\left[p_1(x-\hat{x}_0)+2p_0p_1\mathrm{i}(t-\hat{t}_0)+n\theta_1+k\lambda_1\right]\left[Q_N^{[m]}\right]'(z_0)\left[1+O(|a_m|^{-1/m})\right], \tag{127}$$

where $(\hat{x}_0,\hat{t}_0)$ are given in Equations (78)–(79) of Theorem 5.

Similarly, the second determinant involving $\boldsymbol{x}^{-}(n,k)$ in Equation (103) under the first index choice of $\boldsymbol{\nu}=(0,1,\ldots,N-1)$ contributes the term

$$\alpha^*\,(a_m^*)^{[N(N+1)-1]/m}\left[p_1^*(x-\hat{x}_0)-2p_0^*p_1^*\mathrm{i}(t-\hat{t}_0)-n\theta_1^*-k\lambda_1^*\right]\left[Q_N^{[m]}\right]'(z_0^*)\left[1+O(|a_m|^{-1/m})\right]. \tag{128}$$

(ii) Under the second index choice of $\boldsymbol{\nu}=(0,1,\ldots,N-2,N)$ in Equation (103), the leading-order contribution to the first determinant involving $\boldsymbol{x}^{+}(n,k)$ can be calculated from the asymptotics (104) and the relation (109) as

$$h_0^{N(N-1)/2+1}a_m^{[N(N+1)-1]/m}\det_{1\le i\le N}\left[p_{3i-1}^{[m]}(z_0),p_{3i-2}^{[m]}(z_0),\ldots,p_{3i-(N-1)}^{[m]}(z_0),p_{3i-N-1}^{[m]}(z_0)\right]\left[1+O(|a_m|^{-1/m})\right]. \tag{129}$$

Recalling $p_{j-1}^{[m]}(z) = [p_j^{[m]}]'(z)$, the above contribution can be rewritten as

$$h_0 \alpha\, a_m^{[N(N+1)-1]/m} \left[Q_N^{[m]}\right]'(z_0)\left[1 + O(|a_m|^{-1/m})\right]. \tag{130}$$

Similarly, the second determinant involving $\boldsymbol{x}^-(n,k)$ in Equation (103) contributes

$$h_0^* \alpha^* (a_m^*)^{[N(N+1)-1]/m} \left[Q_N^{[m]}\right]'(z_0^*)\left[1 + O(|a_m|^{-1/m})\right]. \tag{131}$$

Summarizing the above contributions to Equation (103), we find that

$$\sigma_{n,k}^{(Q)}(x,t) = |\alpha|^2 \left|\left[Q_N^{[m]}\right]'(z_0)\right|^2 |a_m|^{[N(N+1)-1]/m} \times \left(\left[p_1(x-\hat{x}_0) + 2\mathrm{i}p_0 p_1 (t-\hat{t}_0) + n\theta_1 + k\lambda_1\right]\right.$$
$$\left. \times \left[p_1^*(x-\hat{x}_0) - 2\mathrm{i}p_0^* p_1^* (t-\hat{t}_0) - n\theta_1^* - k\lambda_1^*\right] + |h_0|^2\right)\left[1 + O(|a_m|^{-1/m})\right]. \tag{132}$$

Under our assumption of all nonzero roots of $Q_N^{[m]}(z)$ being simple, $[Q_N^{[m]}]'(z_0) \neq 0$. Thus, the above leading-order asymptotics for $\sigma_{n,k}^{(Q)}(x,t)$ does not vanish. It is easy to see that this expression of $\sigma_{n,k}^{(Q)}(x,t)$, combined with Equations (28)–(30), gives a fundamental rogue wave $[\hat{u}_1(x-\hat{x}_0, t-\hat{t}_0)\, e^{\mathrm{i}(k_1 x + \omega_1 t)},\ \hat{u}_2(x-\hat{x}_0, t-\hat{t}_0)\, e^{\mathrm{i}(k_2 x + \omega_2 t)}]$ as given in Theorem 5, and the error of this fundamental rogue wave prediction is $O(|a_m|^{-1/m})$. This completes the proof of Theorem 5 for the outer region. □

Proof of Theorem 5 for the inner region. To analyze the large-a_m behavior of Q-type Manakov rogue waves in the inner region, where $x^2 + t^2 = O(1)$, we first rewrite the $\sigma_{n,k}^{(Q)}$ determinant (68) into a $4N \times 4N$ determinant[11]

$$\sigma_{n,k}^{(Q)} = \begin{vmatrix} \mathbf{O}_{\mathbf{N}\times\mathbf{N}} & \Phi_{N\times 3N} \\ -\Psi_{3N\times N} & \mathbf{I}_{3N\times 3N} \end{vmatrix}, \tag{133}$$

where

$$\Phi_{i,j} = \left(\frac{p_1}{p_0 + p_0^*}\right)^{j-1} S_{3i-j}[\boldsymbol{x}^+(n,k) + (j-1)\boldsymbol{s}], \quad \Psi_{i,j} = \left(\frac{p_1^*}{p_0 + p_0^*}\right)^{i-1} S_{3j-i}[\boldsymbol{x}^-(n,k) + (i-1)\boldsymbol{s}^*]. \tag{134}$$

Defining $\boldsymbol{y}^\pm$ to be the vector $\boldsymbol{x}^\pm$ without the a_m term, that is, let

$$\boldsymbol{x}^+ = \boldsymbol{y}^+ + (0, \ldots, 0, a_m, 0, \ldots), \quad \boldsymbol{x}^- = \boldsymbol{y}^- + (0, \ldots, 0, a_m^*, 0, \ldots), \tag{135}$$

it is easy to see from the definition (22) of Schur polynomials that the Schur polynomials of $\boldsymbol{x}^\pm$ are related to those of $\boldsymbol{y}^\pm$ as

$$S_j(\boldsymbol{x}^+ + \nu\boldsymbol{s}) = \sum_{l=0}^{[j/m]} \frac{a_m^l}{l!} S_{j-lm}(\boldsymbol{y}^+ + \nu\boldsymbol{s}), \quad S_j(\boldsymbol{x}^- + \nu\boldsymbol{s}^*) = \sum_{l=0}^{[j/m]} \frac{(a_m^*)^l}{l!} S_{j-lm}(\boldsymbol{y}^- + \nu\boldsymbol{s}^*). \tag{136}$$

The reader is reminded that the notation of $[a]$ represents the largest integer less than or equal to a. Using these relations, we express matrix elements of Φ and Ψ in Equation (133) through Schur polynomials $S_j(\boldsymbol{y}^+ + \nu\boldsymbol{s})$, $S_j(\boldsymbol{y}^- + \nu\boldsymbol{s}^*)$, and powers of a_m and a_m^*.

Next, we perform row operations to the Φ matrix in order to remove certain power terms of a_m. For this purpose, we notice that when $m = 3j + 1$ ($j \geq 1$), coefficients of the highest a_m power terms in Φ's first column are proportional to

$$\hat{S}_2, \hat{S}_5, \ldots, \hat{S}_{3j-1}, \hat{S}_1, \hat{S}_4, \ldots, \hat{S}_{3j-2}, \hat{S}_0, \hat{S}_3, \ldots, \hat{S}_{3j}, \tag{137}$$

and repeating, where $\hat{S}_j \equiv S_j(\boldsymbol{y}^+ + \nu \boldsymbol{s})$. When $m = 3j + 2$ ($j \geq 0$), these coefficients of the highest a_m power terms in Φ's first column are proportional to

$$\hat{S}_2, \hat{S}_5, \ldots, \hat{S}_{3j-1}, \hat{S}_0, \hat{S}_3, \ldots, \hat{S}_{3j}, \hat{S}_1, \hat{S}_4, \ldots, \hat{S}_{3j+1}, \tag{138}$$

and repeating. In the second and higher columns of Φ, elements are of the same form as those in the first column, except that the index j of every $\hat{S}_j$ in them decreases by one with each higher column, and $\hat{S}_j \equiv 0$ for $j < 0$. Using the first m rows, we perform row operations to remove the highest powers of a_m from the second m rows, leaving the second highest power terms of a_m with coefficients proportional to $\hat{S}_{j+m}$, where $\hat{S}_j$ is the highest a_m-power coefficient of each element just being removed. Then, we use the first m rows and the resulting second m rows to eliminate the highest and second highest power terms of a_m from the third m rows, leaving the third highest power terms of a_m with coefficients proportional to $\hat{S}_{j+2m}$ in them. This process is continued to all later rows of Φ. Similar column operations are also applied to the matrix Ψ in Equation (133).

After these row and column operations, we then keep only the highest remaining power of a_m in each matrix element of Φ and the highest remaining power of a_m^* in each matrix element of Ψ. Using these manipulations and the sequence structures in Equations (137) and (138), for m mod 3 = 1 and 2, respectively, we find that $\sigma_{n,k}^{(Q)}$ in (133) is asymptotically reduced to

$$\sigma_{n,k}^{(Q)} = \widehat{\beta}\,|a_m|^{\widehat{K}} \begin{vmatrix} \mathbf{O}_{(\mathbf{N_{1Q}}+\mathbf{N_{2Q}})\times(\mathbf{N_{1Q}}+\mathbf{N_{2Q}})} & \widehat{\Phi}_{(N_{1Q}+N_{2Q})\times\widehat{N}} \\ -\widehat{\Psi}_{\widehat{N}\times(N_{1Q}+N_{2Q})} & \mathbf{I}_{\widehat{N}\times\widehat{N}} \end{vmatrix} \left[1 + O(|a_m|^{-1})\right], \tag{139}$$

where $\widehat{\beta}$ is an (m, N)-dependent nonzero constant, $\widehat{K}$ is an (m, N)-dependent positive integer, (N_{1Q}, N_{2Q}) are nonnegative integers given in Theorem 1, $\widehat{N} = \max(3N_{1Q}, 3N_{2Q} - 1)$,

$$\widehat{\Phi} = \begin{pmatrix} \widehat{\Phi}^{(1)}_{N_{1Q}\times\widehat{N}} \\ \\ \widehat{\Phi}^{(2)}_{N_{2Q}\times\widehat{N}} \end{pmatrix}, \quad \widehat{\Psi} = \begin{pmatrix} \widehat{\Psi}^{(1)}_{\widehat{N}\times N_{1Q}} & \widehat{\Psi}^{(2)}_{\widehat{N}\times N_{2Q}} \end{pmatrix}, \tag{140}$$

$$\widehat{\Phi}^{(I)}_{i,j} = (h_0)^{-(j-1)} S_{3i-I}\left[\boldsymbol{y}^+(n,k) + (j - 1 + \nu_0)\boldsymbol{s}\right], \tag{141}$$

$$\widehat{\Psi}^{(J)}_{i,j} = (h_0^*)^{-(i-1)} S_{3j-J}[\boldsymbol{y}^-(n,k) + (i - 1 + \nu_0)\boldsymbol{s}^*], \tag{142}$$

and $\nu_0 = N - N_{1Q} - N_{2Q}$. Since the constant factor $\widehat{\beta}\,|a_m|^{\widehat{K}}$ in (139) does not affect the Manakov solution and can be dropped, the remaining determinant in (139) can be rewritten as

$$\sigma_{n,k}^{(Q)} = \det \begin{pmatrix} \sigma_{n,k}^{[1,1]} & \sigma_{n,k}^{[1,2]} \\ \sigma_{n,k}^{[2,1]} & \sigma_{n,k}^{[2,2]} \end{pmatrix} \left[1 + O(|a_m|^{-1})\right], \tag{143}$$

$$\sigma_{n,k}^{[I,J]} = \left(\phi^{(n,k,I,J)}_{3i-I,\,3j-J}\right)_{1\leq i\leq N_{IQ},\,1\leq j\leq N_{JQ}}, \tag{144}$$

where the matrix elements in $\sigma_{n,k}^{[I,J]}$ are defined by

$$\phi_{i,j}^{(n,k,I,J)} = \sum_{\nu=0}^{\min(i,j)} \left[\frac{|p_1|^2}{(p_0+p_0^*)^2}\right]^{\nu} S_{i-\nu}\left(\boldsymbol{y}^{+}(n,k)+\nu_0\boldsymbol{s}+\nu\boldsymbol{s}\right) S_{j-\nu}(\boldsymbol{y}^{-}(n,k)+\nu_0\boldsymbol{s}^*+\nu\boldsymbol{s}^*). \quad (145)$$

The largest index j of S_j involved in the above reduced solution is $\max(3N_{1Q}-1, 3N_{2Q}-2)$. It is easy to see from Theorem 1 that $\max(3N_{1Q}-1, 3N_{2Q}-2) < m$. Thus, the above solution only depends on S_j polynomials with $j < m$, and hence, only depends on $y_j^{\pm}(n,k)$ with $j < m$. From the definition (135), we see that $y_j^{\pm}(n,k) = x_j^{\pm}(n,k)$ when $j < m$. This means that in Equation (145), $\boldsymbol{y}^{\pm}(n,k)$ can be replaced by $\boldsymbol{x}^{\pm}(n,k)$. Finally, we lump each constant $\nu_0 s_j$ into a_j of $x_j^{+}(n,k)$, and similarly lump each $\nu_0 s_j^*$ into a_j^* of $x_j^{-}(n,k)$. When $j \bmod 3 = 0$, $x_j^{\pm}(n,k) = 0$ per Theorem 3 and does not contain a_j. In such a case, we just lump $\nu_0 s_j$ into $x_j^{+}(n,k)$ and $\nu_0 s_j^*$ into $x_j^{-}(n,k)$, which eventually can be eliminated from the solution for the same reason we did in Equation (36) of Theorem 3. After these treatments, the above determinant in (143) becomes a (N_{1Q}, N_{2Q})th-order Manakov rogue wave $[u_{1,N_{1Q},N_{2Q}}(x,t), u_{2,N_{1Q},N_{2Q}}(x,t)]$ as given in Theorem 3, whose internal parameters $(\hat{a}_{1,1}, \hat{a}_{2,1}, \hat{a}_{4,1}, \hat{a}_{5,1}, \dots, \hat{a}_{3N_{1Q}-1,1})$ and $(\hat{a}_{1,2}, \hat{a}_{2,2}, \hat{a}_{4,2}, \hat{a}_{5,2}, \dots, \hat{a}_{3N_{2Q}-2,2})$ are related to those in the original rogue wave as

$$\hat{a}_{j,1} = \hat{a}_{j,2} = a_j + \nu_0 s_j, \quad j = 1, 2, 4, 5, \dots, \quad (146)$$

which is the same as the relation (81) in Theorem 5 since $s_j = 0$ for $j \bmod 3 \neq 0$ (see Remark 3 and Appendix D). The error of this lower order rogue wave approximation is $O(|a_m|^{-1})$ in view of Equation (143). This completes the proof of Theorem 5 for the inner region. □

Proof of Theorem 6. The proof of Theorem 6 for R-type Manakov rogue waves is very similar to that for Theorem 5. For that reason, we will only list the differences here.

In the outer region, due to the different matrix indices in Equation (69) for R-type rogue waves, the corresponding polynomials whose roots give leading-order locations of fundamental rogue waves are naturally R-type Okamoto hierarchy polynomials $R_N^{[m]}(z)$. The remaining difference is the calculation of the next-order position shift, that is, the formula for Δ_R in Equations (83)–(84). Repeating earlier calculations for the different R-type matrix indices, we can easily find that

$$\Delta_R = \left(\frac{p_2}{p_1}z_0 + \frac{\mathrm{i}p_1^2}{2\Re(p_0)}\frac{\Im\left(z_0 e^{\mathrm{i}\varphi_m}/p_1\right)}{e^{\mathrm{i}\varphi_m}}\right)\frac{\sum_{j=1}^{N}\det_{1\le i\le N}\left[p_{3i-1-1}^{[m]}(z_0), \dots, p_{3i-j-1-2}^{[m]}(z_0), \dots, p_{3i-N-1}^{[m]}(z_0)\right]}{\left[R_N^{[m]}\right]'(z_0)}. \quad (147)$$

Here, the determinant inside the summation of the above formula is the determinant of $R_N^{[m]}(z_0)$, that is, $\det_{1\le i,j\le N}[p_{3i-j-1}^{[m]}(z_0)]$, except that subindices of its jth column are reduced by two.

In the inner region, where $x^2+t^2 = O(1)$, we also rewrite the $\sigma_{n,k}^{(R)}$ determinant (69) into a $4N \times 4N$ determinant, and then use relations (136) to rewrite every matrix element of Φ and Ψ into powers of a_m and a_m^*, respectively. For R-type rogue waves, when $m = 3j+1$ $(j \ge 1)$, coefficients of the highest a_m power terms in Φ's first column are proportional to

$$\hat{S}_1, \hat{S}_4, \dots, \hat{S}_{3j-2}, \hat{S}_0, \hat{S}_3, \dots, \hat{S}_{3j}, \hat{S}_2, \hat{S}_5, \dots, \hat{S}_{3j-1}, \quad (148)$$

and repeating, and when $m = 3j + 2$ ($j \geq 0$), these coefficients are proportional to

$$\hat{S}_1, \hat{S}_4, \dots, \hat{S}_{3j+1}, \hat{S}_2, \hat{S}_5, \dots, \hat{S}_{3j-1}, \hat{S}_0, \hat{S}_3, \dots, \hat{S}_{3j}, \tag{149}$$

and repeating. Using these sequence structures and performing the same row and column operations as described earlier to remove certain high powers of a_m in the Φ and Ψ matrices, we find that $\sigma_{n,k}^{(R)}$ can be asymptotically reduced to (139)–(142), except that (N_{1Q}, N_{2Q}) are replaced by (N_{1R}, N_{2R}) as given in Theorem 2, and $(\widehat{\beta}, \widehat{K})$ are different constants. The rest of the proof is the same as before, and Theorem 6 is then proved. □

Proof of Theorem 7. The proof of Theorem 7 for Q-type rogue patterns in the three-wave-interaction system is very similar to that of Theorem 5 for the Manakov system. In the outer region where $\sqrt{x^2 + t^2} = O(|a_m|^{1/m})$ at large $|a_m|$,

$$S_j(\boldsymbol{x}^+(n,k) + \nu \boldsymbol{s}) = S_j(x_1^+, x_2^+, \nu s_3, x_4^+, x_5^+, \nu s_6, \dots, x_m^+ + \nu s_m, \dots) \sim S_j(\mathbf{v}), \tag{150}$$

where

$$\mathbf{v} = [(\alpha_1 - \beta_1)x + (c_1\beta_1 - c_2\alpha_1)t,\ 0, \dots, 0, a_m, 0, \dots]. \tag{151}$$

Following similar calculations as in the proof of Theorem 5, we find that the highest power term of a_m in $\sigma_{n,k}^{(Q)}$ of the three-wave system is

$$\sigma_{n,k}^{(Q)} \sim |\alpha|^2 \, |a_m|^{2N(N+1)/m} \left| Q_N^{[m]}(z) \right|^2, \tag{152}$$

where $\alpha = (h_0)^{N(N-1)/2} c_N^{-1}$, $h_0 = p_1/(p_0 + p_0^*)$, and

$$z = a_m^{-1/m}[(\alpha_1 - \beta_1)x + (c_1\beta_1 - c_2\alpha_1)t]. \tag{153}$$

Thus, the solution $[u_{1,N,0}(x,t), u_{2,N,0}(x,t), u_{3,N,0}(x,t)]$ would be on the uniform background (44), except at or near (x,t) locations $(\tilde{x}_0, \tilde{t}_0)$ where

$$z_0 = a_m^{-1/m}[(\alpha_1 - \beta_1)\tilde{x}_0 + (c_1\beta_1 - c_2\alpha_1)\tilde{t}_0] \tag{154}$$

is a root of the polynomial $Q_N^{[m]}(z)$, and such $(\tilde{x}_0, \tilde{t}_0)$ locations are the leading-order terms of $(\hat{x}_0, \hat{t}_0)$ in Equation (88) of Theorem 7.

We can further show that when (x,t) is in the $O(1)$ neighborhood of each of the $(\tilde{x}_0, \tilde{t}_0)$ locations given by Equation (154), the Q-type three-wave rogue solution approaches a fundamental rogue wave that is located within $O(1)$ distance from $(\tilde{x}_0, \tilde{t}_0)$. For this purpose, we denote

$$\hat{x}_2^+(x,t) = (\alpha_2 - \beta_2)x + (c_1\beta_2 - c_2\alpha_2)t, \tag{155}$$

which are the dominant terms of $x_2^+(x,t)$ in Equation (57) with the index "I" removed, when (x,t) is in the outer region. Then, for (x,t) in the $O(1)$ neighborhood of $(\tilde{x}_0, \tilde{t}_0)$, we have a more refined asymptotics for $S_j(\boldsymbol{x}^+(n,k) + \nu \boldsymbol{s})$ as

$$S_j(\boldsymbol{x}^+(n,k) + \nu \boldsymbol{s}) = \left[S_j(\hat{\mathbf{v}}) + \hat{x}_2^+(\tilde{x}_0, \tilde{t}_0) S_{j-2}(\hat{\mathbf{v}})\right] \left[1 + O(|a_m|^{-2/m})\right], \quad |a_m| \gg 1, \tag{156}$$

$$\hat{\mathbf{v}} = \left(x_1^+, 0, \dots, 0, a_m, 0, \dots\right), \tag{157}$$

$$x_1^+ = (\alpha_1 - \beta_1)x + (c_1\beta_1 - c_2\alpha_1)t + n\theta_1 + k\lambda_1. \tag{158}$$

Here, the normalization of $a_1 = 0$ has been utilized. Next, we again rewrite $\sigma_{n,k}^{(Q)}$ in Equation (68) as (103). Then the contribution to the first determinant in Equation (103) from the first index choice of $\nu_j = j - 1$ can be similarly calculated as

$$\begin{aligned} &\alpha\, a_m^{[N(N+1)-1]/m}\left[(\alpha_1 - \beta_1)(x - \tilde{x}_0) + (c_1\beta_1 - c_2\alpha_1)(t - \tilde{t}_0) + n\theta_1 + k\lambda_1 + \hat{\Delta}_Q\right] \\ &\times \left[Q_N^{[m]}\right]'(z_0)\left[1 + O(|a_m|^{-1/m})\right], \end{aligned} \tag{159}$$

where

$$\hat{\Delta}_Q = \frac{\hat{x}_2^+(\tilde{x}_0, \tilde{t}_0)}{a_m^{1/m}} \frac{\sum_{j=1}^N \det_{1\le i\le N}\left[p_{3i-1}^{[m]}(z_0), \dots, p_{3i-j-2}^{[m]}(z_0), \dots, p_{3i-N}^{[m]}(z_0)\right]}{\left[Q_N^{[m]}\right]'(z_0)}. \tag{160}$$

As in the definition of Δ_Q in Equation (126), the determinant inside the summation of the above $\hat{\Delta}_Q$ formula is the determinant of $Q_N^{[m]}(z_0)$, that is, $\det_{1\le i,j\le N}[p_{3i-j}^{[m]}(z_0)]$, except that indices of its jth column are reduced by two. Denoting $\varphi_m \equiv \arg(a_m^{1/m})$ as before, and using the $(\tilde{x}_0, \tilde{t}_0)$ expressions as obtained from Equation (154), we get

$$\frac{\hat{x}_2^+(\tilde{x}_0, \tilde{t}_0)}{a_m^{1/m}} = e^{-\mathrm{i}\varphi_m}\left[(\alpha_2 - \beta_2)\frac{\Im\left[\frac{z_0 e^{\mathrm{i}\varphi_m}}{c_1\beta_1 - c_2\alpha_1}\right]}{\Im\left[\frac{\alpha_1 - \beta_1}{c_1\beta_1 - c_2\alpha_1}\right]} + (c_1\beta_2 - c_2\alpha_2)\frac{\Im\left[\frac{z_0 e^{\mathrm{i}\varphi_m}}{\alpha_1 - \beta_1}\right]}{\Im\left[\frac{c_1\beta_1 - c_2\alpha_1}{\alpha_1 - \beta_1}\right]}\right]. \tag{161}$$

Thus,

$$\begin{aligned} \hat{\Delta}_Q = e^{-\mathrm{i}\varphi_m}&\left[(\alpha_2 - \beta_2)\frac{\Im\left[\frac{z_0 e^{\mathrm{i}\varphi_m}}{c_1\beta_1 - c_2\alpha_1}\right]}{\Im\left[\frac{\alpha_1 - \beta_1}{c_1\beta_1 - c_2\alpha_1}\right]} + (c_1\beta_2 - c_2\alpha_2)\frac{\Im\left[\frac{z_0 e^{\mathrm{i}\varphi_m}}{\alpha_1 - \beta_1}\right]}{\Im\left[\frac{c_1\beta_1 - c_2\alpha_1}{\alpha_1 - \beta_1}\right]}\right] \\ &\times \frac{\sum_{j=1}^N \det_{1\le i\le N}\left[p_{3i-1}^{[m]}(z_0), \dots, p_{3i-j-2}^{[m]}(z_0), \dots, p_{3i-N}^{[m]}(z_0)\right]}{\left[Q_N^{[m]}\right]'(z_0)}, \end{aligned} \tag{162}$$

which is an $O(1)$ quantity. Absorbing this $\hat{\Delta}_Q$ term into $(\tilde{x}_0, \tilde{t}_0)$ in Equation (159), we find that the contribution to the first determinant in Equation (103) under the first index choice of $\nu_j = j - 1$ is

$$\alpha\, a_m^{[N(N+1)-1]/m}\left[(\alpha_1 - \beta_1)(x - \hat{x}_0) + (c_1\beta_1 - c_2\alpha_1)(t - \hat{t}_0) + n\theta_1 + k\lambda_1\right]\left[Q_N^{[m]}\right]'(z_0)\left[1 + O(|a_m|^{-1/m})\right], \tag{163}$$

where $(\hat{x}_0, \hat{t}_0)$ are given in Equation (88) of Theorem 7. The contribution to the first determinant in Equation (103) under the second index choice of $\boldsymbol{\nu} = (0, 1, \dots, N-2, N)$ can be found the

same as that in Equation (130). Using these results and similar ones for the second determinant in Equation (103), we find that

$$\sigma_{n,k}^{(Q)}(x,t) = |\alpha|^2 \left| \left[Q_N^{[m]} \right]' (z_0) \right|^2 |a_m|^{[N(N+1)-1]/m}$$
$$\times \{ \left[(\alpha_1 - \beta_1)(x - \hat{x}_0) + (c_1\beta_1 - c_2\alpha_1)(t - \hat{t}_0) + n\theta_1 + k\lambda_1 \right]$$
$$\times \left[(\alpha_1^* - \beta_1^*)(x - \hat{x}_0) + (c_1\beta_1^* - c_2\alpha_1^*)(t - \hat{t}_0) - n\theta_1^* - k\lambda_1^* \right] + |h_0|^2 \} \left[1 + O(|a_m|^{-1/m}) \right]. \quad (164)$$

This expression of $\sigma_{n,k}^{(Q)}(x,t)$, combined with Equations (50)–(53), gives a fundamental rogue wave of the three-wave system as given in Theorem 7, and the error of this prediction is $O(|a_m|^{-1/m})$.

In the inner region, where $x^2 + t^2 = O(1)$, the proof for Theorem 7 is identical to that for Theorem 5. The reason is that Manakov rogue waves and three-wave ones in Theorems 3 and 4 have the same solution structures, except for minor differences in the $\boldsymbol{x}^{\pm}$ vectors, but the proof of Theorem 5 for the inner region does not rely on the contents of the $\boldsymbol{x}^{\pm}$ vectors. Theorem 7 is then proved. □

Proof of Theorem 8. In the outer region of R-type rogue waves in the three-wave system, following procedures very similar to that in the proof of Theorem 7, we can show that the solution separates into M_R isolated fundamental rogue waves, whose positions are given by Equation (92), with

$$\hat{\Delta}_R = e^{-i\varphi_m} \left[(\alpha_2 - \beta_2) \frac{\Im\left[\frac{z_0 e^{i\varphi_m}}{c_1\beta_1 - c_2\alpha_1}\right]}{\Im\left[\frac{\alpha_1 - \beta_1}{c_1\beta_1 - c_2\alpha_1}\right]} + (c_1\beta_2 - c_2\alpha_2) \frac{\Im\left[\frac{z_0 e^{i\varphi_m}}{\alpha_1 - \beta_1}\right]}{\Im\left[\frac{c_1\beta_1 - c_2\alpha_1}{\alpha_1 - \beta_1}\right]} \right]$$
$$\times \frac{\sum_{j=1}^{N} \det_{1\le i\le N} \left[p_{3i-1-1}^{[m]}(z_0), \ldots, p_{3i-j-1-2}^{[m]}(z_0), \ldots, p_{3i-N-1}^{[m]}(z_0) \right]}{\left[R_N^{[m]} \right]' (z_0)}. \quad (165)$$

As in the definition of Δ_R in Equation (147), the determinant inside the summation of the above $\hat{\Delta}_R$ formula is the determinant of $R_N^{[m]}(z_0)$, that is, $\det_{1\le i,j\le N}[p_{3i-j-1}^{[m]}(z_0)]$, except that indices of its jth column are reduced by two. The error of this fundamental rogue wave approximation is $O(|a_m|^{-1/m})$. The proof for the inner region is identical to that in the proof of Theorem 6. □

6 | CONCLUSION

In this article, we have reported new types of rogue patterns associated with Okamoto polynomial hierarchies in the Manakov and three-wave-interaction systems. These rogue patterns exhibit new shapes such as double triangles, rhombuses, and squares, and they arise when one of the internal free parameters in the rogue wave solutions gets large. The shapes of these patterns are analytically predicted from root structures of Okamoto-hierarchy polynomials through a mapping, which is linear to the leading order but nonlinear to the next order. Due to the nonlinear part of this mapping, rogue patterns are often deformed, sometimes strongly deformed, from Okamoto-hierarchy root structures. Our analytical predictions of rogue patterns have been compared to true solutions,

and excellent agreement has been observed, even when rogue patterns are strongly deformed from Okamoto-hierarchy root structures.

To put these results in perspective, let us recall rogue patterns associated with the Yablonskii–Vorob'ev polynomial hierarchy, which we reported earlier in Refs. [54, 55]. In those cases, rogue patterns were linear transformations of Yablonskii–Vorob'ev-hierarchy root structures, even when the next-order correction term was included. As a consequence, rogue patterns in Refs. [54, 55] were very recognizable from Yablonskii–Vorob'ev-hierarchy root structures. In the current Okamoto case, the associated rogue patterns are deformed from Okamoto-hierarchy root structures, because the mapping between them is nonlinear when the next-order correction term of size $O(1)$ is accounted for. These shape deformations may make the rogue pattern less recognizable from Okamoto-hierarchy root structures, unless the underlying parameter is very large so that the next-order nonlinear correction in the mapping becomes insignificant.

Although we have only demonstrated these Okamoto-hierarchy-related rogue patterns in the Manakov and three-wave-interaction systems, these patterns will definitely also arise in other integrable systems, as long as such systems admit rogue waves whose τ-function determinants can be expressed through Schur polynomials S_j with index jumps of 3. The reason is that such S_j polynomials, under a large internal parameter, can be related to Schur polynomials $p_j^{[m]}(z)$ defined in Equation (6) through a scaling (109) at the leading order. Since Okamoto-hierarchy polynomials are determinants of $p_j^{[m]}(z)$ polynomials with index jumps of three (see Equations (7)–(8)), rogue waves expressed as determinants of Schur polynomials S_j with index jumps of 3 then are naturally linked to Okamoto-hierarchy polynomials. In the Darboux transformation framework, rogue waves in the form of determinants of Schur polynomials with index jumps of 3 would arise when the underlying scattering matrix admits a triple eigenvalue. Many other integrable systems possess such rogue waves, such as the coupled Hirota equations[75] and the two-component long-wave-short-wave resonant interaction system.[76] Thus, rogue patterns we reported in this article will arise in all such systems and are universal as well.

In the end, we mention the connection of our rogue-pattern results to pole locations of rational solutions in Painlevé hierarchies. It is known that roots of the Yablonskii–Vorob'ev polynomial hierarchy give pole locations of rational solutions to the Painlevé-II hierarchy.[63] Thus, our earlier work in Refs. [54, 55] established a connection between rogue patterns and pole structures of the Painlevé-II hierarchy. In this work, we linked rogue patterns to roots of the Okamoto hierarchies. It is known that roots of the original Okamoto polynomials give pole locations of certain rational solutions to the original Painlevé IV equation.[60–62] Just as the Yablonskii–Vorob'ev case, we expect roots of the Okamoto hierarchies to give pole locations of certain rational solutions to the Painlevé-IV hierarchy. Then, our results in this article established a connection between rogue patterns and pole structures of the Painlevé-IV hierarchy. In a different problem of wave breaking in the semiclassical NLS equation, it has been shown in Ref. [77] that locations for isolated copies of Peregrine solutions that are generated in a wedge near the point of gradient catastrophe are determined by pole locations of the tritronqueé solution to the Painlevé I equation, and a similar result has also been shown for the semiclassical sine-Gordon equation.[78] Given these connections between wave patterns and pole locations of Painlevé I, II, and IV equations or their hierarchies, it is likely that connections between wave patterns and pole locations of the other Painlevé equations or their hierarchies would appear in the future too.

ACKNOWLEDGMENTS

We thank the two anonymous referees, whose comments have improved the presentation of this paper considerably. We also thank one of them for showing us how to prove $s_r = 0$ for $r \bmod 3 \neq 0$

in Theorems 3 and 4, which we included in Appendix D. The work of B.Y. was supported in part by the National Natural Science Foundation of China (Grant No. 12201326), and the work of J.Y. was supported in part by the National Science Foundation (U.S.) under award number DMS-1910282.

DATA AVAILABILITY STATEMENT

Data sharing not applicable to this article as no datasets were generated or analyzed during the current study.

ORCID

Jianke Yang https://orcid.org/0000-0001-5247-1152

REFERENCES

1. Akhmediev N, Ankiewicz A, Taki M. Waves that appear from nowhere and disappear without a trace. *Phys Lett A*. 2009;373:675-678.
2. Dysthe K, Krogstad HE, Müller P. Oceanic rogue waves. *Annu Rev Fluid Mech*. 2008;40:287.
3. Kharif C, Pelinovsky E, Slunyaev A. *Rogue Waves in the Ocean*. Springer; 2009.
4. Solli DR, Ropers C, Koonath P, Jalali B. Optical rogue waves. *Nature*. 2007;450:1054.
5. Wabnitz S, ed. *Nonlinear Guided Wave Optics: A Testbed for Extreme Waves*. IOP Publishing; 2017.
6. Peregrine DH. Water waves, nonlinear Schrödinger equations and their solutions. *J Aust Math Soc B*. 1983;25:16.
7. Akhmediev N, Ankiewicz A, Soto-Crespo JM. Rogue waves and rational solutions of the nonlinear Schrödinger equation. *Phys Rev E*. 2009;80:026601.
8. Dubard P, Gaillard P, Klein C, Matveev VB. On multirogue wave solutions of the NLS equation and position solutions of the KdV equation. *Eur Phys J Spec Top*. 2010;185:247.
9. Kedziora DJ, Ankiewicz A, Akhmediev N. Circular rogue wave clusters. *Phys Rev E*. 2011;84:056611.
10. Guo BL, Ling LM, Liu QP. Nonlinear Schrödinger equation: generalized Darboux transformation and rogue wave solutions. *Phys Rev E*. 2012;85:026607.
11. Ohta Y, Yang J. General high-order rogue waves and their dynamics in the nonlinear Schrödinger equation. *Proc R Soc Lond A*. 2012;468:1716.
12. Benney DJ, Newell AC. The propagation of nonlinear wave envelopes. *J Math Phys*. 1967;46:133.
13. Ablowitz MJ, Segur H. *Solitons and the Inverse Scattering Transform*. SIAM; 1981.
14. Ganshin AN, Efimov VB, Kolmakov GV, Mezhov-Deglin LP, McClintock PVE. Observation of an inverse energy cascade in developed acoustic turbulence in superfluid helium. *Phys Rev Lett*. 2008;101:065303.
15. Kibler B, Fatome J, Finot C, et al. The Peregrine soliton in nonlinear fibre optics. *Nat Phys*. 2010;6:790.
16. Chabchoub A, Hoffmann N, Akhmediev N. Rogue wave observation in a water wave tank. *Phys Rev Lett*. 2011;106:204502.
17. Bailung H, Sharma SK, Nakamura Y. Observation of Peregrine solitons in a multicomponent plasma with negative ions. *Phys Rev Lett*. 2011;107:255005.
18. Chabchoub A, Hoffmann N, Onorato M, et al. Observation of a hierarchy of up to fifth-order rogue waves in a water tank. *Phys Rev E*. 2012;86:056601.
19. He JS, Guo LJ, Zhang YS, Chabchoub A. Theoretical and experimental evidence of non-symmetric doubly localized rogue waves. *Proc R Soc A*. 2014;470:20140318.
20. Tsai YY, Tsai JY, I L. Generation of acoustic rogue waves in dusty plasmas through three-dimensional particle focusing by distorted waveforms. *Nat Phys*. 2016;12:573-577.
21. Kaup DJ, Newell AC. An exact solution for a derivative nonlinear Schrödinger equation. *J Math Phys*. 1978;19:798.
22. Mio K, Ogino T, Minami K, Takeda S. Modified nonlinear Schröinger equation for Alfvén waves propagating along the magnetic field in cold plasmas. *J Phys Soc Jpn*. 1976;41:265.
23. Moses J, Malomed BA, Wise FW. Self-steepening of ultrashort optical pulses without self-phase modulation. *Phys Rev A*. 2007;76:021802.
24. Xu SW, He JS, Wang LH. The Darboux transformation of the derivative nonlinear Schrödinger equation. *J Phys A*. 2011;44:305203.

25. Guo BL, Ling LM, Liu QP. High-order solutions and generalized Darboux transformations of derivative nonlinear Schrödinger equations. *Stud Appl Math*. 2013;130:317.
26. Yang B, Chen J, Yang J. Rogue waves in the generalized derivative nonlinear Schrödinger equations. *J Nonl Sci*. 2020;30:3027-3056.
27. Wai PKA, Menyuk CR. Polarization mode dispersion, decorrelation, and diffusion in optical fibers with randomly varying birefringence. *J Lightwave Technol*. 1996;14:148.
28. Kang JU, Stegeman GI, Aitchison JS, Akhmediev N. Observation of Manakov spatial solitons in AlGaAs planar waveguides. *Phys Rev Lett*. 1996;76:3699.
29. Chen Z, Segev M, Coskun TH, Christodoulides DN, Kivshar YS. Coupled photorefractive spatial-soliton pairs. *J Opt Soc Am B*. 1997;14:3066.
30. Baronio F, Degasperis A, Conforti M, Wabnitz S. Solutions of the vector nonlinear Schrödinger equations: evidence for deterministic rogue waves. *Phys Rev Lett*. 2012;109:044102.
31. Baronio F, Conforti M, Degasperis A, Lombardo S, Onorato M, Wabnitz S. Vector rogue waves and baseband modulation instability in the defocusing regime. *Phys Rev Lett*. 2014;113:034101.
32. Ling L, Guo B, Zhao L. High-order rogue waves in vector nonlinear Schrödinger equations. *Phys Rev E*. 2014;89:041201(R).
33. Chen S, Mihalache D. Vector rogue waves in the Manakov system: diversity and compossibility. *J Phys A*. 2015;48:215202.
34. Zhao L, Guo B, Ling L. High-order rogue wave solutions for the coupled nonlinear Schrödinger equations-II. *J Math Phys*. 2016;57:043508.
35. Baronio F, Conforti M, Degasperis A, Lombardo S. Rogue waves emerging from the resonant interaction of three waves. *Phys Rev Lett*. 2013;111:114101.
36. Degasperis A, Lombardo S. Rational solitons of wave resonant-interaction models. *Phys Rev E*. 2013;88:052914.
37. Chen S, Soto-Crespo JM, Grelu P. Watch-hand-like optical rogue waves in three-wave interactions. *Opt Express*. 2015;23:349-359.
38. Wang X, Cao J, Chen Y. Higher-order rogue wave solutions of the three-wave resonant interaction equation via the generalized Darboux transformation. *Phys Scr*. 2015;90:105201.
39. Zhang G, Yan Z, Wen XY. Three-wave resonant interactions: multi-dark-dark-dark solitons, breathers, rogue waves, and their interactions and dynamics. *Physica D*. 2018;366:27-42.
40. Frisquet B, Kibler B, Morin P, et al. Optical dark rogue wave. *Sci Rep*. 2016;6:20785.
41. Baronio F, Frisquet B, Chen S, Millot G, Wabnitz S, Kibler B. Observation of a group of dark rogue waves in a telecommunication optical fiber. *Phys Rev A*. 2018;97:013852.
42. Mu G, Qin Z, Grimshaw R. Dynamics of rogue waves on a multisoliton background in a vector nonlinear Schrödinger equation. *SIAM J Appl Math*. 2015;75:1-20.
43. Chen J, Pelinovsky DE, White RE. Rogue waves on the double-periodic background in the focusing nonlinear Schrödinger equation. *Phys Rev E*. 2019;100:052219.
44. Xu G, Chabchoub A, Pelinovsky DE, Kibler B. Observation of modulation instability and rogue breathers on stationary periodic waves. *Phys Rev Res*. 2020;2:033528.
45. Rao J, Fokas AS, He JS. Doubly localized two-dimensional rogue waves in the Davey-Stewartson I equation. *J Nonl Sci*. 2021;31:1-44.
46. Yang B, Yang J. Rogue waves in (2+1)-dimensional three-wave resonant interactions. *Physica D*. 2022;432:133160.
47. He JS, Zhang HR, Wang LH, Porsezian K, Fokas AS. Generating mechanism for higher-order rogue waves. *Phys Rev E*. 2013;87:052914.
48. Kedziora DJ, Ankiewicz A, Akhmediev N. Classifying the hierarchy of nonlinear-Schrödinger-equation rogue-wave solutions. *Phys Rev E*. 2013;88:013207.
49. Ankiewicz A, Akhmediev N. Multi-rogue waves and triangular numbers. *Rom Rep Phys*. 2017;69:104.
50. Ankiewicz A, Clarkson PA, Akhmediev N. Rogue waves, rational solutions, the patterns of their zeros and integral relations. *J Phys A*. 2010;43:122002.
51. Wang L, Yang CH, Wang J, He JS. The height of an nth-order fundamental rogue wave for the nonlinear Schrödinger equation. *Phys Lett A*. 2017;381:1714-1718.
52. Bilman D, Miller PD. A robust inverse scattering transform for the focusing nonlinear Schrödinger equation. *Commun Pure Appl Math*. 2019;72:1722-1805.

53. Bilman D, Ling L, Miller PD. Extreme superposition: rogue waves of infinite order and the Painlevé-III hierarchy. *Duke Math J*. 2020;169:671-760.
54. Yang B, Yang J. Rogue wave patterns in the nonlinear Schrodinger equation. *Physica D*. 2021;419:132850.
55. Yang B, Yang J. Universal rogue wave patterns associated with the Yablonskii-Vorob'ev polynomial hierarchy. *Physica D*. 2021;425:132958.
56. Chen J, Chen Y, Feng BF, Maruno KI, Ohta Y. General high-order rogue waves of the (1+1)-dimensional Yajima-Oikawa system. *J Phys Soc Japan*. 2018;87:094007.
57. Feng BF, Ma R, Zhang Y. General breather and rogue wave solutions to the complex short pulse equation. *Physica D*. 2022;439:133360.
58. Wu C, Zhang G, Shi C, Feng BF. General rogue wave solutions to the Sasa-Satsuma equation. arXiv:2206.02210 [nlin.SI] 2022.
59. Yang B, Yang J. General rogue waves in the three-wave resonant interaction systems. *IMA J Appl Math*. 2021;86:378-425.
60. Okamoto K. Studies on the Painlevé equations. III. Second and fourth Painlevé equations, P_{II} and P_{IV}. *Math Ann*. 1986;275:221-255.
61. Kajiwara K, Ohta Y. Determinant structure of the rational solutions for the Painlevé IV equation. *J Phys A*. 1998;31:2431-2446.
62. Clarkson PA. The fourth Painlevé equation and associated special polynomials. *J Math Phys*. 2003;44:5350-5374.
63. Clarkson PA, Mansfield EL. The second Painlevé equation, its hierarchy and associated special polynomials. *Nonlinearity*. 2003;16:R1.
64. Noumi M, Yamada Y. Symmetries in the fourth Painlevé equation and Okamoto polynomials. *Nagoya Math J*. 1999;153:53-86.
65. Buckingham RJ, Miller PD. Large-degree asymptotics of rational Painlevé-IV solutions by the isomonodromy method. *Constr Approx*. 2022;56:233-443.
66. Kametaka Y. On poles of the rational solution of the Toda equation of Painlevé-IV type. *Proc Jpn Acad A*. 1983;59:453-455.
67. Fukutani S, Okamoto K, Umemura H. Special polynomials and the Hirota bilinear relations of the second and the fourth Painlevé equations. *Nagoya Math J*. 2000;159:179-200.
68. Manakov SV, Eksp Zh. On the theory of two-dimensional stationary self-focusing of electromagnetic waves. *Teor Fiz*. 1973;65:1392 [Sov. Phys. JETP 38, 248 (1974)].
69. Kivshar YS, Agrawal GP. *Optical Solitons: From Fibers to Photonic Crystals*. Academic Press; 2003.
70. Evangelides SG, Mollenauer LF, Gordon JP, Bergano NS. Polarization Multiplexing with Solitons. *J Lightwave Technol*. 1992;10:28.
71. Frisquet B, Kibler B, Fatome J, et al. Polarization modulation instability in a Manakov fiber system. *Phys Rev A*. 2015;92:053854.
72. Kevrekidis PG, Frantzeskakis DJ, Carretero-Gonzalez R, eds. *Emergent Nonlinear Phenomena in Bose-Einstein Condensates: Theory and Experiment*. Springer; 2008.
73. Hoefer MA, Chang JJ, Hamner C, Engels P. Dark-dark solitons and modulational instability in miscible two-component Bose-Einstein condensates. *Phys Rev A*. 2011;84:041605(R).
74. Wang D, Zhang D, Yang J. Integrable properties of the general coupled nonlinear Schrödinger equations. *J Math Phys*. 2010;51:023510.
75. Wang X, Chen Y. Generalized Darboux transformation and higher-order rogue wave solutions of the coupled Hirota equations. arXiv:1409.5013 [nlin.SI] 2014.
76. Rao J, Malomed BA, Mihalache D, He JS. General higher-order breathers and rogue waves in the two-component long-wave–short-wave resonance interaction model. *Stud Appl Math*. 2022;149:843-878.
77. Bertola M, Tobvis A. Universality for the focusing nonlinear Schrödinger equation at the gradient catastrophe point: rational breathers and poles of the tritronquée solution to Painlevé I. *Comm Pure Appl Math*. 2013;66:678.
78. Lu B, Miller PD. Universality near the gradient catastrophe point in the semiclassical sine-Gordon equation. *Comm Pure Appl Math*. 2022;75:1517-1641.
79. Macdonald IG. *Symmetric functions and Hall polynomials*. Clarendon Press; 1995.
80. Balogh F, Bertola M, Bothner T. Hankel determinant approach to generalized Vorob'ev-Yablonski polynomials and their roots. *Constr Approx*. 2016;44:417-453.

81. Ohta Y, Wang DS, Yang J. General N-dark-dark solitons in the coupled nonlinear Schrödinger equations. *Stud Appl Math*. 2011;127:345-371.

How to cite this article: Yang B, Yang J. Rogue wave patterns associated with Okamoto polynomial hierarchies. *Stud Appl Math*. 2023;151:60–115.
https://doi.org/10.1111/sapm.12573

APPENDIX A

In this appendix, we provide an alternative definition of Okamoto-hierarchy polynomials $Q_N^{[m]}(z)$ and $R_N^{[m]}(z)$ by Schur functions associated with Young diagrams.[63,79,80]

A Young diagram $Y = (i_1, i_2, \dots, i_l)$, or a partition, of length l, is a sequence of descending nonzero numbers such that $i_1 \geq i_2 \geq \cdots \geq i_l > 0$. The Schur function $s_Y(\mathbf{x})$, for vector $\mathbf{x} = (x_1, x_2, \dots)$ and Young diagram $Y = (i_1, i_2, \dots, i_l)$, is defined by

$$s_Y(\mathbf{x}) = \det_{1\leq j,k\leq l}[S_{i_j-j+k}(\mathbf{x})], \tag{A1}$$

where elementary Schur polynomials $S_j(\mathbf{x})$ are as defined in Equation (22). Using these notations, Okamoto-hierarchy polynomials $Q_N^{[m]}(z)$ can be written as

$$Q_N^{[m]}(z) = \frac{s_Y(z, 0, \dots, 0, 1_m, 0, \dots)}{s_Y(1, 0, 0, \dots)}, \tag{A2}$$

where $Y = (2N, 2N-2, \dots, 4, 2)$, and 1_m means that 1 is in the mth position of that vector. Similarly, Okamoto-hierarchy polynomials $R_N^{[m]}(z)$ can be written as

$$R_N^{[m]}(z) = \frac{s_{\widehat{Y}}(z, 0, \dots, 0, 1_m, 0, \dots)}{s_{\widehat{Y}}(1, 0, 0, \dots)}, \tag{A3}$$

where $\widehat{Y} = (2N-1, 2N-3, \dots, 3, 1)$.

APPENDIX B

In this appendix, we prove Theorems 1 and 2 regarding roots of Okamoto polynomial hierarchies $Q_N^{[m]}(z)$ and $R_N^{[m]}(z)$. The two proofs are similar. Thus, we will only present the proof for Theorem 1 below.

First, we derive the multiplicity of the zero root in $Q_N^{[m]}(z)$. For this purpose, we define the Schur polynomial $p_j^{[m]}(z; a)$ as

$$\sum_{j=0}^{\infty} p_j^{[m]}(z; a)\epsilon^j = \exp[z\epsilon + a\epsilon^m], \tag{B1}$$

where a is a constant, and $p_j^{[m]}(z;a) \equiv 0$ when $j < 0$. Through these $p_j^{[m]}(z;a)$ polynomials, we define the following polynomials:

$$Q_N^{[m]}(z;a) = c_N \begin{vmatrix} p_2^{[m]}(z;a) & p_1^{[m]}(z;a) & \cdots & p_{3-N}^{[m]}(z;a) \\ p_5^{[m]}(z;a) & p_4^{[m]}(z;a) & \cdots & p_{6-N}^{[m]}(z;a) \\ \vdots & \vdots & \vdots & \vdots \\ p_{3N-1}^{[m]}(z;a) & p_{3N-2}^{[m]}(z;a) & \cdots & p_{2N}^{[m]}(z;a) \end{vmatrix}, \tag{B2}$$

where c_N is given in Equation (4). It is easy to see that $p_j^{[m]}(z;a)$ is related to the polynomial $p_j^{[m]}(z)$ in Equation (6) as

$$p_j^{[m]}(z;a) = a^{j/m} p_j^{[m]}(\hat{z}), \quad \hat{z} \equiv a^{-1/m} z. \tag{B3}$$

Thus, the polynomial $Q_N^{[m]}(z;a)$ is related to the Okamoto-hierarchy polynomial $Q_N^{[m]}(z)$ in Equation (8) as

$$Q_N^{[m]}(z;a) = a^{N(N+1)/m} Q_N^{[m]}(\hat{z}). \tag{B4}$$

This equation tells us that every term in the polynomial $Q_N^{[m]}(z;a)$ is a constant multiple of $z^i a^j$, where $i + mj = N(N+1)$. Thus, to determine the multiplicity of the zero root $\hat{z} = 0$ in $Q_N^{[m]}(\hat{z})$, which is the exponent i of the lowest power of $\hat{z}$ in $Q_N^{[m]}(\hat{z})$, we need to determine the term $z^i a^j$ in $Q_N^{[m]}(z;a)$ where the power j of a is the highest. To do so, we first expand $p_j^{[m]}(z;a)$ into powers of a as

$$p_j^{[m]}(z;a) = \sum_{l=0}^{[j/m]} \frac{a^l}{l!(j-lm)!} z^{j-lm}. \tag{B5}$$

This expansion can be obtained by splitting the right side of Equation (B1) into the product of two exponentials and expanding both exponentials into Taylor series of ϵ, and then collecting terms of power ϵ^j in that product and equating them to $p_j^{[m]}(z;a)$. Using the above relation, we can express matrix elements in the determinant (B2) for $Q_N^{[m]}(z;a)$ through powers of z and a. Notice that when $m = 3j+1$ ($j \geq 1$), coefficients of the highest a power terms in the first column of that determinant are proportional to

$$z^2, z^5, \ldots, z^{3j-1}, z^1, z^4, \ldots, z^{3j-2}, z^0, z^3, \ldots, z^{3j}, \tag{B6}$$

and repeating, and when $m = 3j+2$ ($j \geq 0$), these coefficients are proportional to

$$z^2, z^5, \ldots, z^{3j-1}, z^0, z^3, \ldots, z^{3j}, z^1, z^4, \ldots, z^{3j+1}, \tag{B7}$$

and repeating. In the second and higher columns of $Q_N^{[m]}(z;a)$, elements are the same as those in the first column, except that the power j of every z^j in them decreases by one with each higher column, and $z^j \equiv 0$ for $j < 0$.

To obtain the highest power term of a in the determinant $Q_N^{[m]}(z;a)$, we perform row operations to this determinant to remove certain power terms of a. Specifically, using the first m rows, we perform row operations to remove the highest powers of a from the second m rows, leaving the

second highest power terms of a with coefficients proportional to z^{j+m}, where z^j is the highest a-power coefficient of each element just being removed. Then, we use the first m rows and the resulting second m rows to eliminate the highest and second highest power terms of a from the third m rows, leaving the third highest power terms of a with coefficients proportional to z^{j+2m} in them. This process is continued to all later rows of $Q_N^{[m]}(z;a)$.

After these row operations, we then keep only the highest remaining power term of a in each matrix element of $Q_N^{[m]}(z;a)$. This reduced determinant will be the $z^i a^j$ term in $Q_N^{[m]}(z;a)$ where the power j of a is the highest, and the corresponding power i of z^i in this term will be the multiplicity of the zero root in $Q_N^{[m]}(\hat{z})$. Recalling the sequence structures in Equations (B6) and (B7), for m mod 3 = 1 and 2, respectively, we can readily calculate this reduced determinant and find its z^i term, where i is equal to the quantity N_Q given in Equation (11) of Theorem 1.

One may notice the close resemblance between the above derivation for the zero root's multiplicity in the Okamoto hierarchy polynomial $Q_N^{[m]}(z)$, and the proof of Theorem 5 for the reduced Q-type rogue wave in the inner region. Indeed, these two seemingly very different topics are actually closely related.

Now, we prove the factorization formula (10) in Theorem 1. The definition (6) of the polynomial $p_j^{[m]}(z)$ implies the symmetry

$$p_j^{[m]}(\omega z) = \omega^j p_j^{[m]}(z), \tag{B8}$$

where ω is any one of the mth root of 1, that is, $\omega^m = 1$. This symmetry of $p_j^{[m]}(z)$ leads to the symmetry of $Q_N^{[m]}(z)$ as

$$Q_N^{[m]}(\omega z) = \omega^{N(N+1)} Q_N^{[m]}(z). \tag{B9}$$

Since we have just established that the multiplicity of the zero root in $Q_N^{[m]}(z)$ is N_Q, we can write

$$Q_N^{[m]}(z) = z^{N_Q} q_N^{[m]}(z), \tag{B10}$$

where $q_N^{[m]}(z)$ is a polynomial of z with a nonzero constant term. The symmetry (B9) of the polynomial $Q_N^{[m]}(z)$ induces a symmetry for $q_N^{[m]}(z)$ as

$$q_N^{[m]}(\omega z) = \omega^{N(N+1)-N_Q} q_N^{[m]}(z). \tag{B11}$$

It is easy to check that $N(N+1) - N_Q$ is a multiple of m. Hence, $\omega^{N(N+1)-N_Q} = 1$, and consequently,

$$q_N^{[m]}(\omega z) = q_N^{[m]}(z). \tag{B12}$$

This symmetry of $q_N^{[m]}(z)$ dictates that $q_N^{[m]}(z)$ can only be a polynomial of $\zeta \equiv z^m$. The form (10) of the polynomial $Q_N^{[m]}(z)$ is then proved.

APPENDIX C

In this appendix, we derive Manakov rogue waves presented in Theorem 3. This derivation is an extension of our earlier derivation in Ref. [55] for a simpler type of Manakov rogue waves.

Under the transformation,

$$u_1(x,t)=\rho_1\frac{g}{f}e^{\mathrm{i}(k_1x+\omega_1t)},\quad u_2(x,t)=\rho_2\frac{h}{f}e^{\mathrm{i}(k_2x+\omega_2t)}, \tag{C1}$$

where f is real and (g,h) complex, and the Manakov system (19) can be converted into the following bilinear equations:

$$\begin{aligned}&\left(D_x^2+\epsilon_1\rho_1^2+\epsilon_1\rho_1^2\right)f\cdot f=\epsilon_1\rho_1^2gg^*+\epsilon_2\rho_2^2hh^*,\\&\left(iD_t+D_x^2+2ik_1D_x\right)g\cdot f=0,\\&\left(iD_t+D_x^2+2ik_2D_x\right)h\cdot f=0.\end{aligned} \tag{C2}$$

This bilinear system can be reduced from the following higher dimensional bilinear system in the two-component Kadomtsev–Petviashvili (KP) hierarchy,[81]

$$\begin{aligned}&(\tfrac{1}{2}D_xD_r-1)\tau_{n,k}\cdot\tau_{n,k}=-\tau_{n+1,k}\,\tau_{n-1,k},\\&(D_x^2-D_y+2aD_x)\tau_{n+1,k}\cdot\tau_{n,k}=0,\\&(\tfrac{1}{2}D_xD_s-1)\tau_{n,k}\cdot\tau_{n,k}=-\tau_{n,k+1}\,\tau_{n,k-1},\\&(D_x^2-D_y+2bD_x)\tau_{n,k+1}\cdot\tau_{n,k}=0,\end{aligned} \tag{C3}$$

where n,k are integers, $\tau_{n,k}$ is a function of four independent variables (x,y,r,s), $a=\mathrm{i}k_1$, and $b=\mathrm{i}k_2$. For rogue waves, the solution $\tau_{n,k}$ to these higher dimensional bilinear equations is chosen as[55]

$$\tau_{n,k}=\det_{1\le\nu,\mu\le N}\left(\phi_{i_\nu,j_\mu}^{(n,k)}\right), \tag{C4}$$

where $(i_1,i_2,\dots,i_N)$ and $(j_1,j_2,\dots,j_N)$ are arbitrary sequences of indices, and the matrix element $\phi_{ij}^{(n,k)}$ is defined as

$$\phi_{ij}^{(n,k)}=\mathcal{A}_i\mathcal{B}_j\phi^{(n,k)}, \tag{C5}$$

$$\phi^{(n,k)}=\frac{(p+1)(q+1)}{2(p+q)}\left(-\frac{p-a}{q+a}\right)^n\left(-\frac{p-b}{q+b}\right)^k e^{\xi+\eta}, \tag{C6}$$

$$\xi=px+p^2y+\frac{1}{p-a}r+\frac{1}{p-b}s+\xi_0(p), \tag{C7}$$

$$\eta=qx-q^2y+\frac{1}{q+a}r+\frac{1}{q+b}s+\eta_0(q), \tag{C8}$$

$$\mathcal{A}_i=\frac{1}{i!}\left[f_1(p)\partial_p\right]^i,\quad \mathcal{B}_j=\frac{1}{j!}\left[f_2(q)\partial_q\right]^j, \tag{C9}$$

p,q are arbitrary complex constants, and $\xi_0(p),\eta_0(q),f_1(p),f_2(q)$ are arbitrary functions of p and q, respectively.

To reduce the higher dimensional bilinear system (C3) to the original system (C2), we need to set

$$f=\tau_{0,0},\quad g=\tau_{1,0},\quad h=\tau_{0,1},\quad y=\mathrm{i}t, \tag{C10}$$

impose the dimension reduction condition

$$\left(2\partial_x + \epsilon_1\rho_1^2\partial_r + \epsilon_2\rho_2^2\partial_s\right)\tau_{n,k} = C\,\tau_{n,k}, \tag{C11}$$

where C is some constant, and impose the conjugation condition

$$\tau_{-n,-k} = \tau_{n,k}^*. \tag{C12}$$

The steps to meet these two conditions are the same as in Ref. [59] for rogue waves in the three-wave resonant interaction system.

First, we consider the dimension reduction condition (C11). Here,

$$\left(2\partial_x + \epsilon_1\rho_1^2\partial_r + \epsilon_2\rho_2^2\partial_s\right)\phi_{ij}^{(n,k)} = \mathcal{A}_i\mathcal{B}_j[\mathcal{F}_1(p) + \mathcal{F}_2(q)]\phi^{(n,k)}, \tag{C13}$$

where

$$\mathcal{F}_1(p) = \frac{\epsilon_1\rho_1^2}{p-a} + \frac{\epsilon_2\rho_2^2}{p-b} + 2p, \tag{C14}$$

and $\mathcal{F}_2(q)$ is the above $\mathcal{F}_1(p)$ function with p switching to q and (a,b) switching to $(-a,-b)$. Suppose the algebraic equation $\mathcal{F}_1'(p) = 0$ admits a nonimaginary double root p_0, which happens under conditions (24), and the corresponding root p_0 is given in Equation (27). In this case, the dimension reduction condition (C11) would be satisfied if we choose $f_1(p)$ to satisfy the differential equation

$$\left(f_1(p)\partial_p\right)^3\mathcal{F}_1(p) = \mathcal{F}_1(p), \tag{C15}$$

choose $f_2(q)$ to satisfy a similar equation except to change the index above from 1 to 2 and change p to q, and choose the $\tau_{n,k}$ determinant (C4) as

$$\tau_{n,k} = \det\begin{pmatrix} \tau_{n,k}^{[1,1]} & \tau_{n,k}^{[1,2]} \\ \tau_{n,k}^{[2,1]} & \tau_{n,k}^{[2,2]} \end{pmatrix}, \tag{C16}$$

where

$$\tau_{n,k}^{[I,J]} = \mathrm{mat}_{1\le i\le N_I, 1\le j\le N_J}\left(\phi_{3i-I,3j-J}^{(n,k)}\Big|_{p=p_0,\, q=q_0,\, \xi_0=\xi_{0I},\, \eta_0=\eta_{0J}}\right), \quad 1\le I,J\le 2, \tag{C17}$$

$\phi_{i,j}^{(n,k)}$ is given by Equations (C5)–(C9), $q_0 = p_0^*$, and N_1, N_2 are nonnegative integers. The reason for this can be found in Ref. [59].

The differential equation (C15) for $\mathcal{F}_1(p)$ is linear and homogeneous. Its solution under the condition of p_0 being a double root of $\mathcal{F}_1'(p) = 0$ is[59]

$$\mathcal{F}_1(p) = \frac{\mathcal{F}_1(p_0)}{3}\left(\mathcal{W}_1(p) + \frac{2}{\sqrt{\mathcal{W}_1(p)}}\cos\left[\frac{\sqrt{3}}{2}\ln\mathcal{W}_1(p)\right]\right), \tag{C18}$$

where $\mathcal{W}_1(p)$ is defined through $f_1(p) = \mathcal{W}_1(p)/\mathcal{W}_1'(p)$. From this equation, one can solve for $\mathcal{W}_1(p)$ from $\mathcal{F}_1(p)$ and then obtain $f_1(p)$. But it turns out this explicit solving for $\mathcal{W}_1(p)$ and $f_1(p)$ is not necessary for our goal of obtaining explicit expressions for matrix elements in Equation (C16), see below.

Regarding the conjugation condition (C12), it can be satisfied when we require $\eta_{0,I} = \xi^*_{0,I}$. To introduce free parameters into these solutions, we set

$$\xi_{0,I} = \sum_{r=1}^{\infty} a_{r,I} \ln^r \mathcal{W}_1(p), \quad I = 1, 2, \tag{C19}$$

where $a_{r,I}$ are free complex constants.

Next, we remove the differential operators in the matrix elements (C5) and derive more explicit expressions of rogue waves through Schur polynomials. This derivation is very similar to that we did in Ref. [59] for the three-wave system. In fact, this derivation is a bit simpler now due to our introduction of the extra factor $(p+1)(q+1)/2$ in Equation (C6). Combining these steps, we obtain the Manakov rogue wave expressions given in Theorem 3, except that the definitions for $x^+_{r,I}(n,k)$ and $x^-_{r,J}(n,k)$ are as given in Equations (34)–(35) for all r indices, including those where $r \bmod 3 = 0$.

But those $x^+_{r,I}(n,k)$ and $x^-_{r,J}(n,k)$ with $r \bmod 3 = 0$ can be removed from the solution. This can be done by using a technique similar to that employed in Appendix A of Ref. [54].

Regarding the regularity of solutions (28)–(29), they can be proved using arguments very similar to that in Ref. [11].

After all these steps, Theorem 3 is then proved.

APPENDIX D

In this appendix, we prove that $s_r = 0$ for $r \bmod 3 \neq 0$ in Theorems 3 and 4.

The functions $\mathcal{F}_1(p)$ and $\mathcal{F}_2(p)$ in Theorems 3 and 4 can be written in a unified scaled form

$$\mathcal{F}(p) = \frac{r}{p-a} + \frac{r}{p-b} + p, \tag{D1}$$

where a and b are distinct purely imaginary (or zero) constants, and r is a real parameter. The simple scaling of $\mathcal{F}_1(p)$ and $\mathcal{F}_2(p)$ to $\mathcal{F}(p)$ does not affect the function $p(\kappa)$ defined in Equations (39) and (64) and thus does not affect the s_r expansions in (38) and (63). When $r = -(a-b)^2$, which is the case in Theorems 3 and 4, the function $\mathcal{F}'(p)$ can be factorized as

$$\mathcal{F}'(p) = \frac{[p^2 - (a+b)p + (a^2 - ab + b^2)]^2}{(p-a)^2(p-b)^2}. \tag{D2}$$

Thus, $\mathcal{F}'(p)$ has a double root p_0 as chosen in Theorems 3 and 4. This double root satisfies the equation

$$p_0^2 - (a+b)p_0 + (a^2 - ab + b^2) = 0, \tag{D3}$$

and its conjugate p_0^* satisfies the equation

$$p_0^{*2} + (a+b)p_0^* + (a^2 - ab + b^2) = 0 \tag{D4}$$

since a and b are purely imaginary.

Equations (39) and (64) that define the function $p(\kappa)$ in Theorems 3 and 4 can be written as

$$\mathcal{F}[p(\kappa)] = \mathcal{F}(p_0)E(\kappa), \tag{D5}$$

where

$$E(\kappa)=\frac{1}{3}\left[e^{\kappa}+2e^{-\kappa/2}\cos\left(\frac{\sqrt{3}}{2}\kappa\right)\right]=\frac{1}{3}\left(e^{\kappa}+e^{\omega\kappa}+e^{\omega^2\kappa}\right)=\sum_{j=0}^{\infty}\frac{\kappa^{3j}}{(3j)!}, \tag{D6}$$

and $\omega=e^{2i\pi/3}$. Notice that $E(\kappa)$ contains only κ^{3j} powers. Inserting the functional form (D1) of $\mathcal{F}(p)$ into the above equation (D5) and simplifying, we get the following cubic equation that defines the function $p(\kappa)$,

$$p^3-(a+b+\alpha)p^2+[ab+\alpha(a+b)+2r]p-[r(a+b)+\alpha ab]=0, \tag{D7}$$

where $\alpha=(3p_0-a-b)E(\kappa)$, and $r=-(a-b)^2$ as mentioned before.

The key idea of the proof is to show that $[p(\kappa)-p_0]^3/[p(\kappa)+p_0^*]^3$ is a function of $E(\kappa)$ only. To do so, we utilize the above equation (D7) for p^3 and Equations (D3)–(D4) for p_0^2 and p_0^{*2} to calculate $[p(\kappa)-p_0]^3$ and $[p(\kappa)+p_0^*]^3$. After simple algebra, we find that

$$[p(\kappa)-p_0]^3=(3p_0-a-b)[E(\kappa)-1][p(\kappa)-a][p(\kappa)-b], \tag{D8}$$

$$[p(\kappa)+p_0^*]^3=\left[(3p_0-a-b)E(\kappa)+(3p_0^*+a+b)\right][p(\kappa)-a][p(\kappa)-b]. \tag{D9}$$

Thus,

$$\frac{[p(\kappa)-p_0]^3}{[p(\kappa)+p_0^*]^3}=\frac{(3p_0-a-b)[E(\kappa)-1]}{(3p_0-a-b)E(\kappa)+(3p_0^*+a+b)}, \tag{D10}$$

which only depends on $E(\kappa)$. When we insert the expansion $p(\kappa)=p_0+p_1\kappa+p_2\kappa^2+\cdots$ into this equation and equate coefficients of the κ^3 term, we further find that

$$p_1^3=\frac{1}{18}(3p_0-a-b)(p_0+p_0^*)^2. \tag{D11}$$

Finally, we put these results together and find that the s_r expansions (38) and (63) in Theorems 3 and 4 are

$$\begin{aligned}\sum_{r=1}^{\infty}s_r\kappa^r&=\frac{1}{3}\ln\left[\frac{1}{\kappa^3}\left(\frac{p_0+p_0^*}{p_1}\right)^3\left(\frac{p(\kappa)-p_0}{p(\kappa)+p_0^*}\right)^3\right]\\&=\frac{1}{3}\ln\left[\frac{18(p_0+p_0^*)}{\kappa^3}\frac{E(\kappa)-1}{(3p_0-a-b)E(\kappa)+(3p_0^*+a+b)}\right].\end{aligned} \tag{D12}$$

Since the right side of this equation is a function of κ^3 only, we then conclude that $s_r=0$ for $r \bmod 3\neq 0$ in Theorems 3 and 4.

For the Manakov system in Theorem 3, if we normalize $k_2=-k_1$ through a Galilean transformation, then $a=-b=ik_1$ and $p_0=\sqrt{3}k_1$. In this case, the above equation reduces to

$$\sum_{r=1}^{\infty}s_r\kappa^r=\frac{1}{3}\ln\left[\frac{12}{\kappa^3}\frac{E(\kappa)-1}{E(\kappa)+1}\right], \tag{D13}$$

which gives s_r values displayed in Equation (42). For the three-wave system in Theorem 4, we have $a = 0$, $b = \mathrm{i}$, and $p_0 = (\sqrt{3} + \mathrm{i})/2$. In this case, the above equation (D12) reduces to

$$\sum_{r=1}^{\infty} s_r \kappa^r = \frac{1}{3} \ln \left[\frac{36\sqrt{3}}{\kappa^3} \frac{E(\kappa) - 1}{(3\sqrt{3} + \mathrm{i})E(\kappa) + (3\sqrt{3} - \mathrm{i})} \right], \tag{D14}$$

which gives s_r values displayed in Equation (67).